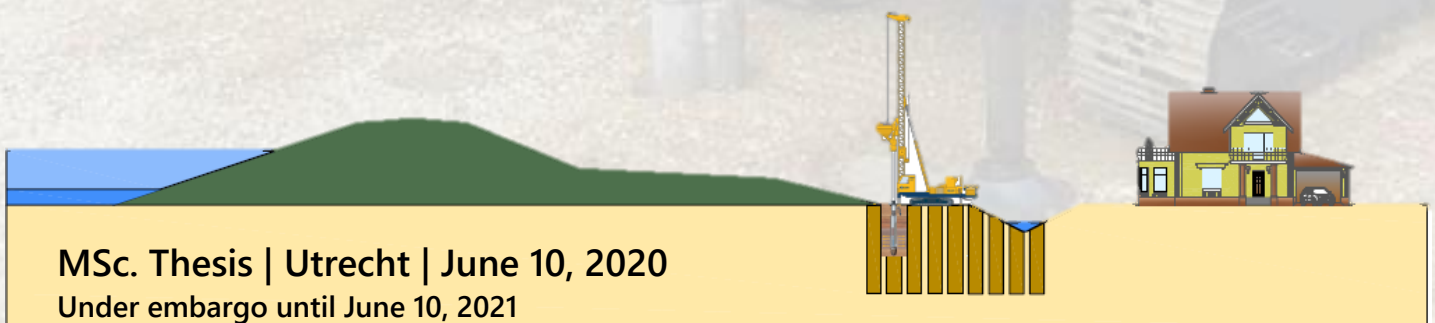


# Dike stabilisation under uplift conditions using stabilisation columns

A study on the technical potential of stabilisation columns for improving  
inner slope stability under uplift conditions



MSc. Thesis | Utrecht | June 10, 2020  
Under embargo until June 10, 2021



# Dike stabilisation under uplift conditions using stabilisation columns

A study on the technical potential of stabilisation columns for improving inner  
slope stability under uplift conditions

Master Thesis

by

P. C. (Peter) van de Stroet

as finalisation to obtain the degree  
Master of Science in Hydraulic Engineering  
at Delft University of Technology  
faculty of Civil Engineering and Geosciences.

To be defended publicly on Wednesday June 10, 2020 at 10:00 AM

|                   |                                  |                    |
|-------------------|----------------------------------|--------------------|
| Student number:   | 4561759                          |                    |
| Project duration: | 2019-2020                        |                    |
| Thesis committee: | Prof. Dr. Ir. S.N. (Bas) Jonkman | TU Delft, chairman |
|                   | Prof. Dr. K.G. (Ken) Gavin       | TU Delft           |
|                   | Ir. M.G. (Mark) van der Krogt    | TU Delft           |
|                   | Ir. B. (Ben) Rijneveld           | Fugro              |

Utrecht, June 10, 2020

Cover image is obtained from: [https://www.bsb-partner.ch/de/vologin-erweiterung-logistikcenter-voigt-niederbipp-\\_content---1--10049--362.html](https://www.bsb-partner.ch/de/vologin-erweiterung-logistikcenter-voigt-niederbipp-_content---1--10049--362.html)



## Preface

This thesis finalises my MSc study Hydraulic Engineering at Delft University of Technology within the specialisation Coastal Engineering. This research has been performed with the support of Delft University of Technology and the Fugro Hydraulic Engineering department.

I would like to thank my graduation committee, Prof. Dr. Ir. S.N. Jonkman, Prof. Dr. K.G. Gavin, Ir. M.G. van der Krogt and Ir. B. Rijnveld. Bas Jonkman, thank you for leading the committee and for your enthusiasm for this subject right from the start. Ken Gavin, thank you for the critical in depth questions during the meetings that helped me to improve my thesis. I would like to express my gratitude to Mark, you have been a really great help throughout this period. Thank you for keeping in touch with me and keeping me posted during Covid-19. And for helping me to provide a theoretical base to practical problems. A special thanks to Ben, for providing a practical base to theoretical problems. Thank you for your endless support, your help was essential to complete this thesis. Prof. Dr. Ir. R.B.J. Brinkgreve thank you for your help with the PLAXIS calculations.

Thanks to my colleagues at Fugro, thank you all for your advice, the enjoyable coffee breaks and the table football games we played. Especially Milan, Mark and Leon, thank you for your support with the PLAXIS calculations.

A special thanks to Ard-Jan Methorst, you have been a great support during my TU Delft study time. Thanks for the fun, the beers, playing FIFA and being a valuable friend. I would also like to thank my family and friends for always supporting me. And last, but certainly not least, from the bottom of my heart, thank you so much my beloved Karlijn. Thank you for always believing in me, supporting me and giving me the possibility to fulfil my dreams. I couldn't have done it without you, you're the best.

*P.C. (Peter) van de Stroet*

*Utrecht/Delft, 2020*



## Summary

Classical solutions to improve inner slope stability, like decreasing the inner slope and/or creating a stabilisation berm, generally have a large footprint. Stabilisation columns are expected to be an effective improvement method for inner slope stability that can prevent the occurrence of uplift within the actual footprint of the dike. Stabilisation columns are a soil improvement method where vertically created holes are filled upwards with a granular material displacing the host soil.

There are three effects of stabilisation columns that can contribute to improving inner slope stability and prevent lifting of the low permeable top layers with this method. The effects described are 1) an increase in weight, 2) an increase in strength and 3) a lateral expansion of the stabilisation columns. Due to the inclusion of a firmer material as gravel, weight and strength increase with respect to the host soil. When the stabilisation columns are installed by means of a vibro displacement method, the host soil displaces laterally. This can lead to an increase in lateral stress, soil stiffness and pore pressures. Until now, no internationally agreed on closed form equations are available to characterise these effects properly, the effects can at best be described by a Finite Element Analysis.

The effects of stabilisation columns are investigated in a case study using the Finite Element program PLAXIS. At first an unimproved homogenous reference dike on a low permeable clay top layer is given. The effects of stabilisation columns on inner slope stability are quantified by means of the improvement in the Factor of Safety (FoS) with respect to this reference dike. The various modelling techniques described in the literature study are used to simulate the stabilisation columns. An increase in weight and strength can be modelled straightforward with all methods described. The lateral expansion of stabilisation columns can only be modelled with a 3D or a 2D Plane Strain model.

The increase in weight improves the FoS by 5-10% for a row of 3-10 stabilisation columns perpendicular to the dike in a triangular grid. A strength increase hardly contributes to the FoS, since the slip surface is directly forced below the stabilisation columns, irrespective of the number of columns applied. Combining the effects of weight and lateral expansion leads to a FoS improvement of 14-24% for a row of 3-10 stabilisation columns perpendicular to the dike in a triangular grid respectively, meaning the lateral expansion contributes for approximately 9-14% to the FoS. The combined effects show the technical potential of applying stabilisation columns as a contributor to inner slope stability within the actual footprint, at the same time the occurrence of uplift is prevented. To improve the FoS of the reference dike by 20% by means of a classical stabilisation berm, the berm present needs to be extended by 15m and heightened by 0.5m. Applying stabilisation columns is therefore a suited alternative to improve primary and regional flood defences. For (regional) flood defences with a road on top they might be used to reduce settlements as well. This was not part of the Thesis and needs to be investigated, as the added weight then contributes to the driving moment.

The effectiveness of the lateral expansion, the largest contributor to the FoS, can be determined by the coefficient of lateral earth pressure ( $K$ ), of which the full potential is achieved if there is a clear increasing trend of  $K$  close to the columns. Scatter of  $K$  indicates physical failure of soil elements from which no strength can be derived, which is the case for the reference design. The sensitivity analysis gives directions in order to design stabilisation columns more efficiently in this respect. Adjusting the column diameter is the most effective way to achieve this. The columns should be long enough in order to force the slip surface down and thereby increasing the FoS. Due to the expansion lateral stresses can be 1-3 times higher than the vertical stresses. It is recommended to perform field tests, to assess whether the changes in stress fields occur in reality as well. Overall, this study shows that stabilisation columns have a good potential for improving inner slope stability of dikes.

## TABLE OF CONTENTS

|  |    |
|--|----|
| PREFACE  | IV |
| SUMMARY  | VI |
| SYMBOLS AND DEFINITIONS                              | IX |
| 1. INTRODUCTION                                      | 1  |
| 1.1 Macro-instability                                | 1  |
| 1.2 Stabilisation columns                            | 2  |
| 1.3 Research gap                                     | 2  |
| 1.4 Objective  | 3  |
| 1.5 Relevance  | 3  |
| 1.6 Approach and Thesis outline                      | 3  |
| 2. THEORETICAL BACKGROUND                            | 5  |
| 2.1 Slope stability                                  | 5  |
| 2.1.1 Stability assessment models                    | 6  |
| 2.1.2 Shear strength                                 | 7  |
| 2.2 Effects of stabilisation columns                 | 9  |
| 2.2.1 Increase in weight                             | 9  |
| 2.2.2 Increase in strength                           | 10 |
| 2.2.3 Lateral expansion                              | 10 |
| 2.2.4 Other effects                                  | 14 |
| 2.3 Modelling the effects of stabilisation columns   | 15 |
| 2.3.1 Modelling techniques                           | 15 |
| 2.3.2 Modelling lateral expansion                    | 18 |
| 3. CASE STUDY  | 20 |
| 3.1 Reference dike design                            | 20 |
| 3.1.1 Geometry                                       | 20 |
| 3.1.2 Soil parameters                                | 20 |
| 3.1.3 Phreatic surface and potential lines           | 21 |
| 3.1.4 Calculated factor of safety                    | 21 |
| 3.2 Reference dike improved by stabilisation columns | 24 |
| 3.2.1 Soil Homogenisation                            | 24 |
| 3.2.2 Plane Strain; width reduction                  | 25 |
| 3.2.3 Plane Strain; strength reduction               | 27 |



|                                       |           |
|---------------------------------------|-----------|
| <b>4. RESULTS</b>                     | <b>28</b> |
| <b>4.1 Increase in weight</b>         | <b>28</b> |
| <b>4.2 Increase in strength</b>       | <b>30</b> |
| <b>4.3 Lateral expansion</b>          | <b>31</b> |
| <b>4.4 Sensitivity analysis</b>       | <b>35</b> |
| 4.4.1 Classical berm solution         | 35        |
| 4.4.2 Weight                          | 36        |
| 4.4.3 Lateral expansion               | 38        |
| 4.4.4 Geometric properties            | 41        |
| 4.4.5 Soil stiffness                  | 43        |
| 4.4.6 Groundwater                     | 44        |
| 4.4.7 Conclusion                      | 45        |
| <b>5. DISCUSSION</b>                  | <b>46</b> |
| <b>5.1 Results</b>                    | <b>46</b> |
| <b>5.2 Design considerations</b>      | <b>47</b> |
| 5.2.1 Geometry                        | 47        |
| 5.2.2 Modelling stabilisation columns | 47        |
| 5.2.3 Modelling lateral expansion     | 48        |
| <b>6. CONCLUSION</b>                  | <b>50</b> |
| <b>6.1 Recommendations</b>            | <b>52</b> |
| <b>7. LITERATURE</b>                  | <b>54</b> |
| <b>APPENDICES</b>                     | <b>56</b> |
| <b>A.1 Plaxis</b>                     | <b>1</b>  |
| A.1.1 Hardening Soil model            | 1         |
| A.1.2 Soft Soil Creep model           | 2         |
| A.1.3 SHANSEP NGI-ADP                 | 3         |
| <b>A.2 D-Stability (2019)</b>         | <b>5</b>  |
| <b>B.1 Green dike layout</b>          | <b>7</b>  |
| <b>B.2 Soil parameters</b>            | <b>8</b>  |

# Symbols and definitions

## Abbreviations

|         |  |
|---------|--|
| FoS     | Factor of Safety   |
| HS      | Hardening Soil model   |
| PSs     | Plane Strain modelling method with effective strength parameters |
| PSw     | Plane Strain modelling method with effective width               |
| SC      | Stabilisation columns  |
| SH      | Soil Homogenisation modelling method                             |
| SHANSEP | Stress History And Normalised Soil Engineering Properties        |
| SSC     | Soft Soil Creep model  |

## Symbols

|                  |                                       |                      |
|------------------|---------------------------------------|----------------------|
| A                | Area                                  | [m <sup>2</sup> ]    |
| c                | Cohesion                              | [kPa]                |
| d                | diameter                              | [m]                  |
| E                | Young's modulus                       | [kPa]                |
| K                | Coefficient of lateral earth pressure | [-]                  |
| m                | Strength increase exponent            | [-]                  |
| OCR              | Over Consolidation Ratio              | [-]                  |
| POP              | Pre Overburden Pressure               | [kN/m <sup>2</sup> ] |
| p'               | Mean effective stress                 | [kN/m <sup>2</sup> ] |
| q                | Deviatoric stress                     | [kN/m <sup>2</sup> ] |
| R                | Plastic radius                        | [m]                  |
| s                | Inter column spacing                  | [m]                  |
| S                | Undrained shear strength ratio        | [-]                  |
| s <sub>u</sub>   | Undrained shear strength              | [kPa]                |
| ε                | Strain                                | [-]                  |
| φ                | Friction angle                        | [°]                  |
| τ                | Shear stress                          | [kPa]                |
| σ'               | Effective stress                      | [kN/m <sup>2</sup> ] |
| φ <sub>z,g</sub> | the limit potential                   | [m±NAP]              |
| γ                | Volumetric weight                     | [kN/m <sup>3</sup> ] |

## Subscripts

|         |                         |
|---------|-------------------------|
| 0       | Initial/ at rest        |
| c       | Column                  |
| n       | normal                  |
| p       | Plastic                 |
| r, θ, z | Cylindrical coordinates |
| w       | Effective width         |

# 1. Introduction

About 60% of the Netherlands is prone to flooding, see Figure 1-1. On the one hand due to high river discharges on one of the major rivers, on the other hand due to the fact that a large part of The Netherlands lies below sea level. Most of the Dutch inhabitants are living in these vulnerable areas. As the possibility of flooding can never be ruled out, there is an urge for sufficiently safe flood defences. We need to constantly improve our understanding of flood defences and come up with innovations that can improve flood defences in a smarter and better way. A large part of the Dutch flood defences are dikes, which are earthen embankments. A distinction has to be made between primary and regional dikes. Where the primary river dikes protect against flooding from the large rivers, sea or lakes, the regional dikes do the same for canals and small rivers. This research focusses on an innovation applied to primary Dutch river dikes with little environmental impact.

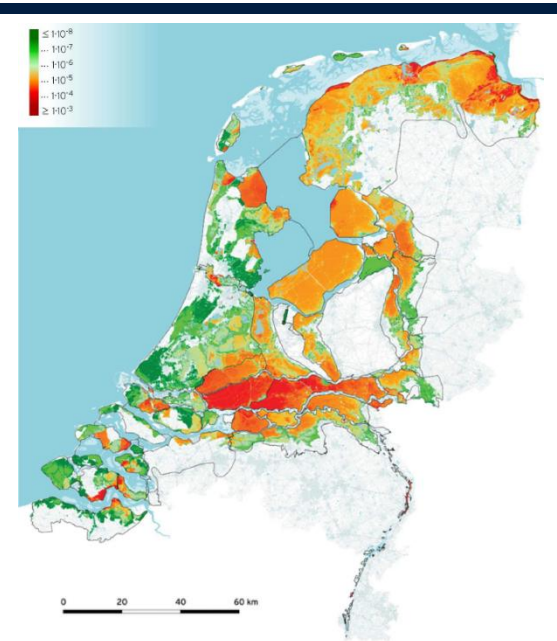


Figure 1-1: Individual risk in The Netherlands in 2015. The individual risk is defined as the annual probability for an imaginary person at a particular place in the protected area to die as a result of flooding in the area. (Vergouwe et al., 2016)

## 1.1 Macro-instability

If dikes fail they lose their primary function, which is preventing flooding of the hinterland. Failing of dikes can occur in various ways, the most important failure mechanisms are shown in Figure 1-2. One of them is sliding of the inner dike slope (panel C in Figure 1-2), known as macro-instability. This thesis focusses on this mechanism.

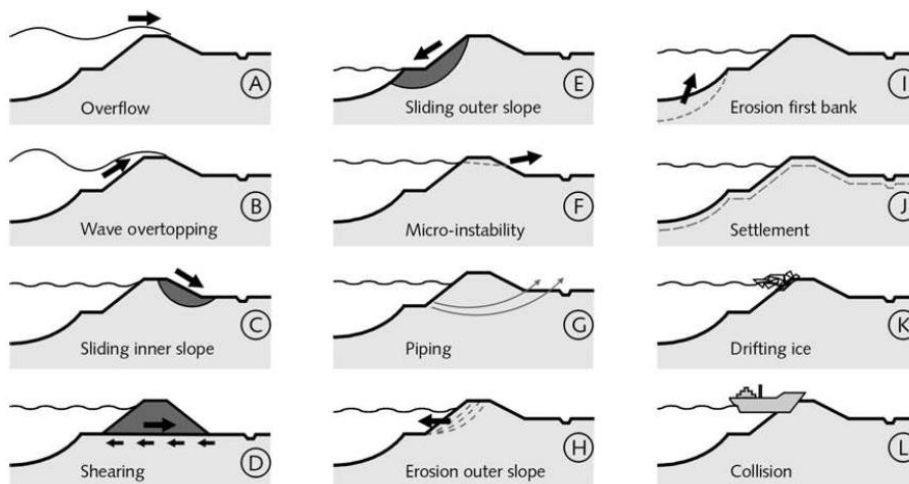


Figure 1-2 List of most important failure modes (Vrijling, Schweckendiek, & Kanning, 2011)

This failure mode is usually caused by an outside (river) water level elevation. Leading to a load increase on the one hand and on the other hand to a decrease in resistance due to an increase of pore water pressures in and beneath the dike. This leads to a decrease of the effective stress and an accompanied decrease of the undrained shear strength. A specific type of macro-instability can occur during uplift conditions. The low lying areas in the Netherlands often consist of soft and low permeable soils like clay and peat on top of a sand layer. Due to high water pressures at the interface

between the permeable sand layer and the low permeable top layers the effective normal stresses decrease to zero, which can cause lifting of the low permeable top layers. As a consequence a deep seated long slip surface of the inward dike face can occur, see Figure 1-2.

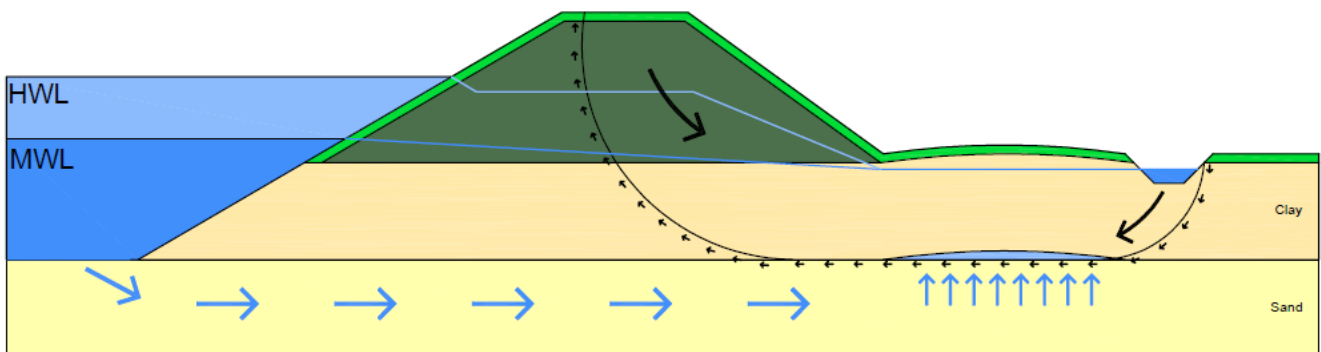


Figure 1-3: Uplift induced failure mechanism. Horizontal blue arrows indicate the flow of water towards the hinterland. The vertical blue arrows indicate the lifting of the low permeable top layer. The small black arrows indicate the shear resistance along the slip surface. HWL = High Water Level, MWL = Mean Water Level. An increasing water level results in an increase in pressure under the low permeable top layer.

Classically, improving inner slope stability was done by either decreasing the dike slope or by constructing a stabilisation berm. Where a well-designed berm works in two ways: “a) it counterbalances the driving momentum of the sliding slope; b) it increases the weight of the top layer to prevent uplift.” (Jonkman, Jorissen, Schweckendiek, & van den Bos, 2018) When there is limited space other solutions, like stability walls, can be applied.

## 1.2 Stabilisation columns

Stabilisation columns (SC) are granular columns, which can be ground displacing or replacing. “These are vertical boreholes in the ground, filled upwards with gravel compacted by means of a vibrator” (Castro, 2017). See Figure 1-4. As SC consist of gravel (or a granular material), material properties as weight and friction angle will be higher than that of the host (soft) soils. By adding granular columns to the host subsoil the strength of the subsoil can significantly increase. It is therefore a ground improvement method. It improves soil properties by 1) an increase in weight 2) an increase in strength and 3) a lateral expansion of the columns.

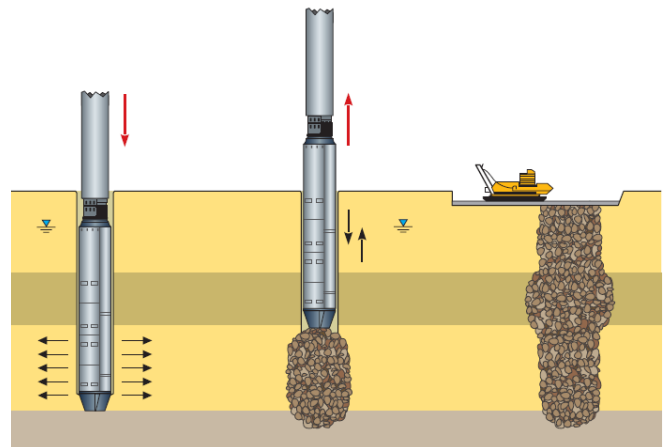


Figure 1-4 Stabilisation Column installation (Keller Group, 2019)

## 1.3 Research gap

Stabilisation columns are readily applied worldwide but mainly in road and rail applications to support embankments and to reduce the accompanying settlements. Numerous studies have been performed on the ground improvement and modelling of stone columns mainly in relationship with settlements. Fewer research has been done on improving slope stability with stone columns. SC are not yet applied in Dutch dikes, because it’s unknown how they will behave under typical Dutch conditions (macro-instability with a deep seated slippage under uplift conditions) and how to meet Dutch regulations for dikes. The 1) increase in weight and 2) increase in strength can be modelled relatively straightforward.

However, no internationally agreed on closed form equations have been derived yet for describing 3) a lateral expansion of stabilisation columns.

According to (Koopmans et al., 2018) stabilisation columns might be a good solution to increase the inner slope stability by adding weight to the resisting moment of the slip surface. Especially in the west of the Netherlands it might be advantageous, because the weight of host clay or peat is usually low. One of the recommendations in this publication is taking the lateral stress increase of the host soil into account.

## 1.4 Objective

The aim of this research is to show the technical potential of applying (floating) granular stabilisation columns to improve the inner slope stability of Dutch dikes under uplift conditions. Floating columns are not founded on a rigid sand layer, but the base of the stabilisation columns is above the sand layer. The stabilisation columns are readily applied worldwide for various applications, however not in Dutch dikes under uplift conditions. This research can be seen as a step towards the application of stabilisation columns in Dutch dikes. The following questions will support this research:

### Research question:

What is the technical potential of using Stabilisation Columns for improving inner slope stability of dikes under uplift conditions in soft soils?

### Sub-questions:

1. What are the effects of stabilisation columns on inner slope stability?
2. How can the effects of stabilisation columns on inner slope stability be modelled?
3. Which aspects are of influence in order to efficiently apply stabilisation columns?

## 1.5 Relevance

Inner slope instability under uplift conditions already is an important mechanism for dikes on soft soils and will become a bigger problem in the near future, due to sea level rise and land subsidence. If a dike doesn't meet the legal safety standards it needs to be reinforced. Traditionally this was achieved by either decreasing the dike slope or by constructing a berm. The traditional measures to stabilise the often very large slip circles are very costly and/or space consuming. The Netherlands are already densely populated and will probably be even more in the future. The available space for dike improvements is therefore limited. So the urge for innovative dike reinforcement methods within the actual dike footprint is rising.

## 1.6 Approach and Thesis outline

In order to answer the research question the thesis is divided into a three parts, namely:

### 1. Introduction and theoretical background

In the introduction the problem is defined. The relevance and research questions are provided. The theoretical background includes a description of slope stability and assessing slope stability. It further focusses on the effects of stabilisation columns on the host soil and slope stability as described in literature. The last part of this chapter focusses on modelling of stabilisation columns.

2. Case study

The fictitious reference case is presented, this is a green dike (only soil). Then the dike reinforced with stabilisation columns is provided. The effect of stabilisation columns on the Factor of Safety is given for various modelling techniques and column configurations. A classical berm solution is presented as well.

3. Discussion, conclusions and recommendations

The results of the research are discussed, as well as the assumptions and limitations. The conclusion will answer the research questions based on the results from the case study. Finally, recommendations for further research and application of stabilisation columns in engineering practice are provided.

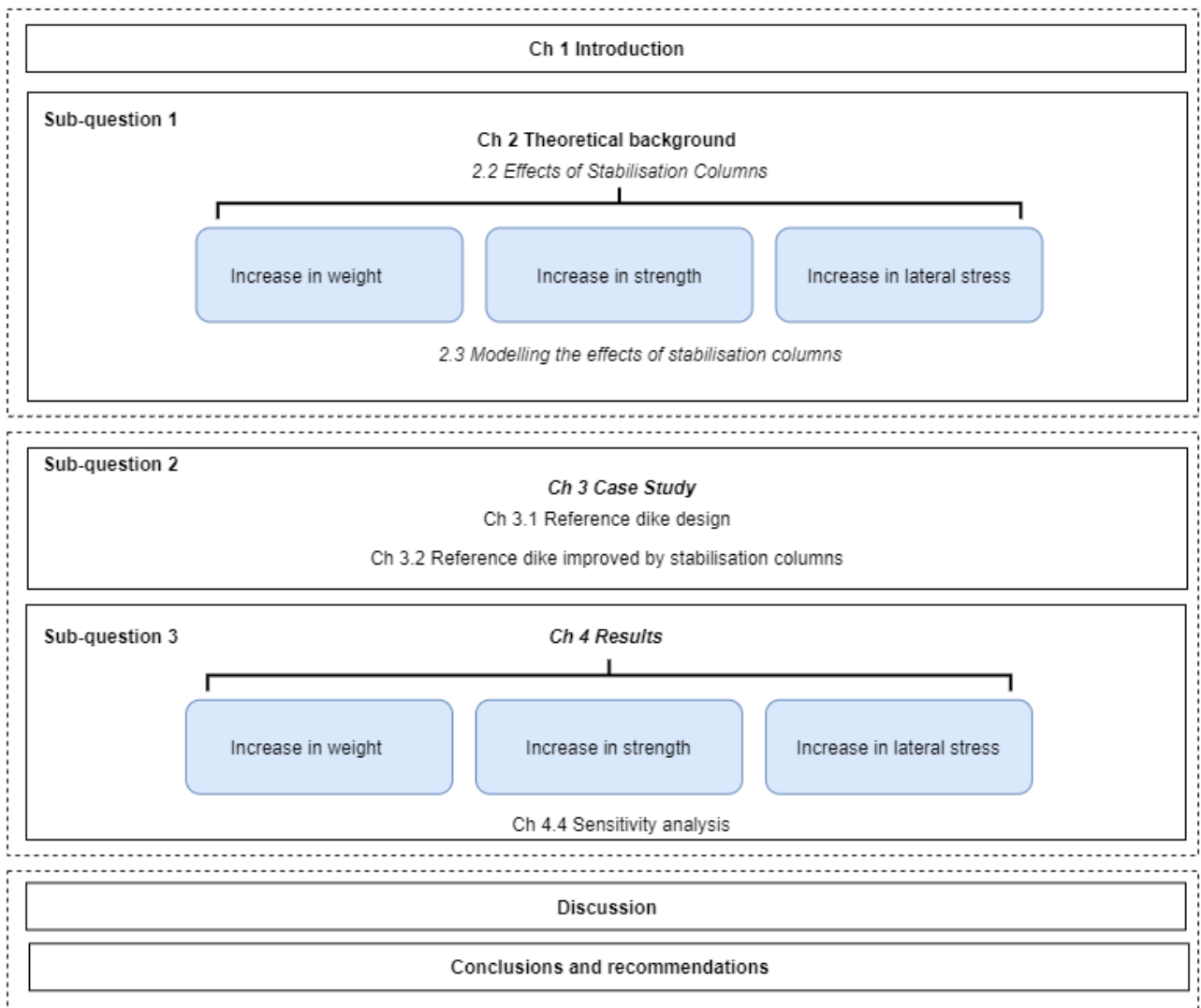


Figure 1-5 - Thesis outline

## 2. Theoretical background

To understand in which way stabilisation columns might improve the inner slope stability, the current Dutch engineering practice to assess inner slope stability is described first. Subsequently the effects that can lead to this improvement are described. This chapter concludes with the modelling options of stabilisation columns and these effects.

### 2.1 Slope stability

When designing or assessing dikes the inner slope instability needs to be checked. The failure mechanism is known as macro-instability. This is the case when large parts of a soil mass slide along straight or curved slip surfaces, see Figure 2-1. The safety of a dike for macro-stability is defined by means of the Factor of Safety (FoS). Generally spoken the FoS is the ratio between the resistance (R) and the load (S). In the case of stability this means the ratio between a driving moment ( $M_d$ ) and a resisting moment ( $M_r$ ), see (eq. 2.1). When a circular slip surface is assumed, the driving moment is the product of the weight of the active soil mass ( $F_{z,actief}$ ) and the arm ( $R_{actief}$ ). The resisting moment is defined as the sum of 1) the product of the weight of the passive soil mass ( $F_{z,passief}$ ) and the arm ( $R_{passief}$ ) and 2) the product of the shear force along the slip surface and the circle radius ('t Hart, 2018), see Figure 2-2.



Figure 2-1 : Inner slope instability (Zwanenburg, van Duinen, & Rozing, 2013)

$$FoS = \frac{R}{S} = \frac{M_r}{M_d} \quad (\text{eq. 2.1})$$

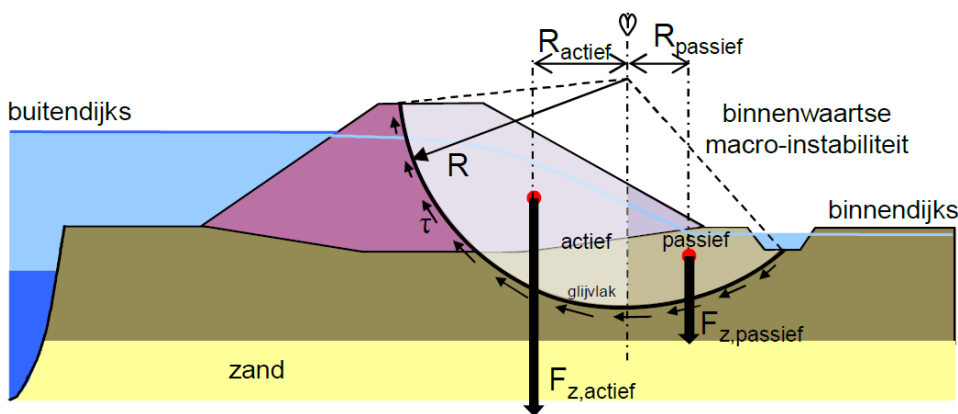


Figure 2-2: Equilibrium for macro-(in)stability of the inner slope. ('t Hart, 2018)

This failure mechanism assumes the loss of equilibrium due to a high water situation is. Water infiltrates into the dike body and its foundation. On the one hand the load increases on the other hand this results in an increase of pore water pressures in and beneath the dike. Leading to a decrease of the effective stress and a decrease of the shear resistance of the soil. Ultimately this can lead to failure of the inner slope.

### 2.1.1 Stability assessment models

To assess slope stability, in other words to calculate the Factor of Safety, various models are available. The first model is the Uplift-Van model. This is a Limited Equilibrium Method (LEM), which is implemented in D-Stability (see Appendix A). The second one is a Finite Element Method which is implemented in PLAXIS (see Appendix A).

#### Uplift-Van

A specific type of macro-instability can occur during uplift conditions. Due to high water pressures at the interface between the permeable sand layer (aquifer) and the low permeable top layers (aquitard), the effective normal stresses decreases to zero, which can cause lifting of the low permeable top layers. As a consequence a deep seated long slippage of the inward dike face can occur, see Figure 2-3.

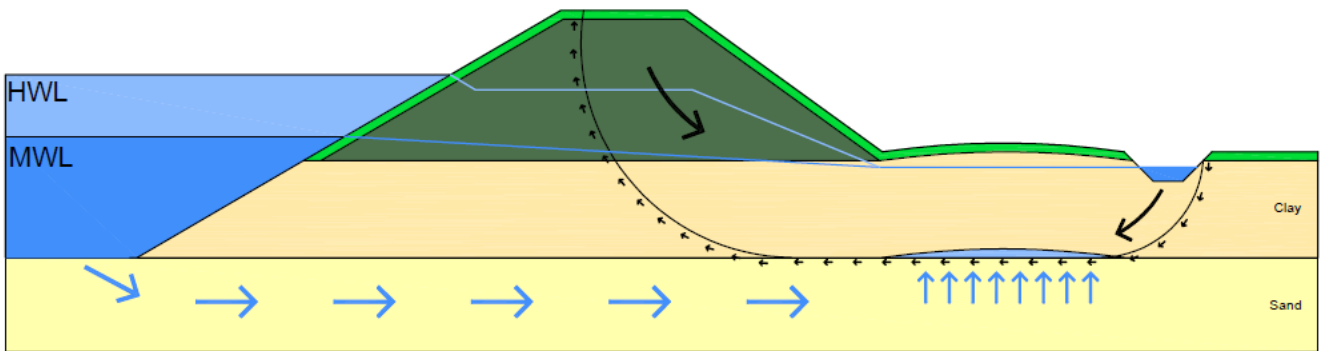


Figure 2-3: Uplift induced failure mechanism. Horizontal blue arrows indicate the flow of water towards the hinterland. The vertical blue arrows indicate the lifting of the low permeable top layer. The small black arrows indicate the shear resistance along the slip surface. HWL = High Water Level, MWL = Mean Water Level. An increasing water level results in an increase in pressure under the low permeable top layer.

The method that is used to describe this process is called the Uplift-Van method. Besides the driving moment (left circular part in Figure 2-4) and the resisting moment (right circular part) there is a horizontal bar (with length  $L$  in Figure 2-4). "This model is similar to the Bishop's model (see Appendix A), but it allows for a non-circular slip circle and can accommodate uplift conditions, which typically occur when a thin blanket layer is located on top of an aquifer connected to the outside water" (Simanjuntak, Goeman, Koning, & Haasnoot, 2018). If  $L$  approaches zero, the slip surface equals the Bishop slip surface. The Factor of Safety is again defined as the ratio of the resisting moment to the driving moment (Simanjuntak et al., 2018).

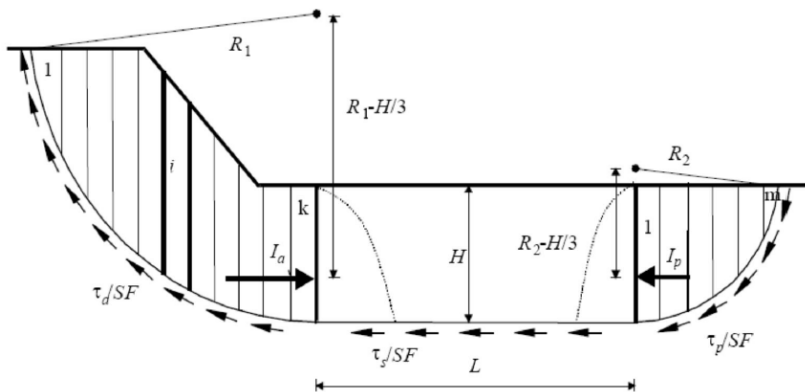


Figure 2-4: Uplift-Van method (Zwanenburg et al., 2013)



### **Critical head**

If there is a relatively thin impervious (clay/peat) top layer on top of a much more permeable sand layer that may be in direct contact with the water pressure in the river (Figure 2-3), the weight of the impervious layer may be insufficient to prevent buoyancy of the soil according to (Bakker & Vrijling, 2013) The head in the sand layer which is just in equilibrium with the weight of the impervious top layer is called the limit potential. If this limit potential is exceeded, bursting or lifting of the top layer might occur. The limit potential for a saturated soil is defined as given in (eq. 2.2) by (Zwanenburg et al., 2013):

$$\phi_{z,g} = h_p + d \frac{\gamma_{wet} - \gamma_w}{\gamma_w} \quad (\text{eq. 2.2})$$

|                |  |
|----------------|--|
| $\phi_{z,g}$   | the limit potential [m±NAP]                                    |
| $h_p$          | the phreatic level in the impervious layer [m±NAP]             |
| $d$            | toplayer thickness [m]   |
| $\gamma_{wet}$ | volumetric weight of impervious top layer [kN/m <sup>3</sup> ] |
| $\gamma_w$     | volumetric weight water [kN/m <sup>3</sup> ]                   |

### **Finite Element Method**

Another possibility to assess slope stability is using PLAXIS (see Appendix A). PLAXIS is a software program in which Finite Element calculations can be performed. Various soil models are implemented to simulate the soil behaviour. In contradiction to the Uplift-Van method, where the shape of the slip surface is predefined, the shape of the slip surface is not bounded for a finite element calculation, but is free.

#### **2.1.2 Shear strength**

The resistance to sliding can be expressed in terms of the shear strength of the soil. The shear strength is amongst others dependent on the type of soil. Besides that it is heavily dependent on how fast the effective stresses react to changes in the stress fields. For every situation it needs to be considered whether an expected failure occurs fast or slow with respect to the consolidation period of the soil (Zwanenburg et al., 2013). If sliding of the inner slope is fast undrained behaviour will occur, resulting in excess- or under pore water pressures along the slip surface. These pore water pressures will definitely influence the effective stresses and thereby the shear strength. Two ways to describe the shear strength are presented here:

#### **Drained shear strength**

We model drained behaviour if the excess pore pressures caused by deformations are small with respect to the ability of the soil to *drain* these pore pressures (Zwanenburg et al., 2013). The draining capacity is of course dependent on the permeability of the soils and the loading speed. A drained response is therefore expected for high permeable soils as sand and gravel.

A commonly used shear strength model to describe the drained shear strength is the well-known material model Mohr-Coulomb. Which assumes a linear relationship between shear strength on a plane and the normal stress acting on it. The soil strength is described by three parameters: the friction angle ( $\varphi$ ), the dilatancy angle ( $\psi$ ) and the cohesion ( $c$ ). The formula defined by Coulomb for  $\varphi = \psi$  is given in (Verruijt, 2001), see eq. 2.3 and the right panel of Figure 2-5. For clay and peat the dilatancy angle is 0 (WBI2017, 2016), the equation for shear stress is defined as given in eq. 2.4.

$$\tau = \sigma'_n \cdot \tan \varphi + c \quad \text{for } \varphi = \psi \quad (\text{eq. 2.3})$$

$$\tau = c \cdot \cos \varphi + \sigma'_n \cdot \sin \varphi \quad \text{for } \psi = 0 \quad (\text{eq. 2.4})$$

|             |                         |       |
|-------------|-------------------------|-------|
| $\tau$      | Shear stress            | [kPa] |
| $\sigma'_n$ | Normal effective stress | [kPa] |
| $\varphi$   | Friction angle          | [°]   |
| $c$         | Cohesion                | [kPa] |

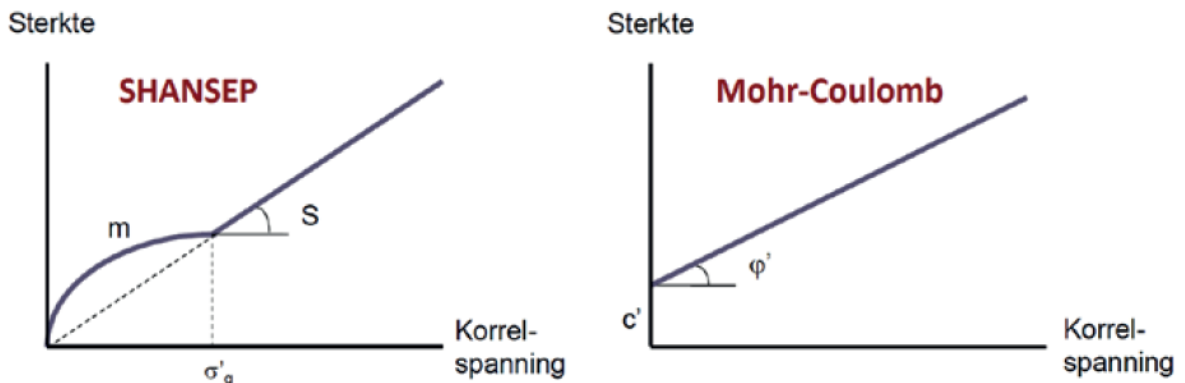


Figure 2-5: Strength curve as a function of the stress for the SHANSEP-model and the MC-model (Koopmans et al., 2018) (Dutch: Korrelspanning -> English: stress; Dutch: Sterkte -> English: Strength)

### Undrained shear strength

Undrained behaviour is modelled if the excess pore pressures caused by deformations are large with respect to the ability of the soil to *drain* these pore pressures. In this case the excess pore pressures cannot drain away quick enough (Zwanenburg et al., 2013). This is typically the case for low permeable soils as clay and peat.

Since 2017 new regulations to assess macro stability are applicable, these are described in the Wettelijk Beoordelings Instrumentarium (WBI). The (WBI) prescribes using the Critical State Shear Strength. This is defined as the strength reached at large shear strain at which the plastic volume change and the pore pressure change equals zero. In case of highwater conditions using undrained shear strength for clay and peat by the SHANSEP (Stress History And Normalized Soil Engineering Properties) model is prescribed (POVM Rekentechnieken – EEM toepassing binnen het ontwerp, 2018). The SHANSEP model describes the undrained shear strength as given in eq. 2.5 and Figure 2-5.

$$s_u = S \cdot \sigma'_{v/p} \cdot (OCR)^m \quad \text{with } OCR = \max\left(\frac{\sigma'_{v/p y}}{\sigma'_{v/p}}, 1\right) \quad (\text{eq. 2.5})$$

|                   |  |       |
|-------------------|--|-------|
| $s_u$             | Undrained shear strength                     | [kPa] |
| $S$               | Undrained shear strength ratio               | [-]   |
| $\sigma'_{v/p}$   | Vertical or principal effective stress       | [kPa] |
| $\sigma'_{v/p y}$ | Vertical or principal effective yield stress | [kPa] |
| OCR               | Over Consolidation Ratio                     | [-]   |
| $m$               | Strength increase exponent                   | [-]   |

## 2.2 Effects of stabilisation columns

According to (Castro, 2017) stabilisation columns are defined as follows: "These are vertical boreholes in the ground, filled upwards with gravel compacted by means of a vibrator." According to (Gaber, Kasa, Abdul-Rahman, & Alsharaf, 2018): "Stone columns improve soft soils due to: (i) The inclusion of a firmer column material such as crushed stones in the soft soil; (ii) the densification of the surrounding soft soil during the installation of stone columns (Choobbasti et al., 2011)." A graphical representation of this process is shown in Figure 1-2.

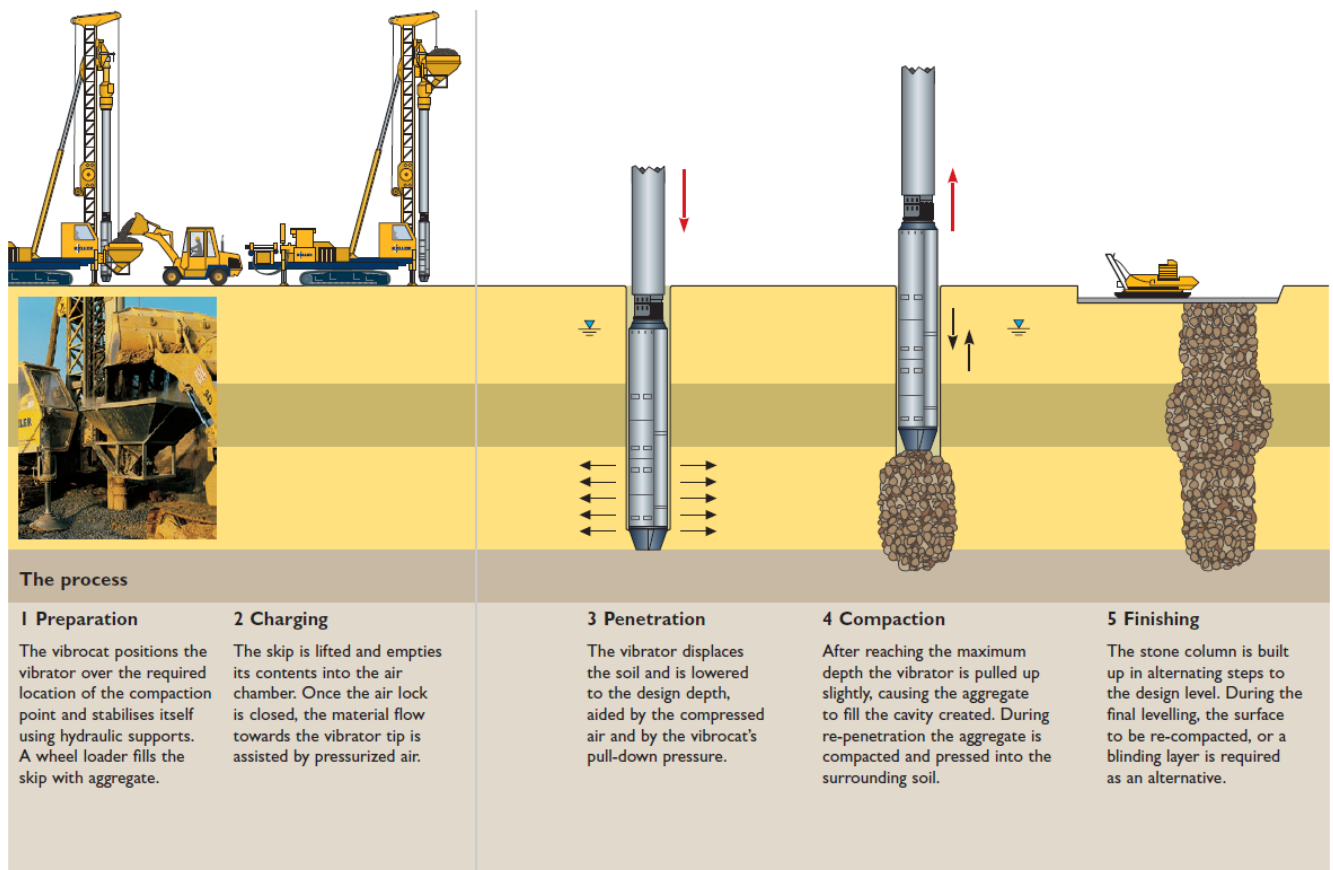


Figure 2-6 Description of the Stabilisation Columns (Keller Group, 2019)

### 2.2.1 Increase in weight

The first effect of installing stabilisation columns in soft soils is an increase in weight. As can be seen in Figure 2-6 the host soil is displaced and the cavity created is filled with an aggregate. The most used aggregate materials are sand and gravel. As can be seen in Table 2-1 these aggregate materials generally weigh (significantly) more than the soft soils (clay and peat). In this way applying stabilisation columns contributes in the same manner to inner slope stability as the classical solution to improve inner slope stability by a berm as a weight solution that stabilises the dike and prevents lifting of the low permeable top layers.

Table 2-1: Common weight properties of various soils (NEN, 2017)

| Material | $\gamma_{sat}$ [kN/m <sup>3</sup> ] |
|----------|-------------------------------------|
| Gravel   | 19-22.5                             |
| Sand     | 19-22                               |
| Clay     | 13-20                               |
| Peat     | 10-12                               |

### 2.2.2 Increase in strength

As stated before the soft soil improves by inclusion of a stronger column material. This strength is amongst others dependent on the friction angle. The friction angle of the material in the stabilisation columns is higher than that of the host soil. So, the average friction angle of the improved soil mass increases. According to (Castro, 2017): "The friction angle of the columns ( $\phi_c$ ) has a notable influence on the results of a stone column treatment. Its value decreases with the confining pressure ( $\sigma_c$ )." A distinction should be made between the effective friction angle and the critical state friction angle ( $\phi_{cv}$ ). Where the friction angle is determined at small strain (2-5%), the critical state friction angle is determined at large strain for non-cohesive soils and soils above the groundwater table. For macro-stability large strains are needed to activate the shear strength along the entire slip plane. These large strains correspond with the critical state. Depending on the design of the stabilisation columns it is questionable whether these large strains will occur. And therefore using small strain friction angles or a strain compatibility method might be useful. Regardless of whether the friction angle is determined at small or large strains, the friction angle of gravel and sand will generally be higher than the friction angle for clay and peat, common values of the effective friction angle are given in Table 2-2. Thus leading to a strength increase of the host soil by means of an increase of friction angle when stabilisation columns are installed.

Table 2-2: Common friction angles for various soils

| Material | $\phi'$ (small strain)[°] |
|----------|---------------------------|
| Gravel   | 30-40*                    |
| Sand     | 30-40*                    |
| Clay     | 15-25*                    |
| Peat     | 15*                       |

\* According to (NEN, 2017)

### 2.2.3 Lateral expansion

When installing stabilisation columns the vibrator displaces the surrounding soil and subsequently the aggregate is compacted and pressed into the surrounding soil, leading to a lateral expansion. This expansion influences the host soil and will lead to 1) a change in horizontal stress and 2) a change in soil stiffness.

#### Influence on lateral stresses

The coefficient of (lateral) earth pressure (K) gives the ratio between the (effective) lateral stress to the vertical (effective) stress (Verruijt, 2001). K is defined for active ( $K_a$ ), passive ( $K_p$ ) and at rest ( $K_0$ ) soil states, as can be seen in eq. 2.6.

$$K_a = \frac{1 - \sin \phi}{1 + \sin \phi} \quad K_p = \frac{1 + \sin \phi}{1 - \sin \phi} \quad K_0 \approx 1 - \sin \phi \quad (\text{eq. 2.6})$$

(Priebe, 1995) assumes the at rest coefficient of earth pressure for stone columns equal to 1 and states that "It has to be considered that with decreasing lateral deformations the coefficient of earth pressure from the columns changes from the active value  $K_a$  to the value at rest  $K_0$ ." For both cases this means an increase in lateral stress for every friction angle.

(Elshazly, Elkasabgy, & Elleboudy, 2007) present values of the post-installation coefficient of lateral earth pressure ( $K^*$ ) of the surrounding soil in the range of 0.4-2.5 based on literature and values of 0.7 – 2 with an average of 1.2 by back analysis. These values can, at best, be used as a guide. Values of  $K^*$

fit in the in the range between the at-rest coefficient ( $K_0$ ) and the ultimate coefficient ( $K_p$ ). The inter column spacing plays a significant role on  $K^*$ , with according to (Elshazly et al., 2007) a “declining trend of  $K^*$  with the increase of inter column spacing.”

(Sexton & McCabe, 2014) consider another definition of  $K$  as given in eq. 2.7, where  $\sigma'_r$  is the radial effective stress and  $\sigma'_\theta$  is the circumferential effective stress (see Figure 2-9). The horizontal stress is the average of both the radial and the circumferential stress.

$$K = (\sigma'_r + \sigma'_\theta) / 2\sigma'_z \quad (\text{eq. 2.7})$$

Since the vertical effective stress ( $\sigma'_z$ ) hardly changes after consolidation it is practical to take  $\sigma'_z = \sigma'_{z0}$ . Which simplifies the radial and circumferential lateral earth pressure coefficients respectively:

$$K_r = \frac{\sigma'_r}{\sigma'_{z0}} \quad K_\theta = \frac{\sigma'_\theta}{\sigma'_{z0}} \quad (\text{eq. 2.8})$$

In Figure 2-7 the ratio of both  $K_r$  and  $K_\theta$  with respect to the initial coefficient of lateral earth pressure ( $K_0$ ) is given. In Figure 2-8 the numerical predicted results for  $K_r/K_0$  are compared with  $K/K_0$  of two field measurements by (Kirsch, 2006). According to (Benmebarek, Abdeldjalil, & Benmebarek, 2018): “Between  $r/d=4$  and  $r/d=10$  the numerical values of  $K_r/K_0$  are very close to the measured values ( $K/K_0$ )”. Close to the column the field measurements are lower than the numerical results. However, the opposite was measured in field tests by (Watts, Johnson, Wood, & Saadi, 2000).

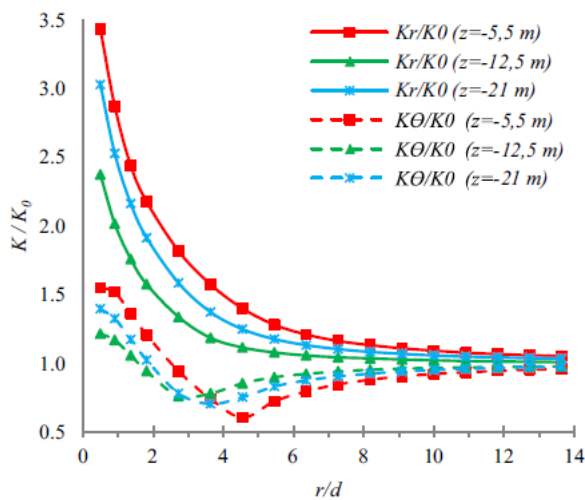


Figure 2-7: Comparison between the two lateral earth coefficients  $K_r/K_0$  and  $K_\theta/K_0$ .  $r/d$  is the normalized radial distance, where  $d$  is the column diameter. (Benmebarek et al., 2018)

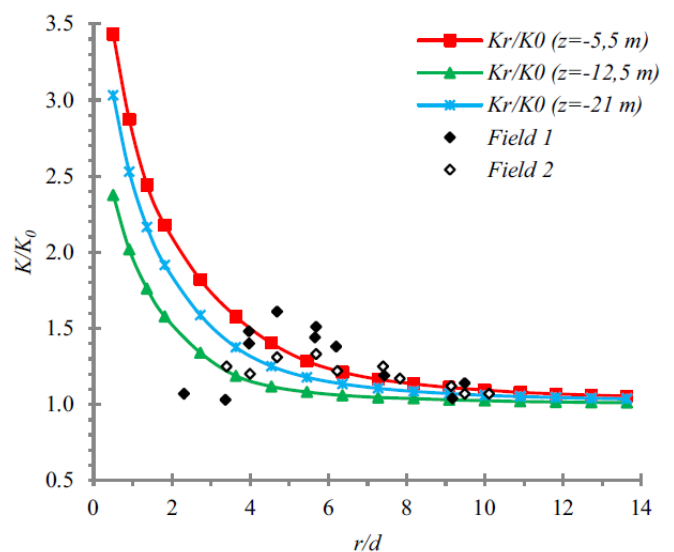


Figure 2-8: Comparison of  $K_r/K_0$  evaluated numerically with  $K/K_0$  of field measurements by (Kirsch, 2006), (Benmebarek et al., 2018).

As can be concluded from (Benmebarek et al., 2018) a good match can be found between a numerical analysis and field measurements. (Sivasithamparam & Castro, 2018) give an analytical solution for the stress state at the elastic/plastic boundary. As can be seen in Figure 2-9 they distinguish various zones

after column installation. The formulas to describe the stress states in various directions at the elastic/plastic boundary are given in eq. 2.9.

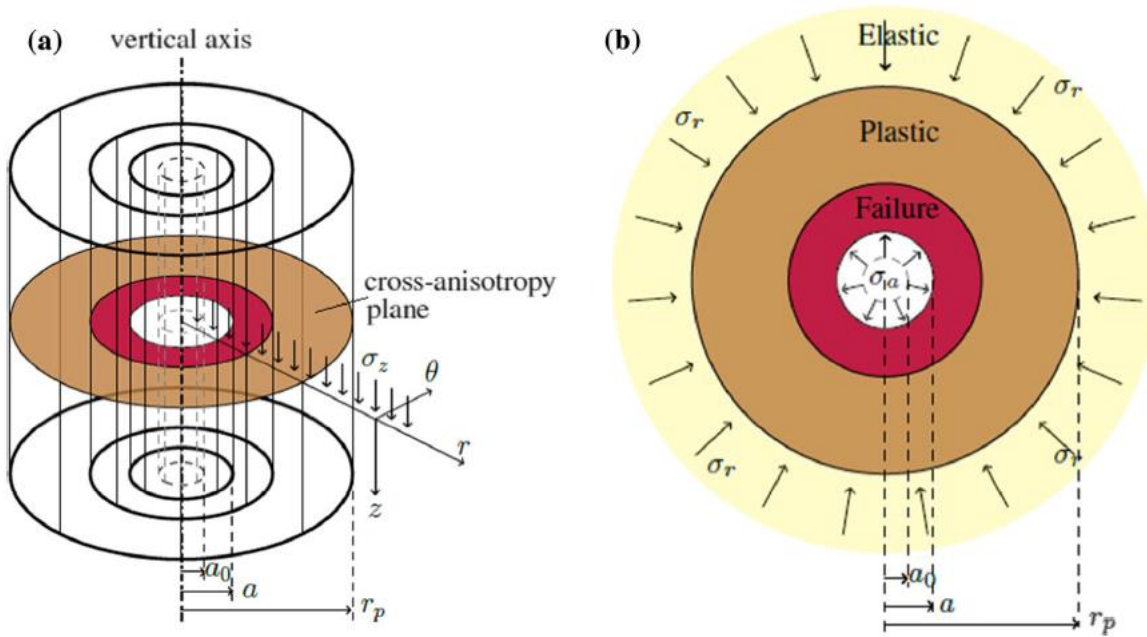


Figure 2-9: Geometry of cylindrical cavity expansion: a cylindrical cavity; b horizontal cross section (Sivasithamparam & Castro, 2018)

$$\begin{aligned} \sigma'_{zp} &= \frac{3}{1 + 2K_0} p'_0 \\ \sigma'_{rp} &= \sigma'_{r0} + \sqrt{\frac{1}{3}(q^2 - (\sigma'_{z0} - K_0\sigma'_{z0})^2)} \\ \sigma'_{\theta p} &= \sigma'_{\theta 0} - \sqrt{\frac{1}{3}(q^2 - (\sigma'_{z0} - K_0\sigma'_{z0})^2)} \end{aligned} \quad (\text{eq. 2.9})$$

#### Symbols

|           |   |
|-----------|---|
| $\sigma'$ | Effective stress                              |
| $p'$      | Mean effective stress                         |
| $q$       | Deviatoric stress                             |
| $K$       | Coefficient of lateral earth pressure at rest |

#### Subscripts

|                |                         |
|----------------|-------------------------|
| 0              | Initial                 |
| p              | Plastic                 |
| $r, \theta, z$ | Cylindrical coordinates |

#### Influence on soil stiffness

The soil stiffness can be expressed as the Young's modulus (E), it is expressed as the ratio between the soil stress and strain along an axis. (Benmebarek et al., 2018) give a relation between the soil stiffness and the effective stress ( $p'$ ):

$$\frac{E}{E_0} = \left( \frac{p'}{p'_0} \right)^m \quad \text{with: } p' = (\sigma'_r + \sigma'_\theta + \sigma'_z) / 3 \quad (\text{eq. 2.10})$$

$\sigma'_r$  is the effective radial stress,  $\sigma'_z$  the effective vertical stress and  $\sigma'_\theta$  the effective circumferential stress. The index "0" refers to the initial state.

Different zones are considered after column installation (Benmebarek et al., 2018):

- Zone 1: The first zone is the plastic zone, where stresses are in a plastic state. This zone can be expressed in terms of the plastic radius (R), since the column is a circle and therefore axial symmetric (Randolph & Wroth, 1979):

$$\frac{a^2}{R^2} = \frac{c_u}{G} \quad (\text{eq. 2.11})$$

|       |                          |                      |
|-------|--------------------------|----------------------|
| a     | Column radius            | [m]                  |
| $c_u$ | Undrained shear strength | [kN/m <sup>2</sup> ] |
| R     | Plastic radius           | [m]                  |
| G     | Shear modulus            | [Pa]                 |

For a cohesive and frictional soil and Mohr-Coulomb behaviour eq. 2.12 can be used to determine the plastic radius (R).

$$\frac{a^2}{R^2} = \frac{(\sigma_{h0} + c \cdot \cot \varphi) \cdot \sin \varphi}{G} \quad (\text{eq. 2.12})$$

|               |                           |       |
|---------------|---------------------------|-------|
| $\sigma_{h0}$ | Initial horizontal stress | [kPa] |
| $\varphi$     | Friction angle            | [°]   |

Directly after column installation the effective stress ( $p'$ ) is expected not to change. The increase in effective radial stress is compensated by the decrease in effective circumferential and effective vertical stress, as can be seen in Figure 2-10(a). After consolidation a significant improvement can be seen, see Figure 2-10(b).

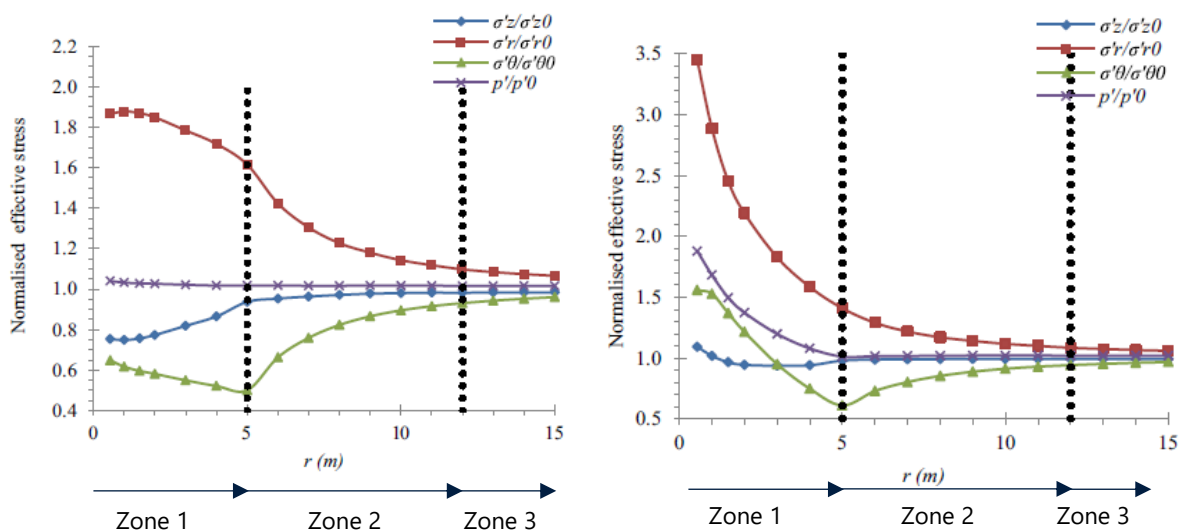


Figure 2-10: Variation of normalised effective stress a) after column installation b) after consolidation (Benmebarek et al., 2018)

(Randolph & Wroth, 1979) assume that the excess pore pressure ( $\Delta u$ ) only occurs in the plastic area. The Finite Element Analysis conducted by (Benmebarek et al., 2018) confirms well to this assumption. (Randolph & Wroth, 1979) proposed the following relation for  $\Delta u$  at each radial distance ( $r$ ) in the plastic zone (zone 1):

$$\Delta u = 2c_u \cdot \ln\left(\frac{R}{r}\right) \quad (\text{eq. 2.13})$$

- Zone 2: The second zone is the elastic zone where stresses are in an elastic state. The numerical analysis performed by (Benmebarek et al., 2018) shows that the effective stress ( $p'$ ) immediately after column installation and after consolidation is practically unchanged, see Figure 2-10. Zone 2 is not clearly defined by a formula but is based on the point where the different stress lines converge in the situation after consolidation, as can be seen in Figure 2-10(b).
- Zone 3: In the third zone stresses return to their initial values, see Figure 2-10.

(Benmebarek et al., 2018) evaluated the change in soil stiffness by a numerical analysis for different depths and compared it with field data, see Figure 2-11. The numerical analysis does not fit well to the field data. Close to the column the stiffness increases 1.5 to 1.8 times the original value and returns to this value at a distance of 5 times the column diameter for the numerical analysis. The field data shows points close to the column with a significant reduction of the soil stiffness. Even for a significant improvement it should be noted that this improvement is for soft soils which typically have a low stiffness. An indication for typical values of  $E_{50,ref}$  are given in (CUR, 2003). For clay this value is in the range of 1-7 MPa, so even if the stiffness increases 100% it is still lower than the stiffness of sand, this is in the range of 15-60 MPa.

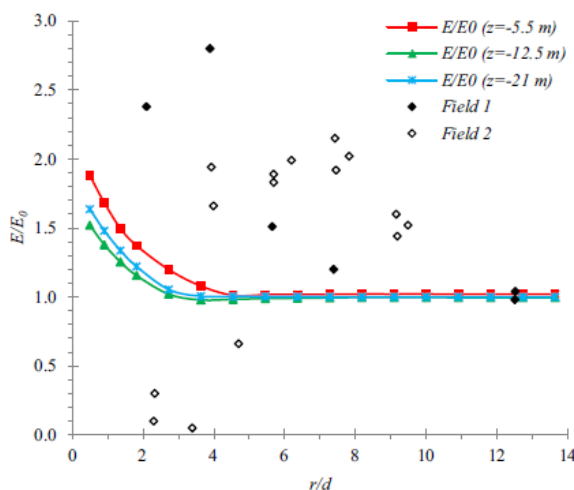


Figure 2-11: Comparison of  $E/E_0$  evaluated numerically and measured in the field by (Kirsch, 2006). (Benmebarek et al., 2018)

### Conclusion on lateral expansion

As stated by (Egan, Scott, & McCabe, 2008): "Where groups of columns are installed interaction of the stress fields from each column occurs in a way that cannot, at present, be described by simple closed form equations." This is supported by the variety of formulas that are presented in this paragraph. Describing the change in lateral stress as presented by (Sexton & McCabe, 2014) and (Benmebarek et al., 2018) seems to give the best results based on field data, but not in the vicinity of the columns. The influence on the soil stiffness doesn't give adequate results, besides that the contribution to slope stability is probably limited as the soil stiffness is still low. Until now the lateral expansion can at best be described by a Finite Element Analysis.

### 2.2.4 Other effects

Multiple studies have been performed on the total (combined) settlement behaviour of floating stone columns under footings. Applying floating columns in high area replacement ratios will significantly reduce settlements according to (Zahmatkesh, 2010). As concluded by (K.S. Ng & Tan, 2015) the



stiffness of the soil ( $E$ ) is the key geotechnical parameter in settlement calculations for floating stone columns under footings. They propose the stiffness parameter to be a constant. Their study was valid for loadings from 0-150 kPa, but only for columns with an optimal length. Based on (Al-Ani & Wanatowski, 2017) the relative settlement reduction is about 45 to 60% for floating columns with a foundation surcharge. And they state that at lower loading levels, the settlement improvement is marginally higher than at higher load levels. However, the relative settlement ratio decreases as the thickness of the soft layer increases.

## 2.3 Modelling the effects of stabilisation columns

Three effects are mentioned in which ways stabilisation columns can possibly contribute to inner slope stability, namely: Weight, Strength and Lateral Expansion.

### 2.3.1 Modelling techniques

Various modelling techniques are available to model stabilisation columns. An overview of these techniques is given by (Castro, 2017) and is shown graphically in Figure 2-12. Method (b) and (d) are not suited for stability analysis, as only one column can be modelled in axisymmetric conditions. The other methods will be explained in this paragraph.

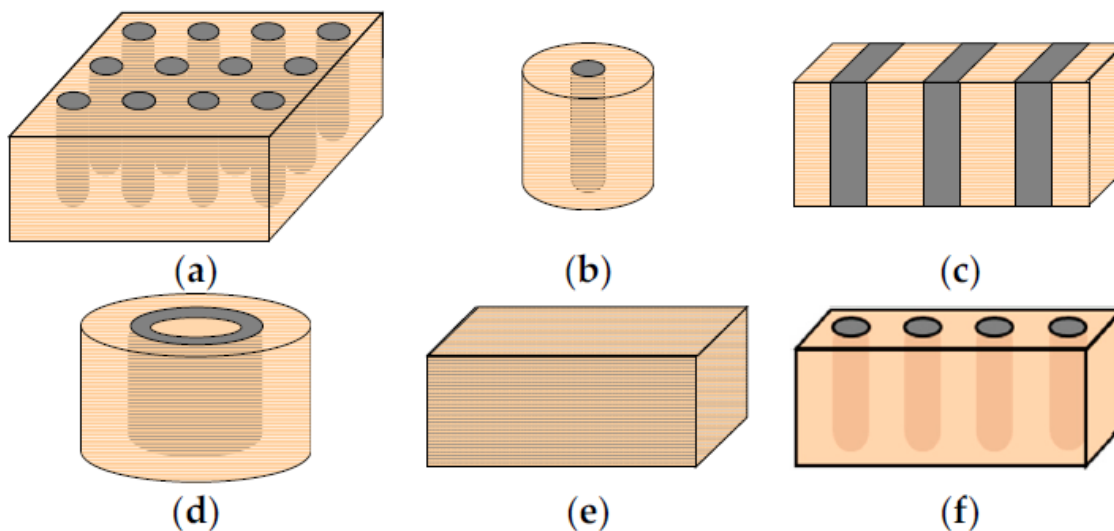


Figure 2-12: Main geometrical models for stone columns studies. (a) Full 3D model; (b) Unit cell; (c) Longitudinal gravel trenches; (d) Cylindrical gravel rings; (e) Equivalent homogenous soil; (f) 3D slice of columns. (Castro, 2017)

### Soil homogenisation

The first modelling technique to translate a 3D situation to a 2D schematization is the Soil Homogenisation technique. Instead of modelling all the columns individually, the columns and the surrounding soil are modelled as a homogenous mass. The soil homogenisation method assumes average soil parameters for stabilisation column improved soil. The improved soil is indicated as a box in Figure 2-13. The average values are expressed by the replacement factor  $a$  as given in eq. 2.14.

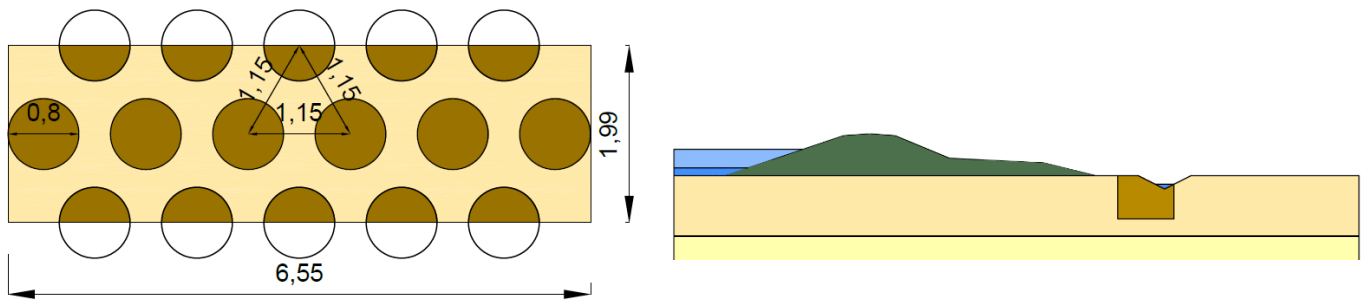


Figure 2-13: Column layout and soil homogenisation, dimensions in [m]

This replacement factor is used to translate material properties into equivalent properties. An example is given for the friction angle in eq. 2.15. In the same manner this can be done for other soil properties.

Table 2-3: Symbol definitions input and an applied example

|                     |   |                   | Example |
|---------------------|---|-------------------|---------|
| $A_{col}$           | Column Area in unit cell                    | [m <sup>2</sup> ] | 5.5     |
| $A_{sol}$           | Area of soil in unit cell                   | [m <sup>2</sup> ] | 7.5     |
| $A$                 | Area of unit cell                           | [m <sup>2</sup> ] | 13      |
| $\varphi'_{column}$ | Effective friction angle of column material | [°]               | 32.5    |
| $\varphi'_{soil}$   | Effective friction angle of host soil       | [°]               | 15      |

$$a_{SH} = A_{col} / (A_{col} + A_{sol}) \quad (\text{eq. 2.14})$$

$$\varphi'_{comb} = \varphi'_{column} a_{SH} + \varphi'_{soil} (1 - a_{SH}) \quad (\text{eq. 2.15})$$

Table 2-4: Output applied example

|                      |  |     | Example |
|----------------------|--|-----|---------|
| $a_{SH}$             | replacement factor for Soil Homogenisation   | [-] | 0.42    |
| $\varphi'_{comb-SH}$ | Effective friction angle Soil Homogenisation | [°] | 22.35   |

### Plane strain modelling; width reduction

The second modelling technique is modelling the stabilisation columns as longitudinal trenches, where the column width is reduced to an equivalent width. Other (strength) properties remain the same. For stone columns installed in a square pattern a relation is given by (Zhang, Han, & Ye, 2013) in eq. 2.16. Where  $d_w$  is an equivalent column width,  $d_c$  the column diameter and  $s$  the column spacing. In a triangular grid each row will have alternatingly  $n$  and  $n-1$  columns, see Figure 2-14.

$$d_w = \frac{d_c^2 \pi}{4s} \quad (\text{eq. 2.16})$$

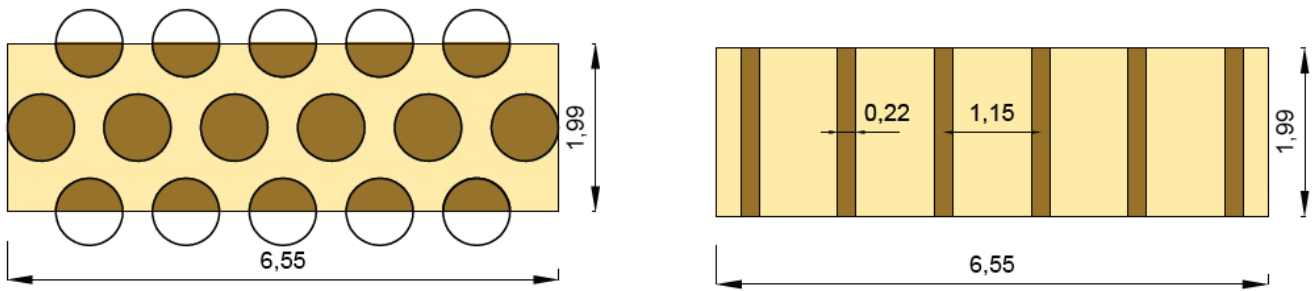


Figure 2-14: Plane Strain Modelling; width reduction technique. [m]

**Plane strain modelling; strength reduction**

The third modelling technique is similar to the second one. Instead of a width reduction material (strength) properties are reduced to equivalent properties. For this method only one row of columns is considered. A graphical representation is given in Figure 2-15. Strength parameters are multiplied with the calculated replacement factor (eq. 2.18) and thereby reduce the strength, for example for the friction angle eq. 2.18.

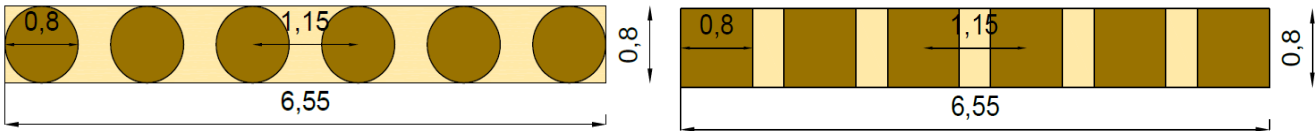


Figure 2-15: Plane Strain Modelling; strength reduction technique. [m]

$$a_{PSS} = A_{col,row} / (A_{col,row} + A_{sol,row}) \tag{eq. 2.17}$$

$$\varphi'_{comb} = \varphi'_{column} a_{PSS} + \varphi'_{soil} (1 - a_{PSS}) \tag{eq. 2.18}$$

Table 2-5: Symbol definitions and an applied example

|               |                                     |                   | Example |
|---------------|-------------------------------------|-------------------|---------|
| $A_{PS}$      | replacement factor for Plane Strain | [-]               | 0.73    |
| $A_{col,row}$ | Column Area in unit cell            | [m <sup>2</sup> ] | 3.84    |
| $A_{sol,row}$ | Area of soil in unit cell           | [m <sup>2</sup> ] | 1.4     |
| A             | Area of unit cell                   | [m <sup>2</sup> ] | 5.24    |

**3D model**

The last modelling technique discussed is a full 3D model. Obviously a 3D model geometrically represents reality the best, because no simplifications or translations from a 3D situation to a 2D model are needed. An example of a 3D model is PLAXIS 3D. When a problem is symmetric it is often sufficient to model only a 3D-slice.

**Conclusion on modelling techniques**

An overview of the various modelling techniques and their suitability to model the various effects is given in Table 2-6.

Table 2-6: Overview of modelling techniques and its suitability

| Modelling technique                  | Stability of Stabilisation Columns |                                 | Model complexity |
|--------------------------------------|------------------------------------|---------------------------------|------------------|
|                                      | No lateral expansion <sup>1)</sup> | Lateral expansion <sup>2)</sup> |                  |
| Weight                               | [1]                                | [4]                             | [1]              |
| 2D Soil Homogenisation               | +                                  | -                               | +++              |
| 2D Plane Strain (Width reduction)    | ++                                 | ++                              | ++               |
| 2D Plane Strain (Strength reduction) | ++                                 | +                               | ++               |
| 3D Full model                        | +++                                | +++                             | +                |

+++ Completely suitable, ++ Moderately suitable, + Slightly suitable, - Not suitable

- 1) From (Castro, 2017)
- 2) The soil homogenisation method cannot simulate cavity expansion of single columns, since a homogenous mass is assumed. The strength reduction method is assumed to be less accurate than the width reduction method. With the strength reduction method large strains will occur. While the cavity behaviour is dependent on the soil properties E and G, as follows from eq. 2.10 and eq. 2.11.
- 3) Modelling a homogenous mass is straightforward. Complexity increases if every column needs to be modelled individually. The time needed for calculations follows this same pattern. However, when the calculations are performed by means of remote scripting, the complexity and calculation time does not really vary for the first three methods.

For studying the effects of an increase in weight and strength the 2D Plane Strain (Strength reduction) method is not suited, the other methods can be used. Using a 3D model to study these effects is very time consuming for these relatively straightforward calculations. So, the 2D Soil Homogenisation and the 2D Plane Strain (Width reduction) are best suited for studying these effects. For studying the effects of a lateral expansion the 2D Plane Strain (width reduction) method is suited. Calculation time is limited, this makes this method suitable for varying various parameters. A final design should be checked by a 3D model or by rules of thumb to exclude the occurrence of soil cutting between the columns.

### 2.3.2 Modelling lateral expansion

As described in Figure 2-6 installing stabilisation columns leads to a lateral displacement of the host soil, leading to a change in soil state. Three methods to account for this behaviour are explained in this paragraph.

#### Back analysis

The first method to account for changes in soil state is by back analysis. According to (Hurley, Nuth, & Karray, 2015) this can be done by varying the lateral to vertical stress ratio (K) to obtain the field test behaviour. In this way the stress field can be represented well, but the effects are not known a priori.

#### Line displacement

“Some authors impose a uniform lateral displacement equal to the final stone column average diameter using a axisymmetric model in 2D.” as stated by (Hurley et al., 2015). This easy to use method is only suited for axisymmetric models. An example of using a line displacement is given in Figure 2-16.

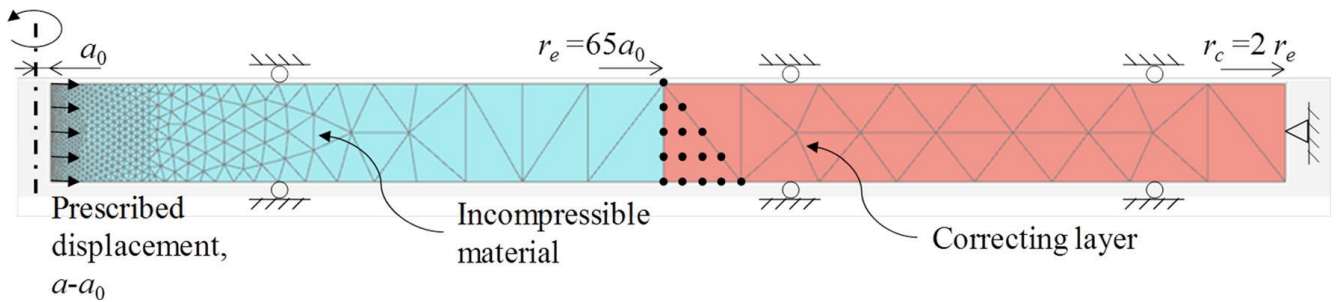


Figure 2-16: Finite element model for cylindrical cavity expansion by a line displacement (Sivasithamparam & Castro, 2018)

### Volumetric strain

The third option that is suggested by (Egan et al., 2008) is applying a volumetric strain to the stabilisation columns. This option can be used in PLAXIS 2D and PLAXIS 3D and can be applied in various directions, see Figure 2-17. To simulate lateral expansion, the volumetric strain in x-direction ( $\epsilon_{xx}$ ) should be modified, a positive value represents an expansion. The updated mesh option should be selected as well to allow large strains. (Egan et al., 2008) state that the amount of radial strain that is applied in the model is a key issue in the modelling of cavity expansion to replicate field conditions. Modelling a stabilisation column as indicated in Figure 2-6 would actually mean expanding an infinite thin line to full column width. This is not possible from a theoretical point of view, since this would mean infinite strain. It's also practically not feasible to have very large strains in PLAXIS. Therefore a decent initial column radius is needed that represents the actual column expansion. (Kok Shien Ng, 2013) and (Sivasithamparam & Castro, 2018) state that doubling the initial radius is able to give adequate approximations to simulate field conditions. For studying the effects of stabilisation columns on the behaviour of a soft clay (Foray, Flavigny, Nguyen, Lambert & Briançon, 2009) used lateral expansion between 5-15% volumetric strain in PLAXIS 3D.

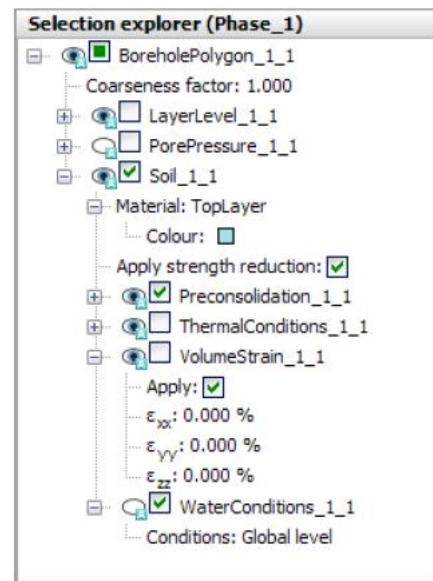


Figure 2-17 Volumetric strain in the selection explorer (Brinkgreve, Zampich, & Ragi Manoj, 2019)

As stated by (Castro & Karstunen, 2010) using a prescribed line displacement is preferred from a numerical stability point of view. To minimise the chance of numerical errors due to volumetric expansion in PLAXIS, the numerical input parameter *max load fraction per step* can be lowered. This results in longer calculation times. The default value is 0.5, which means that the applied load will be solved in at least  $1/0.5=2$  steps according to (Brinkgreve et al., 2019). They even state that: "The user might want to use small values in order to observe the kinetics of the deformation process."

### Conclusion

A dike cannot be described by an axi-symmetric model and there is no field data available. Therefore using volumetric strain to describe the lateral expansion is the best option. The definition of the initial radius by (Kok Shien Ng, 2013) gives most confidence, as he fitted results of analytical solutions, PLAXIS calculations and field data with focus on the lateral expansion behaviour of stabilisation column installation effect.

### 3. Case study

In this chapter a reference dike design is presented. This case will be used to quantify the three effects (weight, strength and lateral expansion) that are caused by stabilisation columns.

#### 3.1 Reference dike design

As stated in the main research question, the technical potential of applying stabilisation columns needs to be investigated. Technical potential can only be shown with respect to a reference case. This reference case is an unimproved dike with a Factor of Safety (FoS) deficit of 20%. The reference case is presented in this paragraph.

##### 3.1.1 Geometry

The geometry of the reference dike is given in Figure 3-1, an enlarged figure is given in Appendix B.1. The dike and the berm consist of dike material. The underlying soil is a soft clay blanket with a thickness of seven meters. Underneath the clay blanket there is a firm Pleistocene sand layer. Next to the berm there is a five meters wide maintenance strip, followed by a 1.5 meters deep ditch. The water depth in the ditch is 0.5 m.

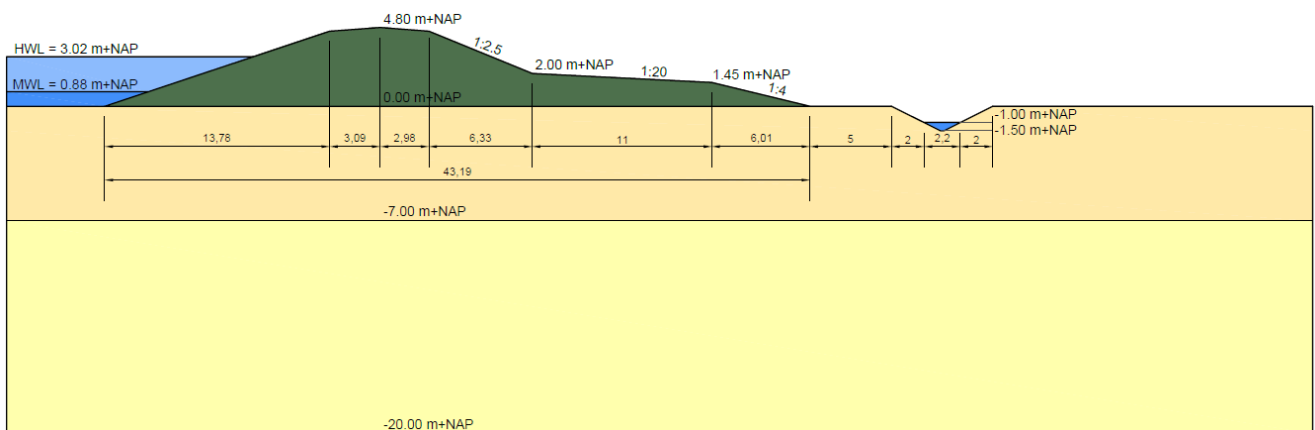


Figure 3-1: Geometry reference dike

##### 3.1.2 Soil parameters

The calculation workflow is as it is prescribed by (POVM, 2018), also known as PPE (POVM Publication EEM). Sand is modelled with drained parameters. To represent this drained behaviour, this will be modelled by applying the Hardening Soil (HS) model in PLAXIS and the C-phi model with dilatancy in D-Stability. According to (POVM, 2018), during the first calculation phases drained conditions should be assumed for clay, peat and sand. For the drained behaviour of low permeable materials as clay and peat the Soft Soil Creep (SSC) model is applied. The Critical State friction angle is of importance for macro stability. Large strains are needed to mobilize the shear strength of the soil along the entire slip surface. For both models (SSC and HS) the Critical State friction angle  $\phi_{cs}$  is applied (WBI2017, 2016). For undrained behaviour the SHANSEP model is applied for clay and dike material.

Relevant soil parameters are given in Table 3-1. These parameters are determined in laboratorial tests by Deltares and are retrieved from (POVM, 2018).

Table 3-1: Soil parameters

| Soil type                   | $\gamma_{unsat}$<br>[kN/m <sup>3</sup> ] | $\gamma_{sat}$<br>[kN/m <sup>3</sup> ] | $c^{1)}$<br>[kN/m <sup>2</sup> ] | $\phi'$<br>[°] | S<br>[-] | m    | POP <sup>2)</sup><br>[kN/m <sup>2</sup> ] |
|-----------------------------|--|--|----------------------------------|----------------|----------|------|---|
| Clay Gorkum light (organic) | 11.86                                    | 11.86                                  | 1                                | 31.2           | 0.25     | 0.76 | 15  |
| Dike material               | 18.45                                    | 18.45                                  | 2                                | 27.2           | 0.25     | 0.76 | 7   |
| Sand Pleistocene            | 18.00                                    | 20.00                                  | 0.1                              | 32.5           | -        | 0.5  | -   |

- 1) To prevent numerical calculation errors, in theory it should be zero in critical state conditions.
- 2) The Pre-Overburden Pressure (POP) is assumed to be the values mentioned.

### 3.1.3 Phreatic surface and potential lines

The piezometric head in the hinterland during a daily outside water level in PLAXIS is NAP-0.3m. This is little higher than typical values (NAP-1m - NAP-0.5m) for the western parts of the Netherlands. In PLAXIS 2D uplift conditions occur if the vertical effective stress at the separation of the clay top layer and the sand sublayer is positive. A value between -1 and 0 kN/m<sup>2</sup> is needed for a stable calculation close to uplift conditions, a negative value means a stress increase in PLAXIS. The limit potential for which this is the case during a high outside water level is NAP+0.77m.

### 3.1.4 Calculated factor of safety

The reference dike as described before is modelled in PLAXIS 2D (FEM) and D-Stability (LEM). PLAXIS 2D calculates a Factor of Safety (FoS) of 0.989, see Figure 3-2 and Figure 3-3. This is the reference FoS, the FoS of the improved dike should thus at least be 1.19 ( $\approx 0.989 \cdot 1.2$ ). D-Stability calculates a FoS of 0.912 when using the Uplift-Van model, see Figure 3-4. This is a 8.5% difference. According to (POVM, 2018) the calculated FoS between both models should be within a 6% range and the slip surface should match. The latter is the case, but the FoS does not match. To verify the outcome of the Uplift-Van calculation, the Factor of Safety has also been calculated by means of the Spencer method. The outcome of the Spencer and Uplift-Van methods are compared by means of the Net FoS (Table 3-2), both methods show comparable results.

### Stress distribution

PLAXIS 2D takes soil stress distribution into account. Due to this stress distribution the vertical effective stresses are higher under the ditch than in D-Stability. This has a positive effect on the calculated FoS. In D-Stability this stress distribution is not taken into account. The effective stresses at the interface of the clay and sand layer are 0 and thus lifting of the clay layer occurs. For a vertical line in the middle of the ditch the stresses are replicated as they are present in PLAXIS. This is done by manually filling the ditch and thus adding weight to the ditch. The vertical effective stresses under the ditch increase. In this way a conservative indication of the influence of stress distribution is given, as this is not a fully replicated stress distribution. Including the manual stress distribution leads to a FoS of 0.948. This is within the 6% range compared to PLAXIS.

Table 3-2 Calculated Factors of Safety for Green Dike

| Slip surface model                                | Calculated Factor of Safety | Model factor <sup>1)</sup> | Net FoS <sup>2)</sup> |
|---|-----------------------------|----------------------------|-----------------------|
| Uplift-Van  | 0.912                       | 1.06                       | 0.86                  |
| Uplift-Van (including manual stress distribution) | 0.948                       | 1.06                       | 0.89                  |
| Spencer   | 0.957                       | 1.07                       | 0.89                  |
| FEM (PLAXIS)                                      | 0.989                       | 1.06                       | 0.93                  |

1) From (WBI2017, 2016) and (POVM, 2018)

2) Net FoS = Calculated Factor of Safety/Model Factor

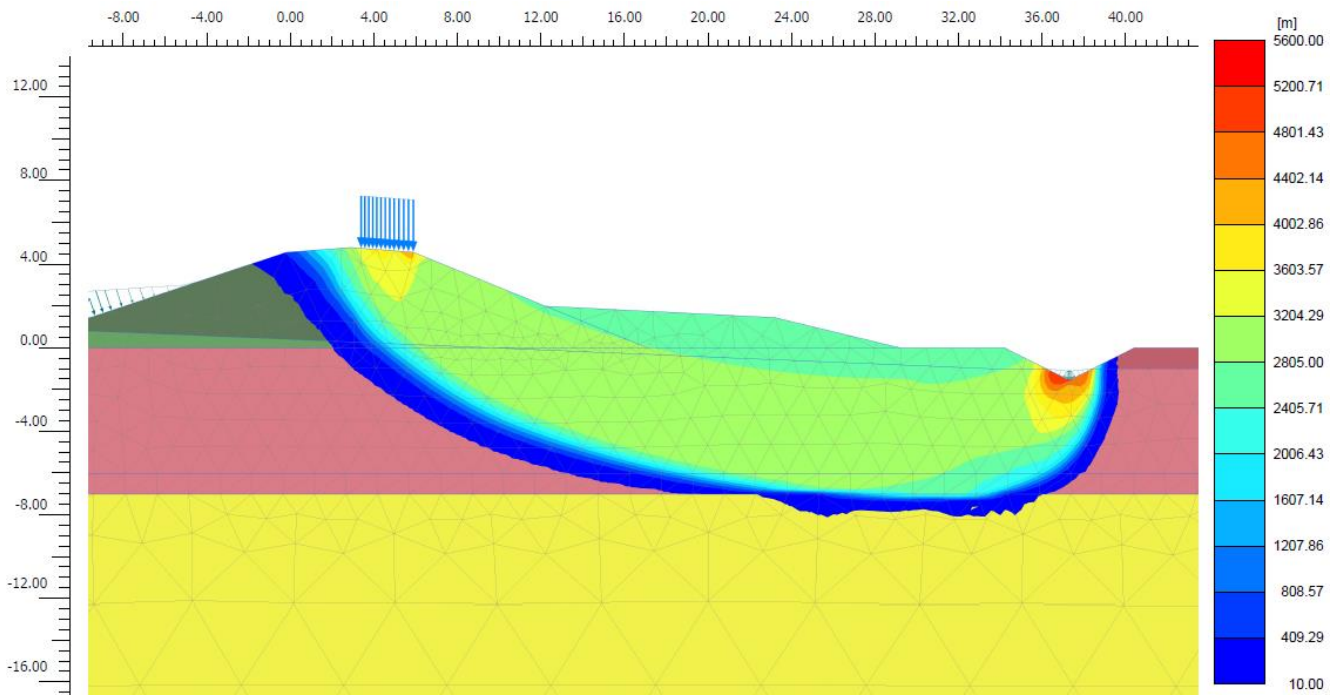


Figure 3-2: PLAXIS Reference dike (FoS = 0.989), Total displacements ( $|u|$  in m) in Safety Phase indicating the slip surface.

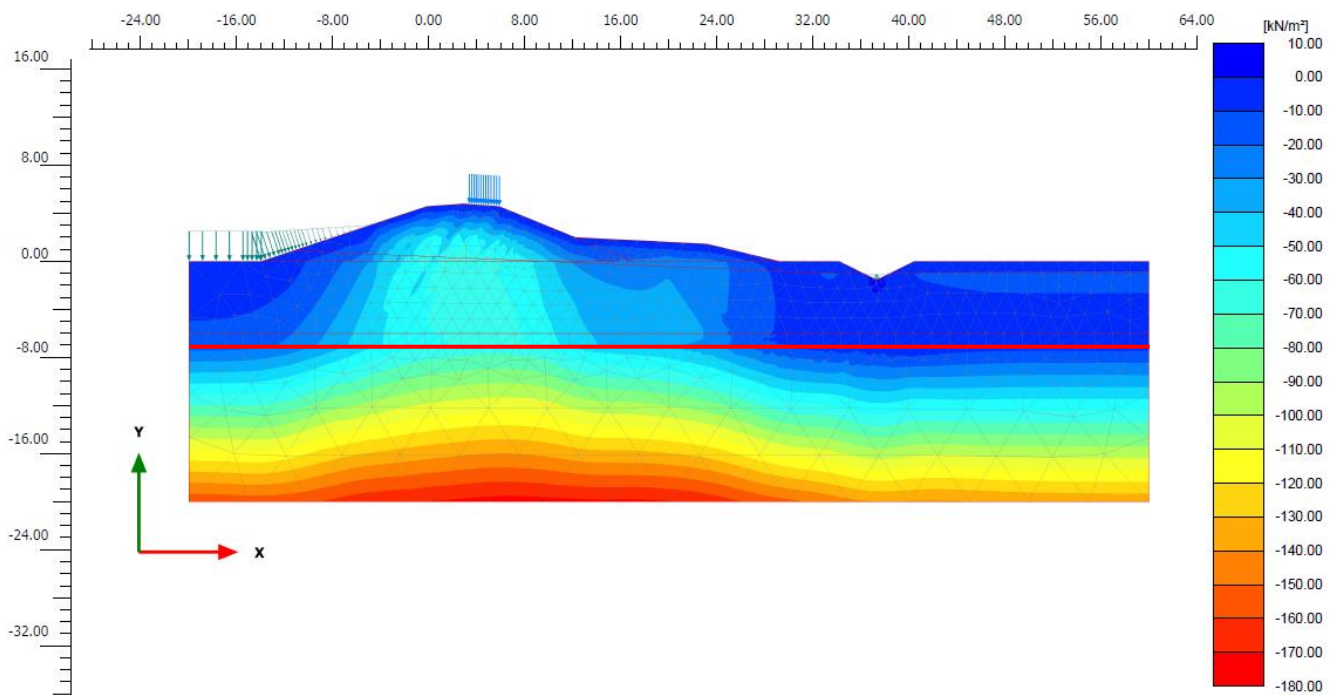


Figure 3-3: PLAXIS reference dike, Vertical effective stresses  $[kN/m^2]$ , the red horizontal line indicates the top of the sand layer.



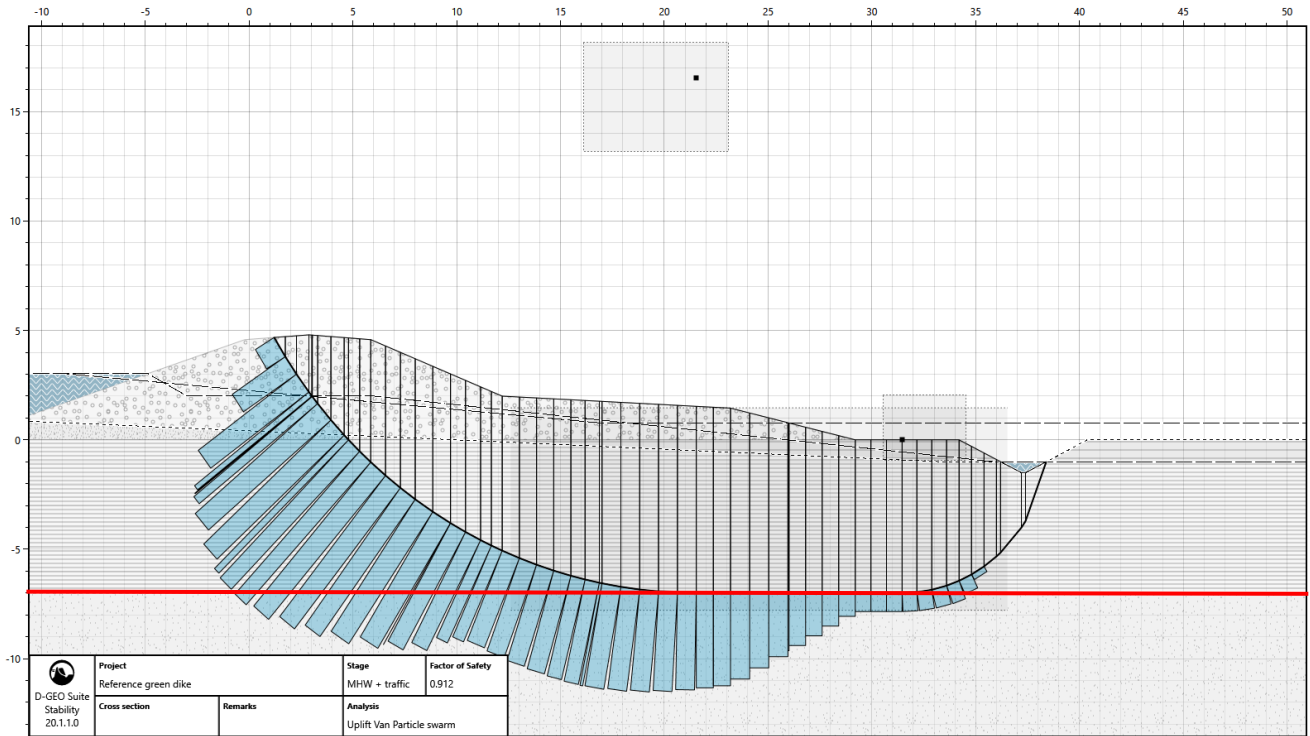


Figure 3-4: D-Stability slip surface - Uplift-Van - FoS = 0.912. The blue bars represent the vertical effective stresses, the red horizontal line indicates the top of the sand layer.

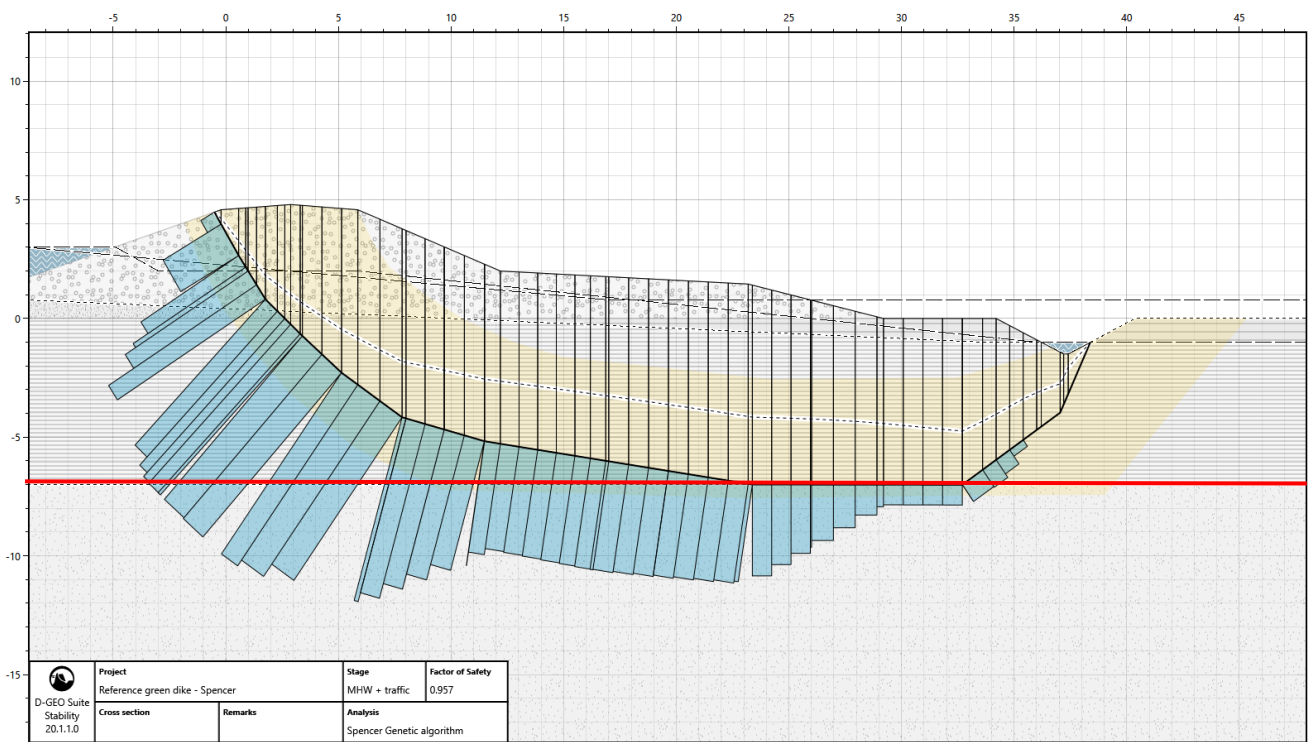


Figure 3-5: D-Stability slip surface - Spencer - FoS = 0.957. The blue bars represent the vertical effective stresses, the red horizontal line indicates the top of the sand layer.

### 3.2 Reference dike improved by stabilisation columns

This paragraph describes how the stabilisation columns applied to the case study are modelled. The reference design is given in Figure 3-6. The applied number of columns is defined for the middle row in Figure 3-6, this row is perpendicular to the river. In this case six columns are applied in a triangular grid.

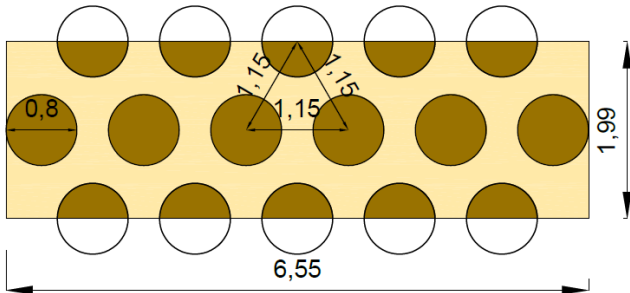
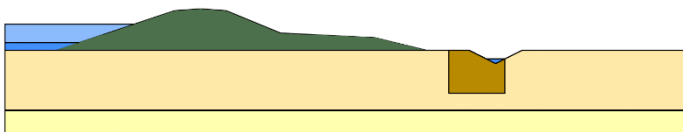


Figure 3-6: Reference design column layout [top view], dimensions in [m]

#### 3.2.1 Soil Homogenisation

The soil homogenisation method assumes average soil parameters for a block of stabilisation column improved soil, see Figure 3-7. This is done by means of the replacement factor ( $a_{SH}$ ) as defined in eq. 3.1 and given in Table 3-3.



$$a_{SH} = A_{col} / (A_{col} + A_{soil}) \quad (\text{eq. 3.1})$$

Figure 3-7 Soil homogenisation

Table 3-3: Symbol definitions and case study

|            |  |                   | Case study                               |
|------------|--|-------------------|--|
| $a_{SH}$   | Replacement factor for Soil Homogenisation | [-]               | 0.42                                     |
| $A_{col}$  | Column Area in unit cell                   | [m <sup>2</sup> ] | $(11 \times \pi \times 0.8^2 / 4) = 5.5$ |
| $A_{soil}$ | Area of soil in unit cell                  | [m <sup>2</sup> ] | 7.5                                      |
| A          | Area of unit cell                          | [m <sup>2</sup> ] | $(6.55 \times 1.99) = 13$                |

#### Increase in weight

The volumetric weight for the Soil Homogenisation ( $\gamma_{SH}$ ) method is given in eq. 3.2 and Table 3-4. This is a combined volumetric weight assigned to the block of soil indicated in Figure 3-7.

$$\gamma_{SH} = \gamma_{column} a_{SH} + \gamma_{soil} (1 - a_{SH}) \quad (\text{eq. 3.2})$$

Table 3-4: Volumetric weight numerical values for case study

|                   |                            | Units                | Case study |
|-------------------|----------------------------|----------------------|------------|
| $\gamma_{clay}$   | Volumetric weight clay     | [kN/m <sup>3</sup> ] | 11.86      |
| $\gamma_{column}$ | Volumetric weight gravel   | [kN/m <sup>3</sup> ] | 20.00      |
| $\gamma_{SH}$     | Combined Volumetric weight | [kN/m <sup>3</sup> ] | 15.30      |

### Increase in strength

The effective friction angle for the Soil Homogenisation method ( $\varphi'_{SH}$ ) is given in eq. 3.3 and Table 3-5. This is a combined friction angle assigned to the block of soil indicated in Figure 3-7.

$$\varphi'_{SH} = \varphi'_{column}a_{SH} + \varphi'_{soil}(1 - a_{SH}) \quad (\text{eq. 3.3})$$

Table 3-5: Symbol definitions and numerical values for case study

|                     |  | Units | Case study |
|---------------------|--|-------|------------|
| $\varphi'_{soil}$   | Effective friction angle of clay             | [°]   | 31.2       |
| $\varphi'_{column}$ | Effective friction angle of column material  | [°]   | 35         |
| $\varphi'_{SH}$     | Effective friction angle Soil Homogenisation | [°]   | 32.8       |

### Lateral expansion

Since there is no field data available for back analysis the Soil Homogenisation method cannot be used to model a lateral expansion.

### 3.2.2 Plane Strain; width reduction

#### Increase in weight

For this method the column width is reduced to an equivalent width, other properties remain the same. Thus the volumetric weight of the stabilisation column is 20 kN/m<sup>3</sup>.

#### Increase in strength

For this method the column width is reduced to an equivalent width, other properties remain the same. Thus the friction angle of the stabilisation column is 35°.

#### Lateral expansion

The effects of a weight and strength increase are applied directly to the host clay by adjusting the volumetric weight and friction angle. In this way the contribution of each of these effects to inner slope stability is clear. This was also intended for the effect of a lateral expansion, but no stable calculations can be performed when applying a volumetric strain to clay modelled by the SSC soil model, because stresses and stiffness of the clay are low and in contradiction to the HS model no shear hardening can occur. Therefore the stabilisation columns are modelled as gravel with the Hardening Soil model, which is the way they should be modelled eventually.

The general workflow used in PLAXIS 2D to model column expansion and to calculate the Factor of Safety is as follows. Phases 1, 3, 4 and 5 are common phases for any calculation in PLAXIS 2D, Phase 2 is explained below and shown in Figure 3-8.

- 1a. Initial Phase
- 1b. 0-step
- 1c. Consolidation Phase

- 2a. Closing of ditch
- 2b. Installing Stabilisation Columns
- 2c1. Cavity Expansion (1/2)
- (2c2. Cavity Expansion (2/2))
- 2d1. Excavating ditch (1/2)
- 2d2. Excavating ditch (2/2)
- 3a. High water
- 3b. High water + traffic load
- 4. Switch to SHANSEP
- 5. Safety calculation Phase

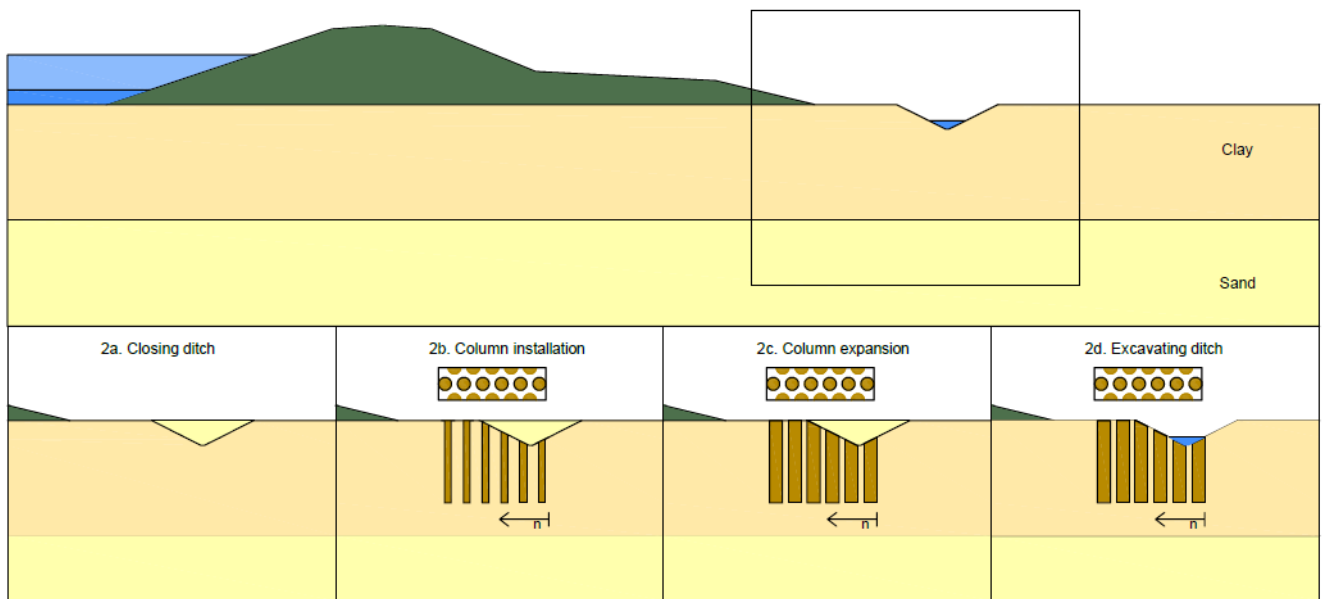


Figure 3-8: Workflow Phase 2

## Phase 2: Column installation

Phase 2 is the step where the stabilisation columns are installed. In practice contractors will close the ditch before installing the stabilisation columns in order to prevent local instabilities at the ditch during construction. The effect of closing and excavating the ditch on the Factor of Safety is +0.004, this is negligible.

As stated before it is sufficient to start with half a column to simulate the expansion behaviour of a stabilisation column. This half column is installed in **step 2b**. The stabilisation columns are modelled as a material with gravel properties.

In **step 2c**, the actual column expansion is modelled. The column expansion is modelled as an volumetric strain in x-direction. The applied volumetric strain in x-direction is 100%, which means the initial radius in 2D (0.22m) is doubled to final column radius (0.44m), this represents a 3D equivalent by means of eq. 2.16. PLAXIS increases the applied load by a predefined maximum load fraction per calculation step, the default fraction is 0.5. To perform stable calculations this value is lowered to 0.2. A work-around method is splitting the volumetric strain into two phases. In this way it is there is no need to change the numerical input parameters, it is clearly stated when this option is used.

In **step 2d**, the columns are at final dimensions and the ditch can be excavated. As the ditch is very large and steep, excavating it at once leads to physical and numerical problems, resulting in very local failures in the ditch. The fill of the ditch functions as a support for the ditch slopes. The stresses generated by the column expansion are still present in the soil. Excavating the ditch directly after column installation will force the expanded soil into the ditch.

### **3.2.3 Plane Strain; strength reduction**

As described in 2.3.1 the width of the Plane Strain equivalent stabilisation column equals the column diameter ( $d_c$ ), so  $d_c=0.8$  m. The 3D width is maintained for the 2D calculations, therefore all other material properties need to be reduced at the same time to effective material properties to reproduce the effect of column installation properly. This method is therefore not suited to study the effects of weight and strength separately.

#### **Lateral expansion**

The approach for modelling a lateral expansion is the same as for the Plane Strain; width reduction (0). In this case half a column thus equals  $0.8*0.5=0.4$ m. This is the width assigned to the Plane Strain equivalent column, that will be expanded to full column width.

## 4. Results

The results are presented in this chapter. The influence of various effects of stabilisation columns are quantified by means of the calculated Factor of Safety.

The following abbreviations, referring to the modelling techniques, are used frequently in the graphs presented:

- **SH:** Soil Homogenisation
- **PSw:** Plane Strain – Width reduction
- **PSs:** Plane Strain – Strength reduction

### 4.1 Increase in weight

Adding stabilisation columns leads to an increase in weight. The influence of this extra weight on the Factor of Safety is shown in Figure 4-1.

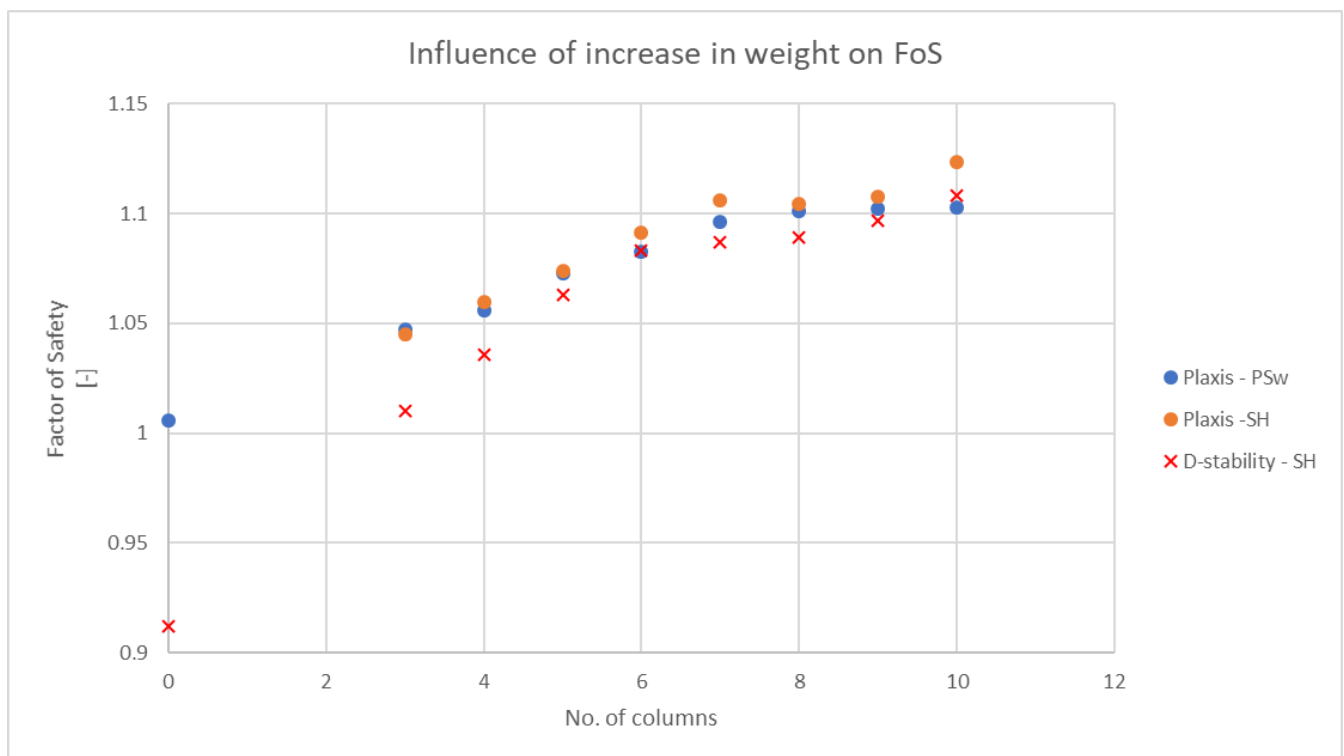


Figure 4-1: Number of columns versus Factor of Safety for an increase in weight.

The undrained shear strength ( $s_u$ ) is described as shown in eq. 2.5. A brief reminder,  $s_u = S \cdot \sigma'_{v/p} \cdot OCR^m$  with  $OCR = \max(\sigma'_{v/p,y} / \sigma'_{v/p}, 1)$ . Weight is directly taken into account in the vertical or principal effective stress and indirectly in  $OCR^m$ . The strength increase exponent ( $m$ ) is 0.76. An increase in weight will thus lead to an increase in  $s_u$ , see the example. If the position of the slip surface is fixed and  $S$  is constant, the increase in  $s_u$  is constant for every extra column applied and thus the FoS increases linearly. This can be seen in Figure 4-1 for applying 3-6 columns, then

#### Example SH:

*-1m w.r.t. ground level, above phreatic level*

|             | Reference     | Stab. Col.    | %   |
|-------------|---------------|---------------|-----|
| $\sigma'_v$ | 11.86x1       | 15.30x1       | +29 |
| $OCR^m$     | 1.86          | 1.53          | -18 |
| $S$         | <u>0.25 x</u> | <u>0.25 x</u> | -   |
| $s_u$       | 5.52          | 5.87          | +6  |

the slip surface cuts through the columns, see Figure 4-2. When 7 or more columns are applied the slip surface is forced below the stabilisation columns, see Figure 4-3. The phreatic level and the potential in the aquifer increase towards the dike from the point ( $\pm x=32$ ) where 6 columns are applied. Every extra column will be less effective as the effect on vertical effective stress is relatively lower. The difference in calculated FoS between PLAXIS and D-Stability due to stress distribution diminishes quickly. In the reference case lifting of the clay layer occurred in D-stability, this is prevented by adding stabilisation columns and thus by adding weight.

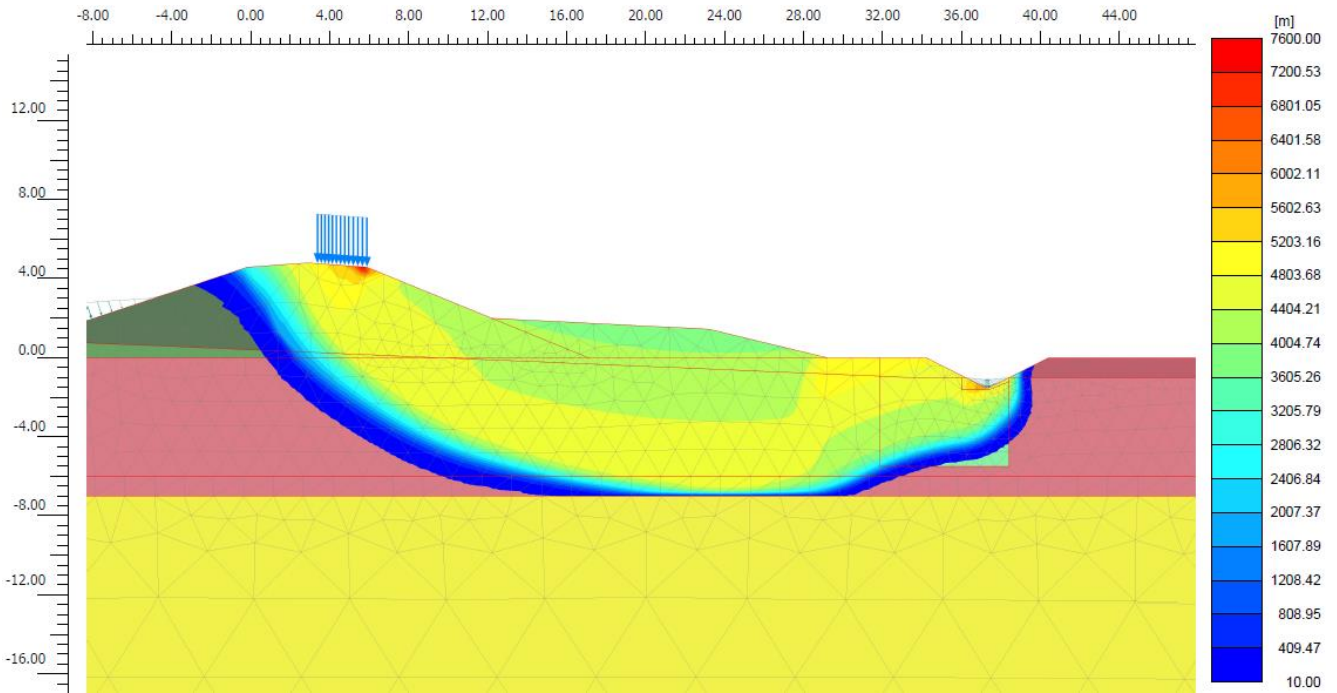


Figure 4-2: Slip surface indicated by total displacements  $|u|$  in m for 6 columns. The Soil Homogenisation method is used, the block of columns is located between  $x=31.85$  and  $x=38.4$ .

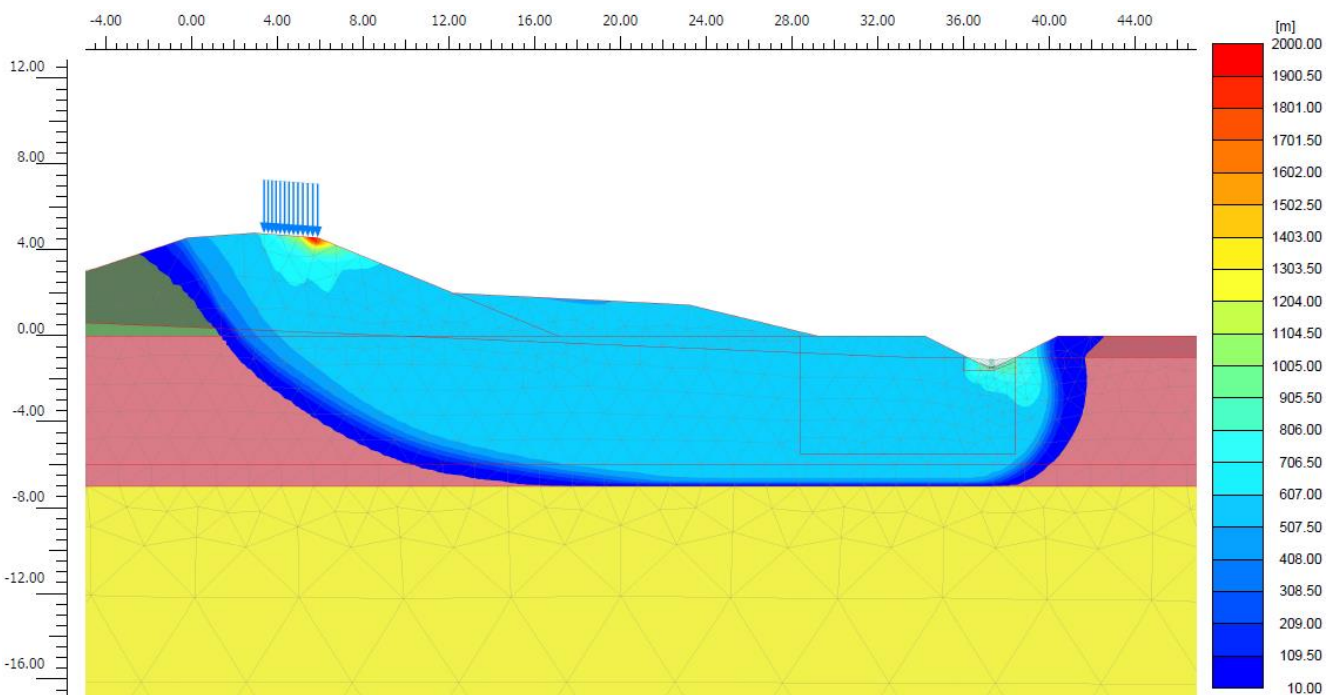


Figure 4-3: Slip surface indicated by total displacements  $|u|$  in m for 9 columns. The Soil Homogenisation method is used, the block of columns is located between  $x=28.4$  and  $x=38.4$ .

## 4.2 Increase in strength

The effect of a strength increase is shown in Figure 4-4. When the slip surface cuts through the stabilisation columns the shear strength for this part is higher due to the increase in strength. However, only assigning a higher friction angle to the clay forces the slip surface directly below the columns, already for applying 3 columns. Thus it is not using this additional shear strength. The position of the slip surface does not change when an extra column is applied and thus the FoS will not improve.

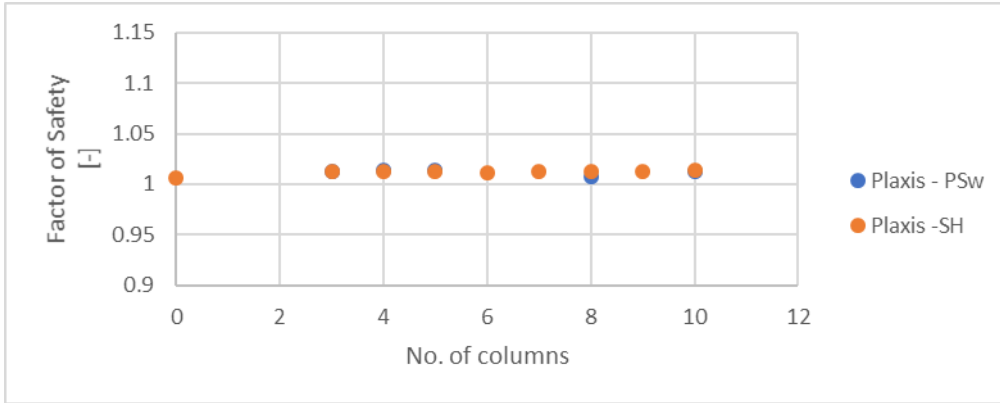


Figure 4-4: Effect on FoS by assigning an increased friction angle to host clay.

When the effects of weight and strength are combined the effect of a higher friction angle might be noticeable. For example for the case as shown in Figure 4-2 where the slip surface cuts through the stabilisation columns. A higher friction angle will then force the slip surface below the stabilisation columns, leading to a higher FoS. The friction angle of the host clay was already high, so the effect is very limited, see Figure 4-5. For clays with a lower friction angle the improvement in FoS will be higher.

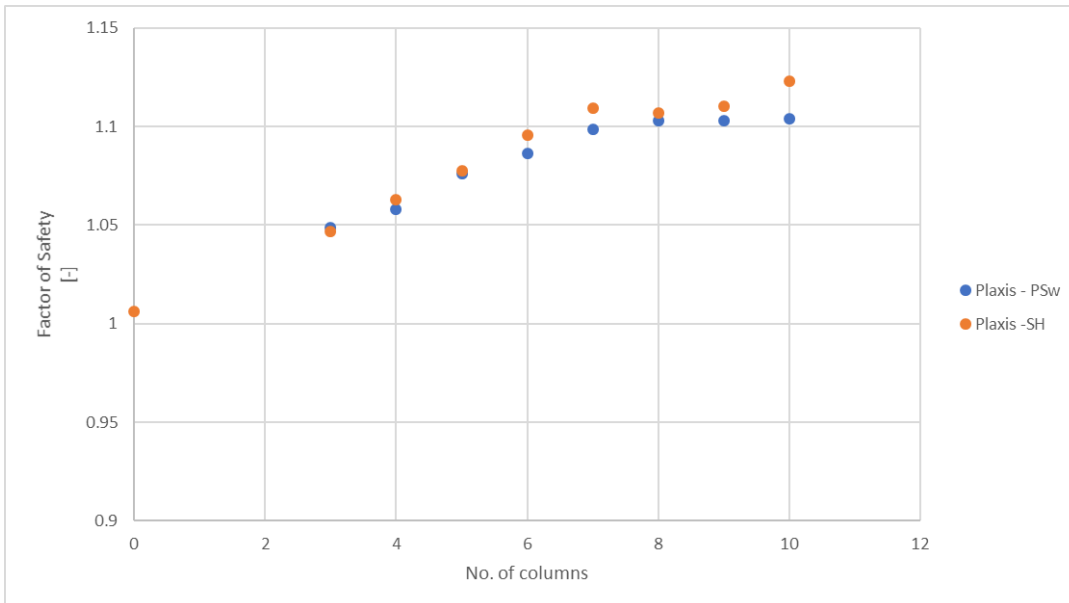


Figure 4-5: Combined effect of weight and strength



### 4.3 Lateral expansion

As stated before in par. 3.2.2 it is not possible to apply a lateral expansion to the host clay. A lateral expansion is modelled to stabilisation columns with gravel properties, this includes a higher weight of the gravel. The effect on the FoS shown in Figure 4-6 is partly caused by a weight increase (40-50%). The slip surface for 6 columns is shown in Figure 4-9 for PLAXIS 3D and in Figure 4-10 for PLAXIS 2D.

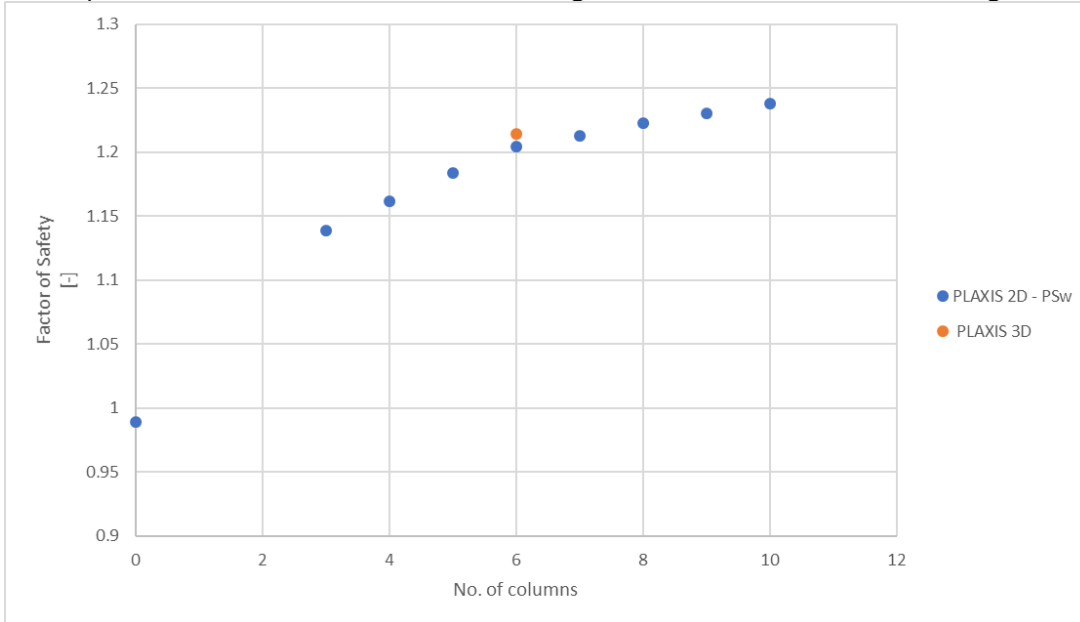


Figure 4-6: Effect of lateral expansion on Factor of Safety for PLAXIS Plane Strain - width reduction and PLAXIS 3D

In Figure 4-11 the principal effective stresses directly after column installation are shown, the columns are not expanded yet. In Figure 4-12 the principal effective stresses after column expansion are shown. Due to the lateral expansion there's a significant increase in principal effective stresses ( $\sigma'_1$ ). As stated before PLAXIS uses ( $\sigma'_1$ ) to calculate the undrained shear strength ( $s_u$ ). Figure 4-12 and Figure 4-13 show a same pattern, so the change in  $s_u$  is mainly dependent on the change in  $\sigma'_1$ . Due to the column expansion there is a significant increase in the coefficient of lateral earth pressure ( $K_r = \sigma'_r / \sigma'_z$ ), see Figure 4-7. A similar trend was found by (Benmebarek et al., 2018) as shown in Figure 2-8. The change in  $K_r$  presented here is higher than the one described by (Benmebarek et al., 2018) and extends further away from the columns. The analysis they conducted was deeper with respect to ground level and for another type of clay with a much higher volumetric weight.

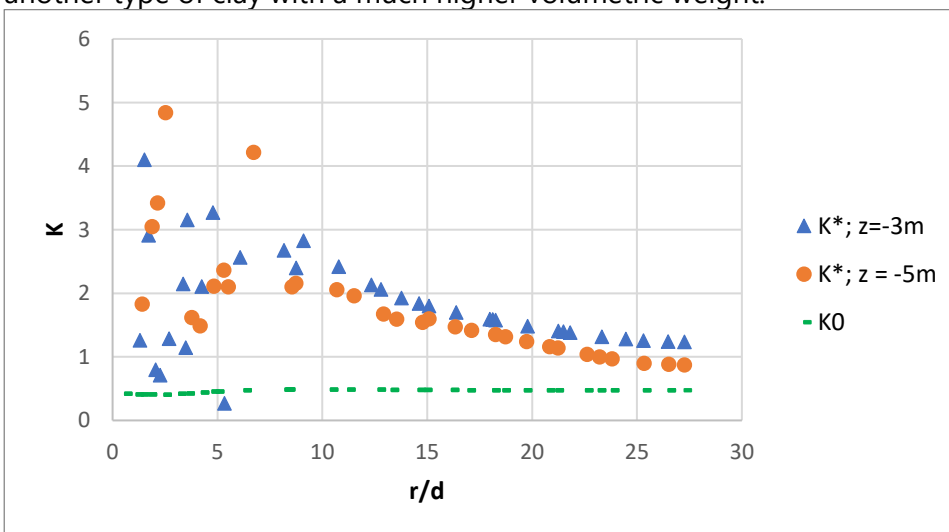


Figure 4-7:  $K^*$  at  $z=-3m$  and  $z=-5m$ , starting from the most right column to the right.  $K_0$  is the initial coefficient of lateral earth pressure,  $K^*$  is the one after column expansion.  $r$  is the distance from the column [m],  $d$  the column diameter [m].

That the influence of the lateral expansion is present at some distance from the stabilisation columns is expected. Looking at the change of the coefficient of lateral earth pressure this can still be seen at the model boundary. Although it is not likely that this boundary influences the result, since it is far away, it cannot be excluded. When the boundary is moved further away PLAXIS cannot solve the stiffness matrix. The expectation is that the low weight of the host clay plays a role in combination with the updated mesh calculations. Due to the low weight the effective stresses are low and are therefore sensitive to minor changes in the stress field. (Benmebarek et al., 2018) show a similar result, where plastic points close to ground level extent until the model boundary, as can be seen in Figure 4-8.

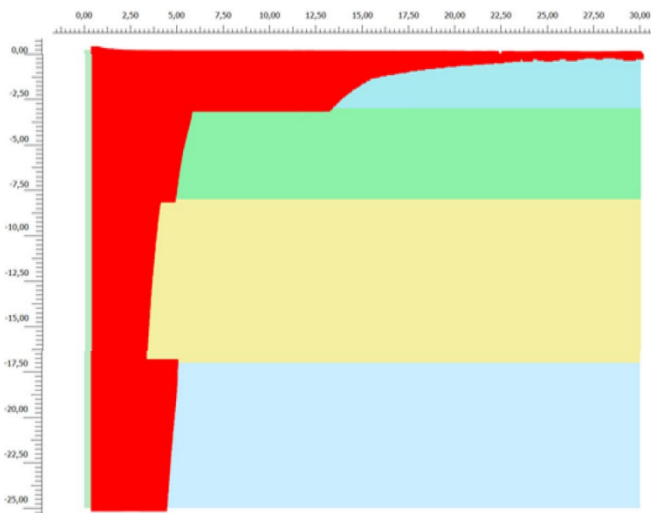


Figure 4-8: Plastic points in soft soil after column installation. (Benmebarek et al., 2018)

The slip surface for 6 columns is shown in Figure 4-9 for PLAXIS 3D and in Figure 4-10 for PLAXIS 2D. Only one calculation has been performed in PLAXIS 3D, as the calculation time is in the order of days. The middle row perpendicular to the dike consists of six stabilisation columns. The position of the slip surface is similar for PLAXIS 2D and 3D. The FoS for PLAXIS 3D calculates is 1.214 and 1.204 for PLAXIS 2D. One of the main concerns arising from modelling in 2D is that cutting of soil between stabilisation columns occurs. As can be seen in Figure 4-9 this does not occur in the 3D calculation and this can be excluded for applying a row of 6 or more columns. For other design configurations a 3D calculation or an analytical solution can be performed to exclude this effect. These results give confidence in the 2D model and its simplifications to translate a 3D situation to a 2D model.

In reality the stabilisation columns are installed by means of a ground displacing method, while modelling them can only be done by replacing part of the host clay by a stabilisation column. Thus, the added amount of weight is underestimated. Assigning a higher weight to the columns that represents the actual stress field leads to good approximation of the added weight, but leads to an overestimation of the amount of lateral expansion, as this is stress dependent. It is therefore a safe assumption to not take this into account, but the FoS can be higher. The sensitivity analysis gives directions, a higher column weight by a heavier material leads to a FoS increase of  $\pm 4\%$ .

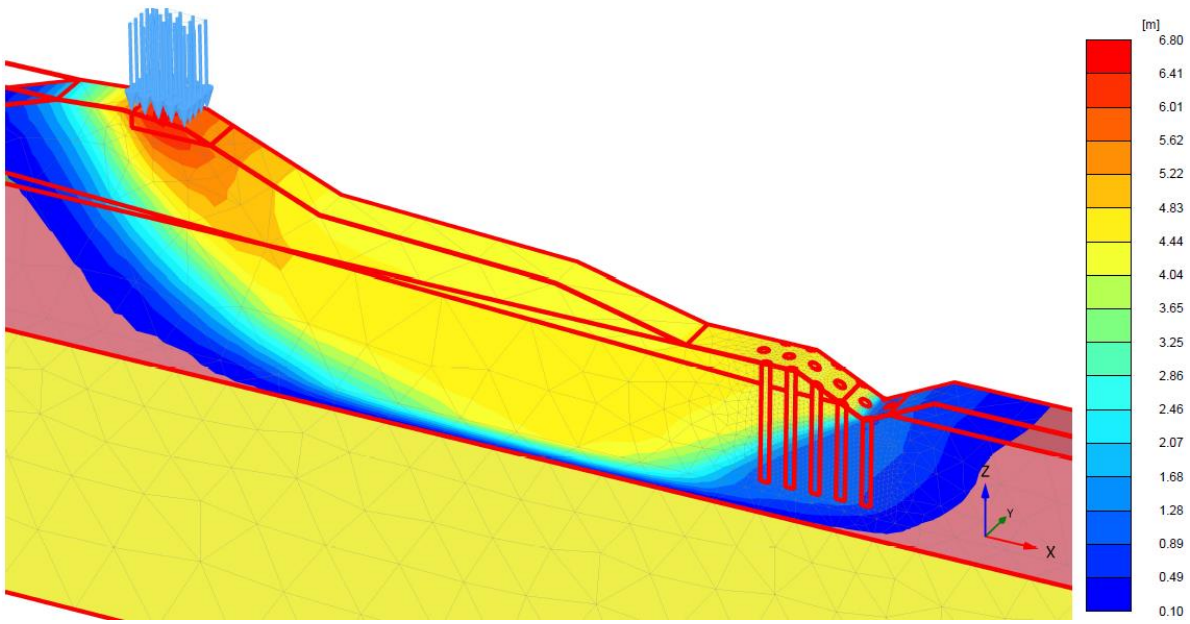


Figure 4-9: Slip surface for 6 stabilisation columns indicated by total displacements  $|u|$  [m] in PLAXIS 3D

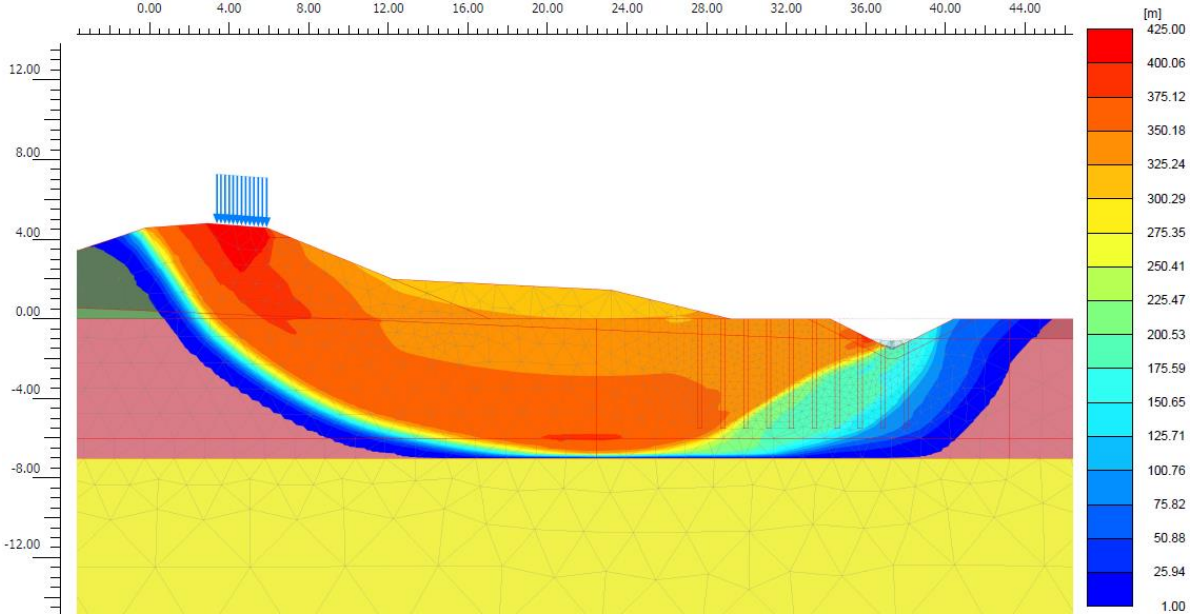


Figure 4-10: Slip surface for 6 stabilisation columns indicated by total displacements  $|u|$  [m]. FoS = 1.204

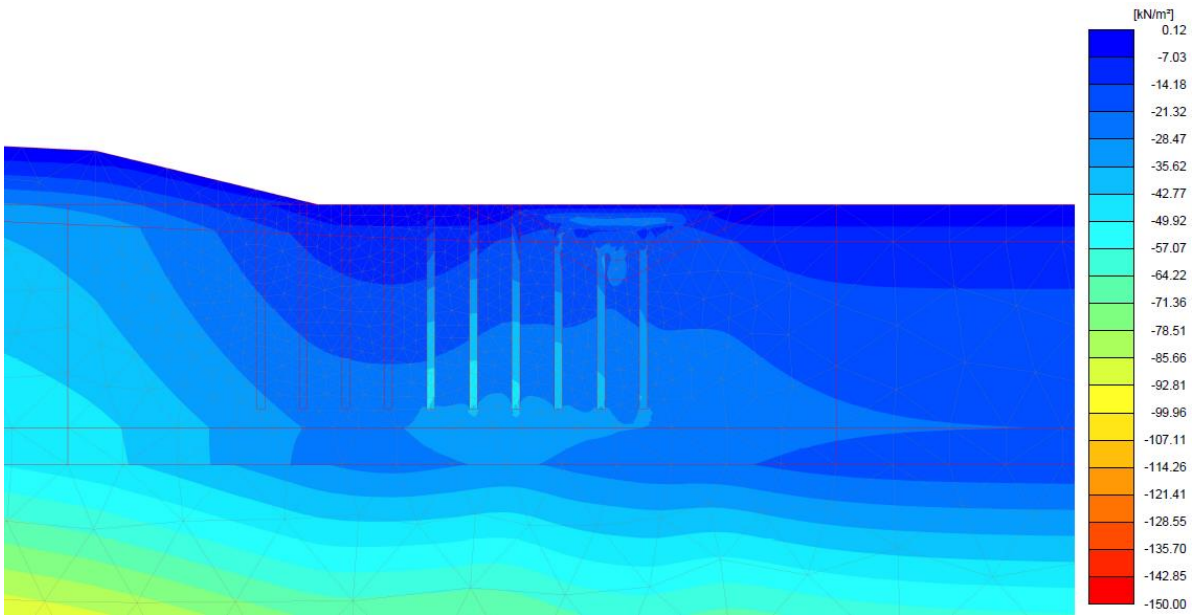


Figure 4-11: Principal effective stresses ( $\sigma'_1$ ) directly after 6 columns are installed.

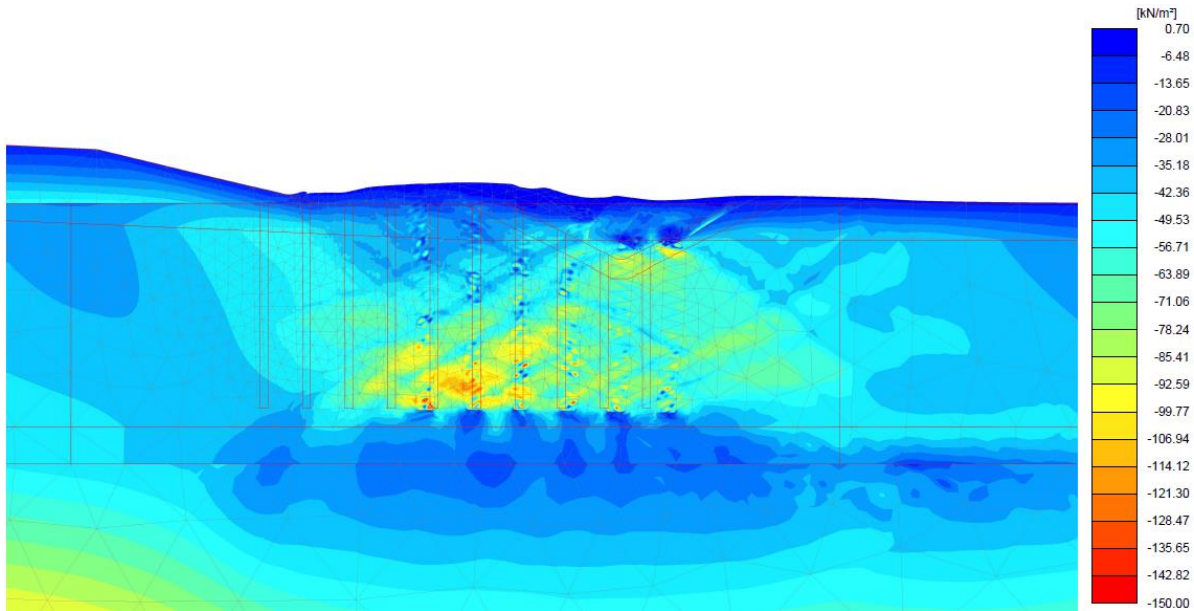


Figure 4-12: Principal effective stresses ( $\sigma'_1$ ) after 6 columns are expanded.

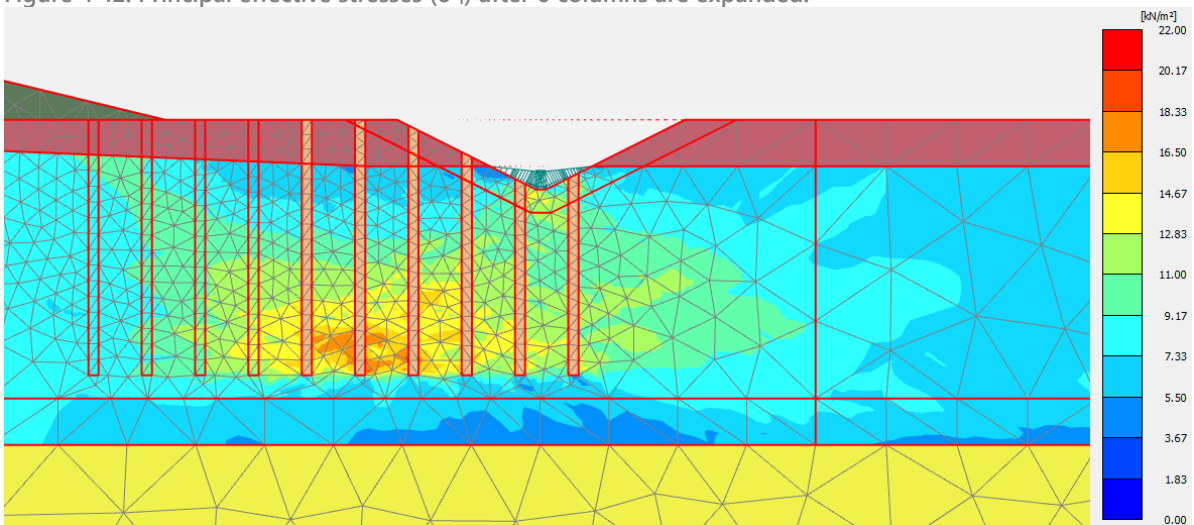


Figure 4-13: Calculated undrained shear strength ( $s_u$ ) for 6 stabilisation columns below phreatic level. The yellow layer at the bottom is the sand layer.

## 4.4 Sensitivity analysis

In the previous paragraphs the various effects of stabilisation columns on inner slope stability were investigated separately. It turns out that the lateral expansion contributes most to the improvement of the FoS, about 50-60%. The contribution of the weight is in the same order of magnitude. As the improvement is largely dependent on the effect of the weight and a lateral expansion, their sensitivity to changes in input parameters is investigated in this paragraph. This is done directly by adjusting weight properties and the applied amount of volumetric strain. And indirectly by adjusting geometrical properties as column diameter, spacing, etc. Also the various effects on the phreatic surface and the head are addressed. All calculations performed in this sensitivity analysis are based on the Plane Strain width reduction technique and include a lateral expansion, unless it's stated otherwise. The calculations were performed by means of scripting. If single calculations failed numerically they are not adjusted and therefore not shown in the graphs. First a classical berm solution is presented.

### 4.4.1 Classical berm solution

The technical potential was defined as a 20% increase of the FoS, this means the required  $FoS_{req} = 1.19$ . This can be reached when 6 stabilisation columns per row are applied, as can be seen in Figure 4-6. To put this technical potential in perspective, a dike with a classical stabilisation berm is designed. The current berm needs to be extended 15 m, the ditch is moved 15 m and the height is increased 0.5 m (see Figure 4-14). The required amount of soil is  $\pm 26 \text{ m}^3/\text{m}$ . The berm is designed with the same material as the current berm consists of (Dike material, see B.2).

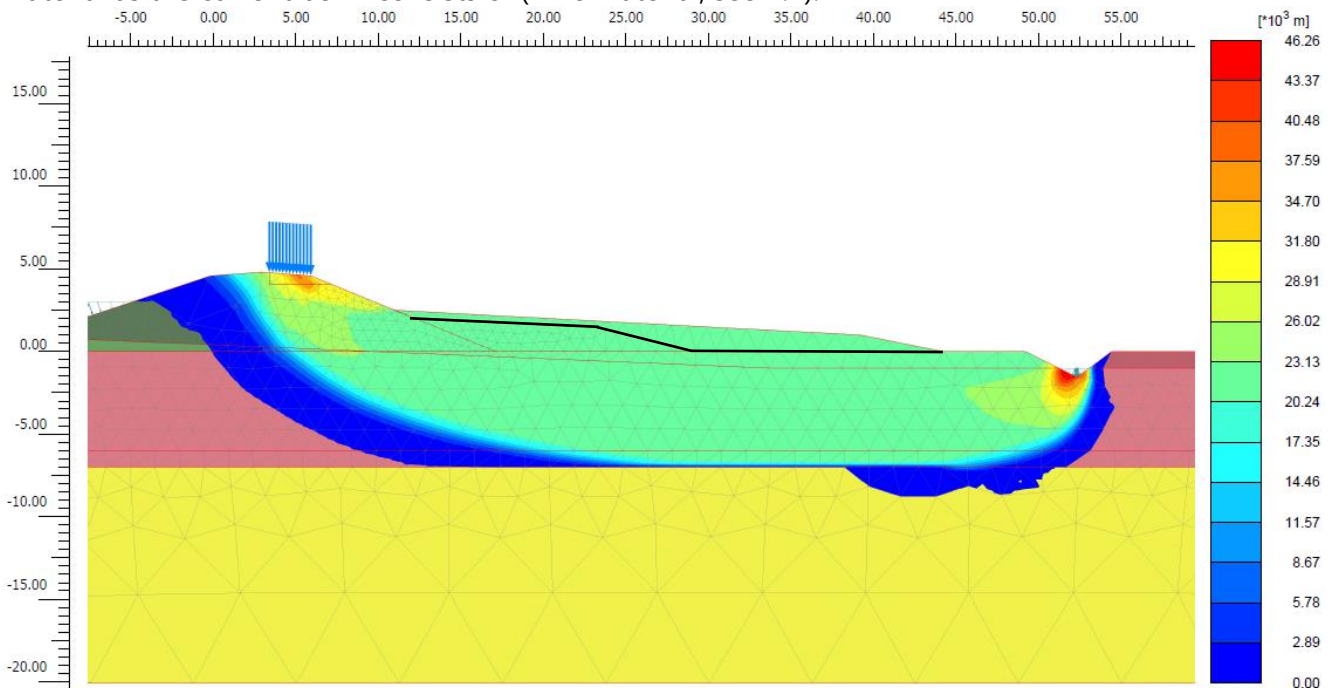


Figure 4-14: Slip surface PLAXIS 2D for a classical stabilisation berm, total displacement ( $|u|$  in m).

In Table 4-1 a comparison between applying a row of 6 stabilisation columns and a classic berm solution. Both methods have a  $FoS \approx 1.2$ .

Table 4-1: Comparison between stabilisation columns and classical berm

| Method                        | Material             | Material volume [m <sup>3</sup> /m] | Additional space required [m] | FoS [-] | FoS improvement [%] |
|-------------------------------|----------------------|-------------------------------------|-------------------------------|---------|---------------------|
| Row of 6 stabilisation column | Gravel               | 15                                  | 0                             | 1.204   | +21.6               |
| Classical berm                | Clay (Dike Material) | 26                                  | 15                            | 1.197   | +20.9               |

#### 4.4.2 Weight

##### Weight of the host clay

The effect of an increase in host clay weight is studied in this paragraph. The weight is increased as indicated in Table 4-2. For the current weight of the host clay as for the increased weight, a situation with and without lateral expansion are considered. An increase of the host soil weight also influences the FoS of the initial situation without stabilisation columns, this FoS is 1.17.

Table 4-2: Weight variation host clay

| Material  | $\gamma_{sat}$ old [kN/m <sup>3</sup> ] | $\gamma_{sat}$ new [kN/m <sup>3</sup> ] | Weight improvement [%] |
|-----------|---|---|------------------------|
| Host clay | 11.86                                   | 14                                      | +18                    |

##### No lateral expansion (◆)

For these calculations only gravel is added, the stabilisation columns are not laterally expanded. The improvement of the FoS with respect to unimproved dike is therefore mainly caused by the weight increase due to the inclusion of gravel, as concluded earlier in this chapter. The relative contribution of the gravel weight is lower for a heavier host clay.

##### Lateral expansion (●)

For these calculations gravel is added and the stabilisation columns are laterally expanded. The difference in FoS ( $\pm 0.18$ ) for light and heavier clay is the same for the unimproved dike (0 columns) as for the improved dike (3-6 columns). As just concluded, the influence of weight is lower for a heavier clay, this means that the effect of a lateral expansion must be larger for heavier clay. This is confirmed by Figure 4-16. Close to the columns, where the slip surface is located, the coefficient of lateral earth pressure (K) is comparable for the light and the heavy clay. For a heavy clay the vertical effective stresses are higher and thus if K is comparable, the horizontal effective stresses as well. The horizontal stress is the principal stress after column expansion, PLAXIS uses the principal stress to calculate the shear strength. For the case where the host clay weight is increased to 14 kN/m<sup>3</sup> and the stabilisation columns are expanded the result is not shown for more than six columns. In this case the slip surface is forced on the outer dike slope.

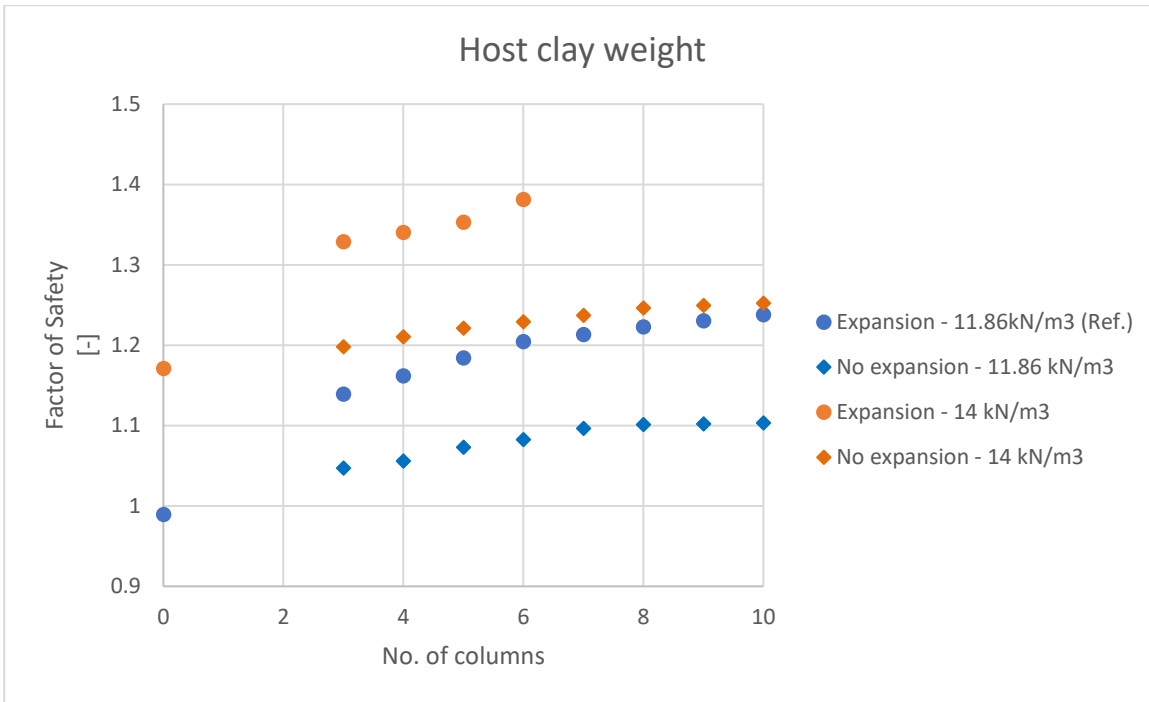


Figure 4-15: Effect of increase in host clay weight on Factor of Safety.

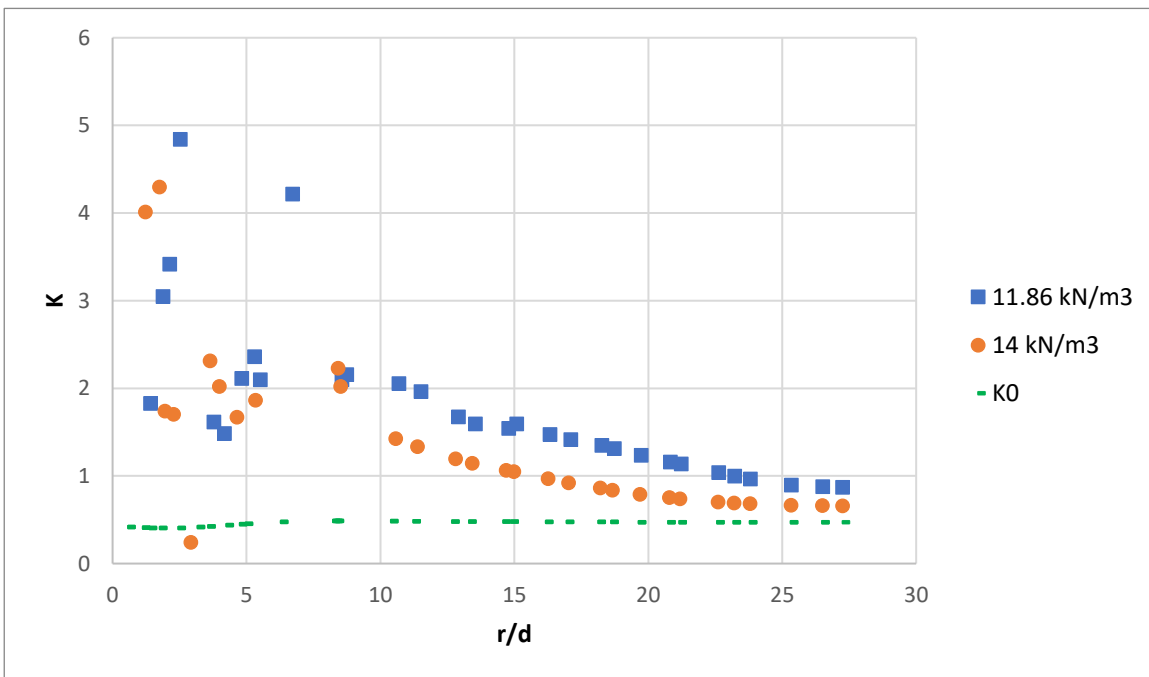


Figure 4-16: Influence of stabilisation columns including a lateral expansion on the coefficient of lateral earth pressure at a depth of  $z=-5\text{m}$ . Six stabilisation columns are installed.

### Weight of the column material

For the reference case gravel properties are assumed. A higher weight for the stabilisation column fill can be reached by using alternative materials, such as Rodense. Table 4-3 contains the values used.

Table 4-3: Weight variation host clay

| Material        | $\gamma_{\text{sat old}}$<br>[kN/m <sup>3</sup> ] | $\gamma_{\text{sat new}}$<br>[kN/m <sup>3</sup> ] | Weight improvement<br>[%] |
|-----------------|---|---|---------------------------|
| Column material | 21  | 27.3  | +30                       |

The effect on the Factor of Safety is shown in Figure 4-17. When more than 6 columns were applied the slip surface was forced to the outer slope. There's a stronger linear increasing trend than when using gravel, which is expected according to paragraph 4.1 Increase in weight. The effect seems limited for applying 3 stabilisation columns. These columns are all under the ditch and are shorter than the other columns. When the ditch is shallower or the columns are larger this effect will be larger.

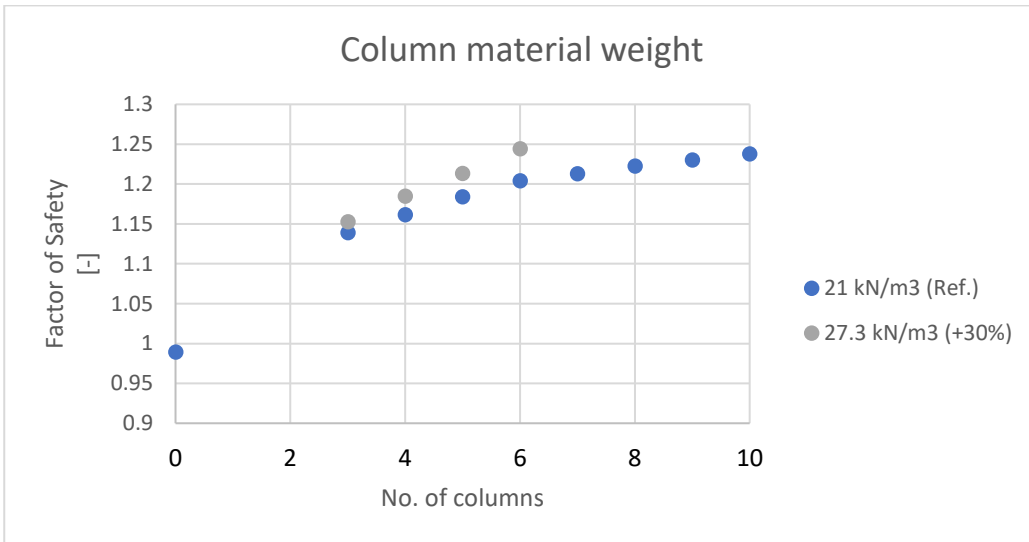


Figure 4-17: Effect of increase in column material weight on Factor of Safety.

#### 4.4.3 Lateral expansion

The lateral expansion is modelled as an imposed volumetric strain of 100%. In Figure 4-18 the effect on the Factor of Safety is shown when the imposed volumetric strain is only 50%.

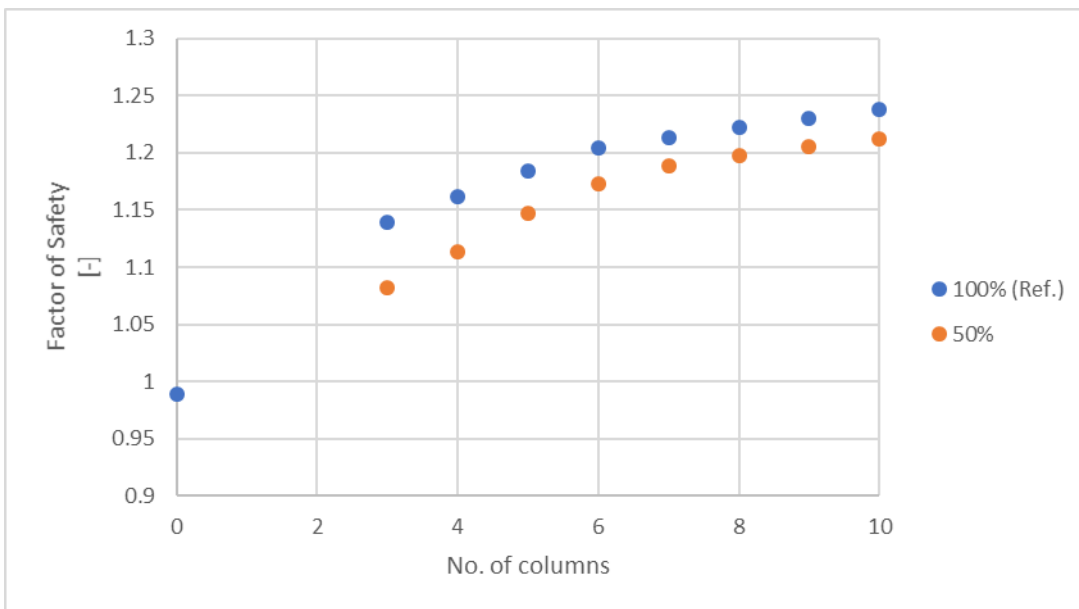


Figure 4-18: Effect of imposed volumetric strain [%] on the Factor of Safety. 100% is the reference value.

Large part of the FoS improvement is already achieved when only 50% strain is imposed. On the one hand this gives confidence that execution uncertainties do not really influence the result. On the other hand, looking at figure Figure 4-19, close to the column K is lower for 100% imposed strain than for 50%. If the position of the slip surface is the same, one expects a lower FoS, since the horizontal and therefore the principal effective stress is lower. Comparing Figure 4-20 and Figure 4-21 the position of



the slip surface changes. For 100% imposed volumetric strain the improved soil mass as a whole moves further to the right, forcing the slip surface up to the left.

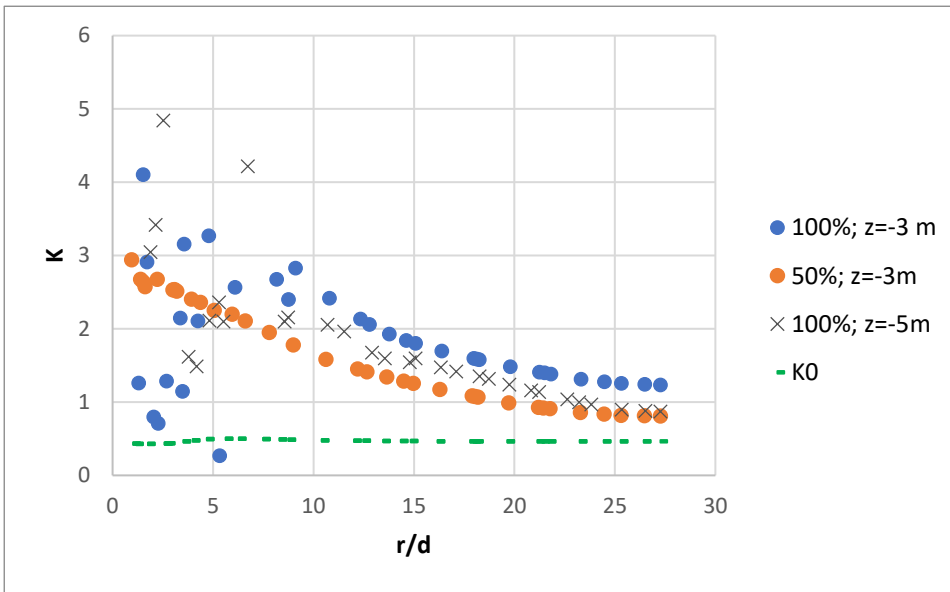


Figure 4-19: Effect of imposed volumetric strain on the coefficient of lateral earth pressure (K) at z=-3 m, in the case were six columns are installed.

Close to the column the values of K decrease for an increase in imposed volumetric strain. The number of failure points in PLAXIS increases significantly for higher imposed strain. According to (Brinkgreve et al., 2019) a failure point indicates that the stresses lie on the surface of the failure envelope. An element in PLAXIS consists of 15-nodes, a failure point indicates that one node fails. For multiple elements close to the stabilisation columns most of the nodes are failure points. Continuous deformations occur here, no strength can be derived from these elements. If 100% imposed volumetric strain does not lead to scatter of K close to the last column, the FoS might be higher than it is now. This can be achieved as can be seen in Figure 2-8 by (Benmebarek et al., 2018), but is case specific. Optimising design parameters like stabilisation column position, spacing, diameter and placement depth might lead to a design where the full potential of the lateral expansion is used.

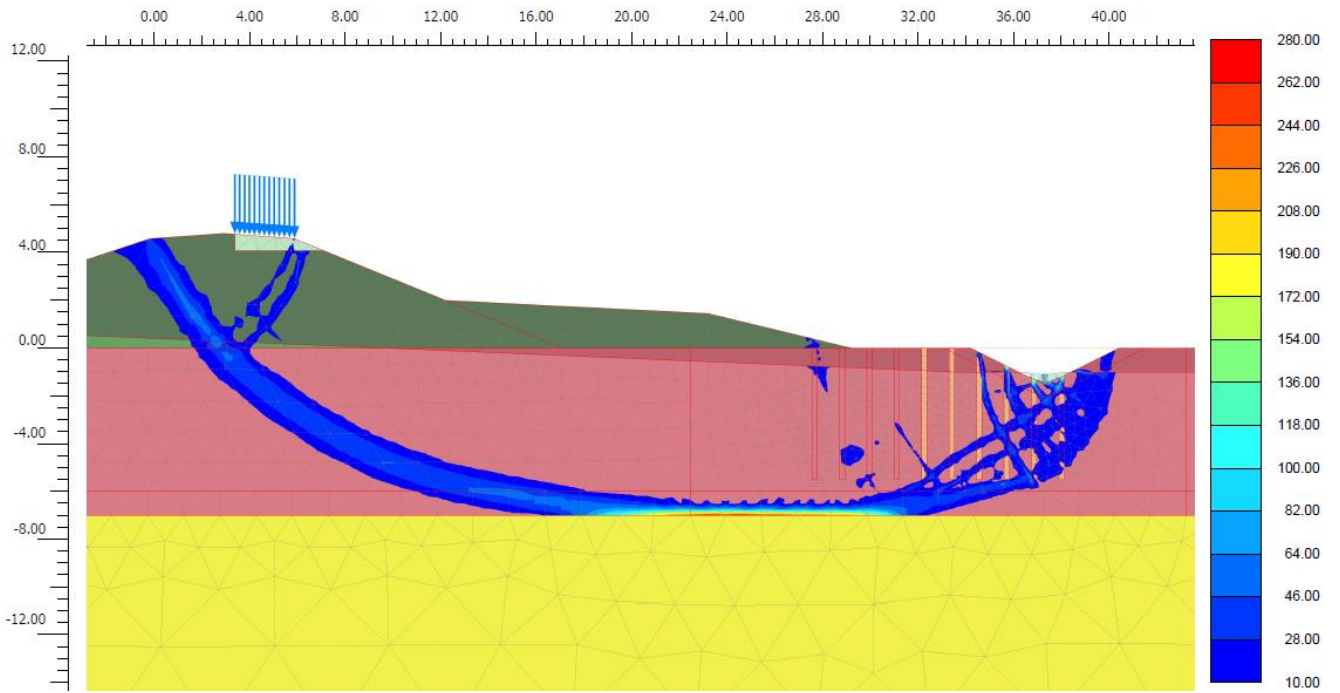


Figure 4-20: Indicated slip surface by means of incremental deviatoric strain [-] for 50% imposed lateral strains for 6 stabilisation columns.

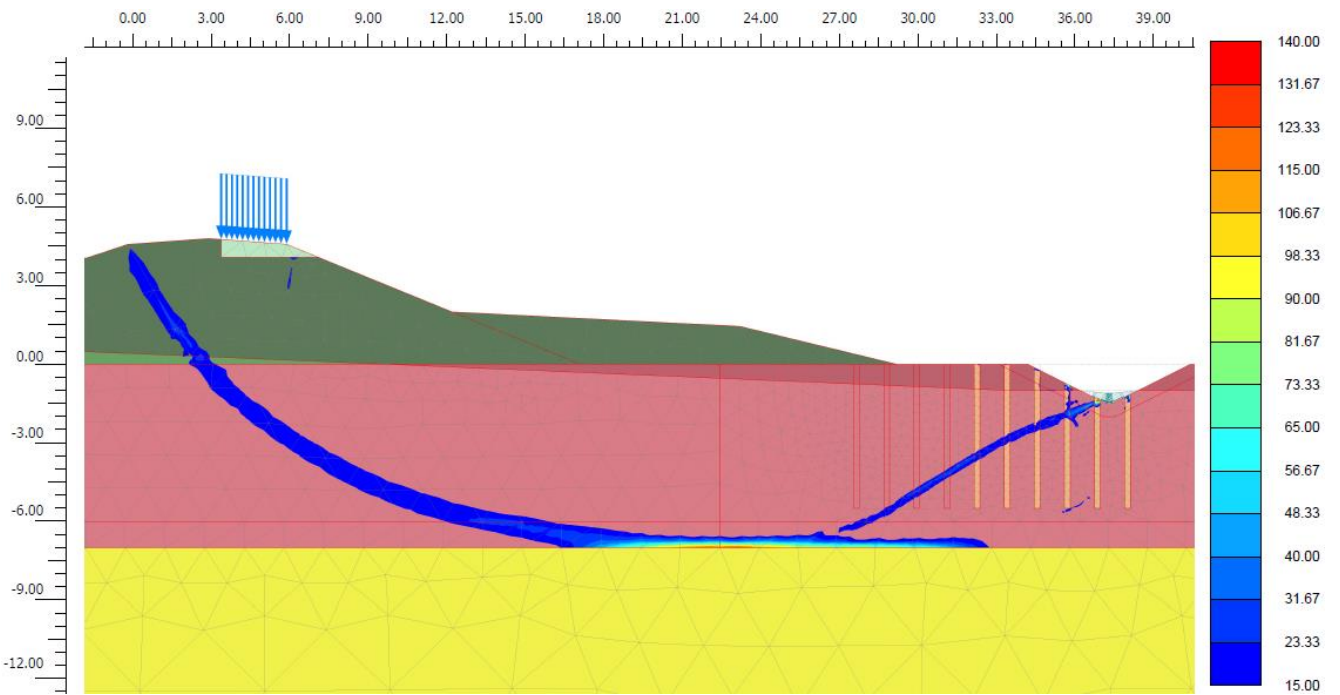


Figure 4-21: Indicated slip surface by means of incremental deviatoric strain [-] for 100% imposed lateral strains for 6 stabilisation columns.

#### 4.4.4 Geometric properties

##### Spacing

In Figure 4-22 the influence of the inter column spacing on the FoS is shown. A larger stabilisation column spacing means the replacement ratio of the host clay is lower, relatively fewer gravel is added to every cubic meter of host clay. Besides that, the effective column width is inversely proportional to the inter column spacing, see eq. 2.16. The total lateral expansion is proportional to the effective column width and will therefore be lower. Therefore, the FoS is lower for a larger column spacing.

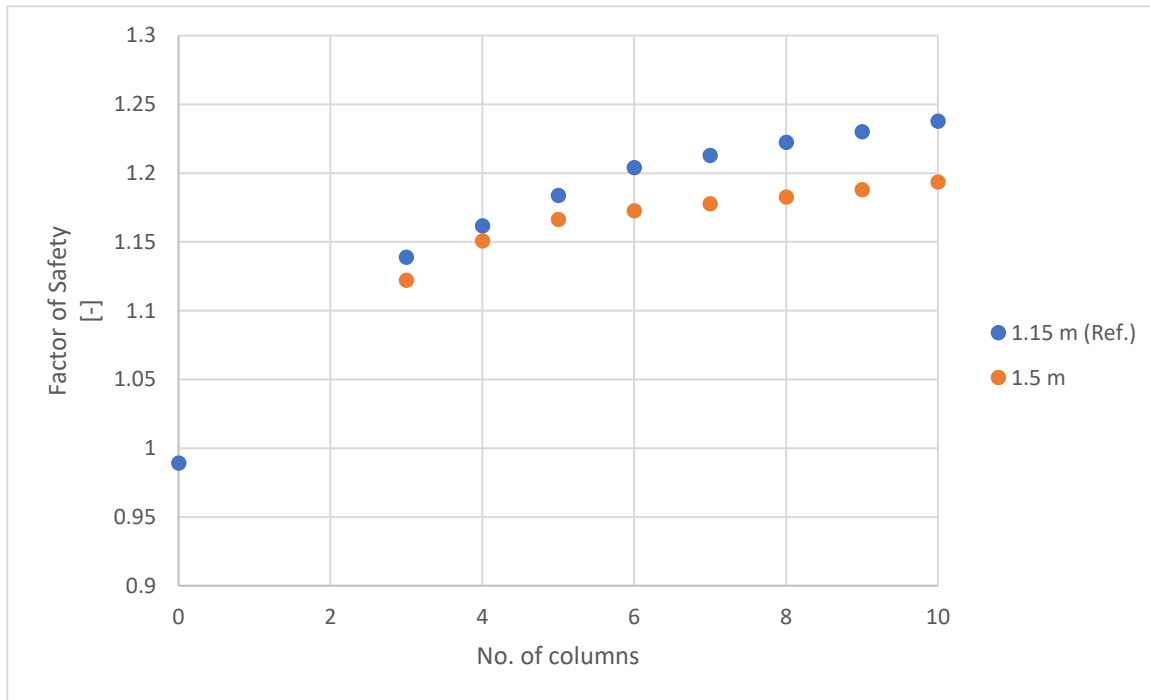


Figure 4-22: Influence of stabilisation column spacing on the FoS.

##### Column depth

The reference design column depth is 5.5 m. The effect on the FoS of 1.5 meters shorter (4 m) and longer (7 m) is shown in Figure 4-23. A column length of 7 meters means that the column is founded on the sand layer. In other cases (4 and 5.5 m) the columns are floating columns. The contribution to the FoS is limited for longer columns. While applying shorter columns leads to a significant reduction of the FoS. This result makes sense, as it affects the main contributors weight and the total lateral expansion. The slip surface for column depths of 5.5m and 7m is similar, for 4m the slip surface is closer to ground level, thus vertical effective stresses are lower, resulting in a lower undrained shear strength.

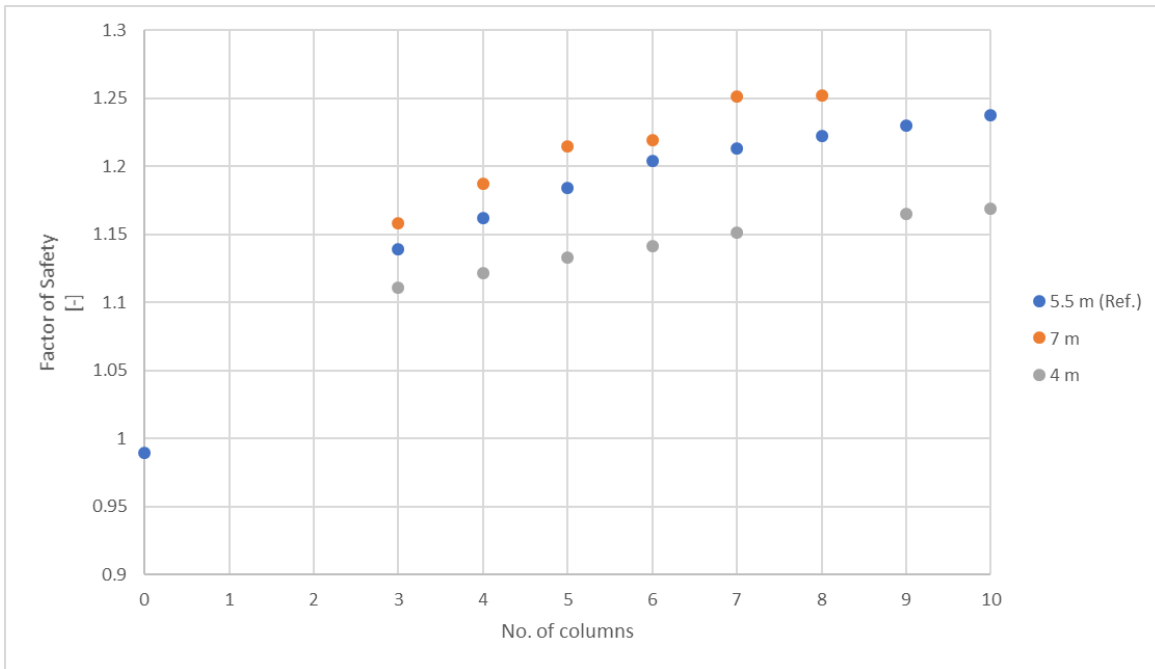


Figure 4-23: Various column lengths versus Factor of Safety.

### Diameter

In the reference design columns of 0.8 m diameter are used. In Figure 4-24 the effect of using a smaller diameter (0.5 m) on the FoS is shown.

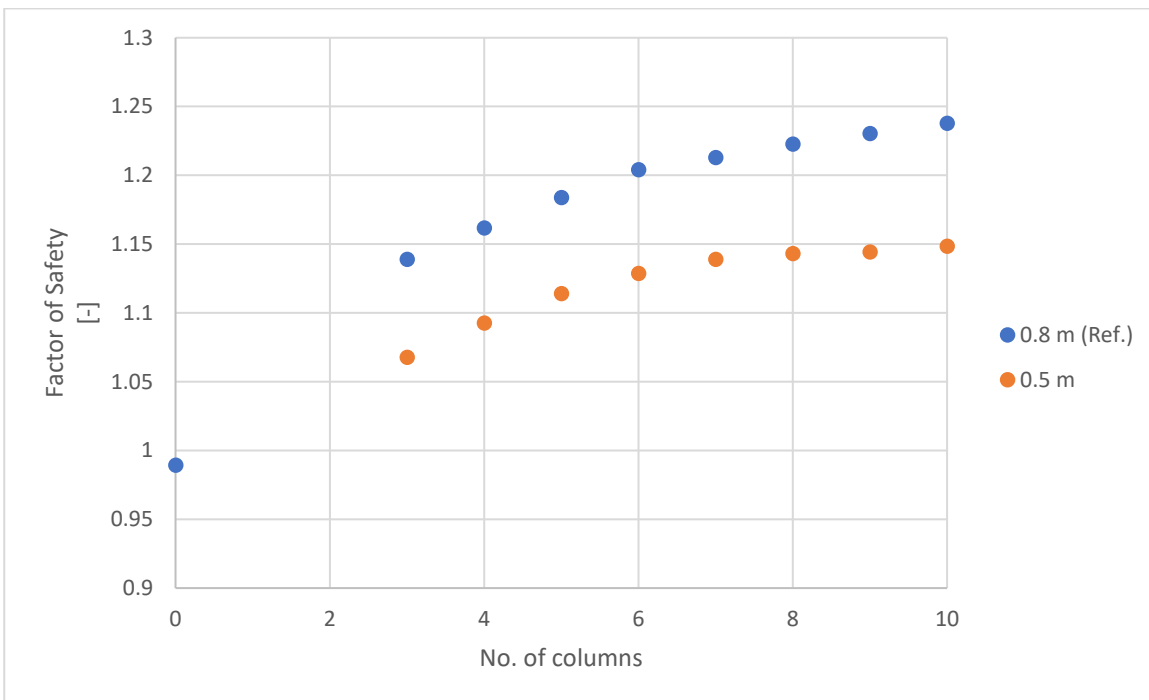


Figure 4-24: Effect of column diameter on FoS.

When a smaller column diameter is applied the FoS is lower. Smaller stabilisation columns means a smaller amount of gravel is added, so the total weight of the columns is less. Besides that, the amount of lateral expansion is less for a column of 0.5 m than for a column of 0.8 m diameter. The column diameter largely determines the effectiveness of the stabilisation columns.

#### 4.4.5 Soil stiffness

In Figure 4-25 the influence of the host clay stiffness on the FoS is shown. The reference FoS is logically a little higher as well and amounts 1.008. The effect of a higher stiffness is negligible. However, looking at Figure 4-26, close to the columns the dots tend to move more towards the trend. For an ever stiffer soil this could mean that points close to the column follow the trend. The influence on K will be higher and therefore the FoS as well.

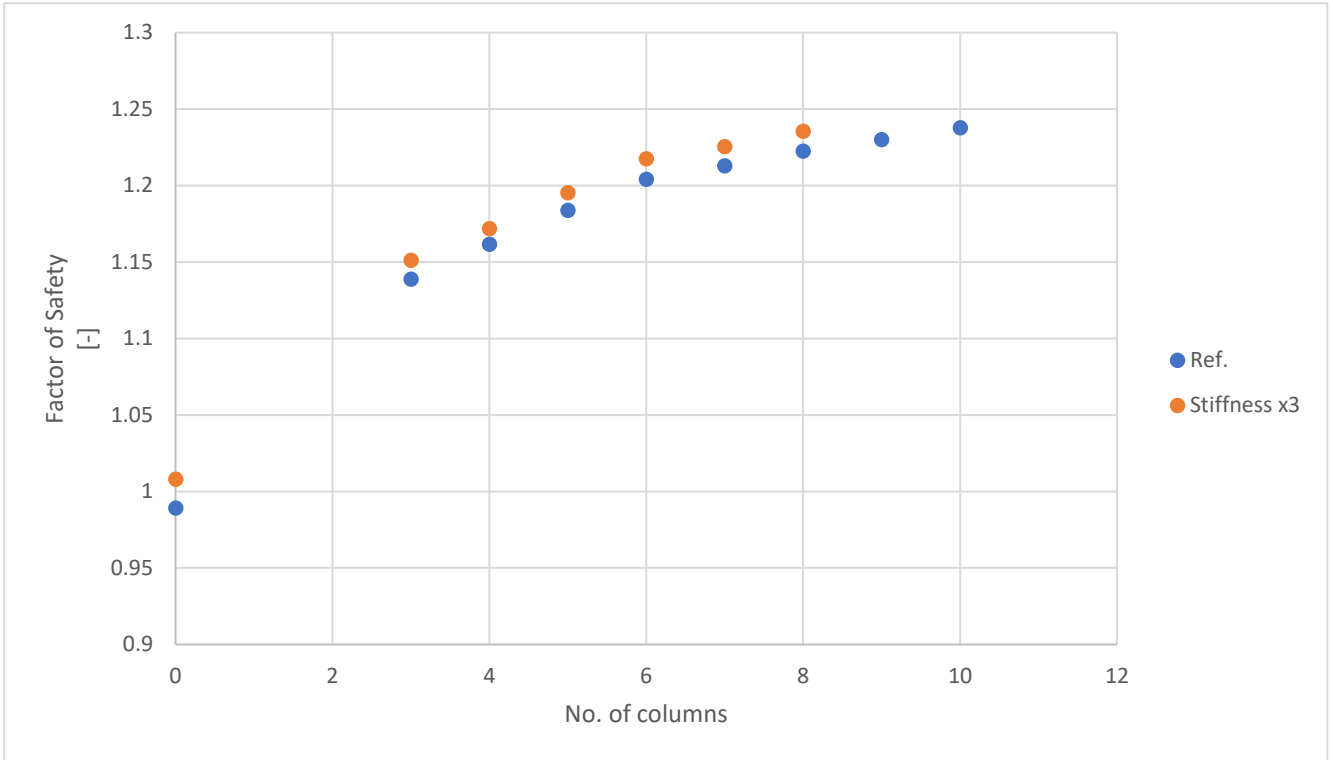


Figure 4-25: Influence of host clay stiffness on the FoS.

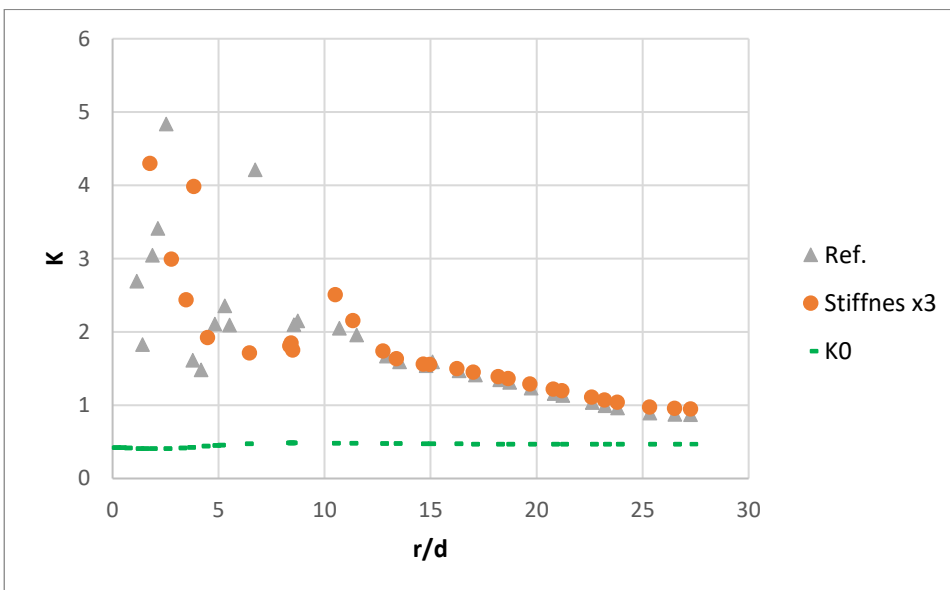


Figure 4-26: Influence of host clay stiffness on the coefficient of lateral earth pressure (K).

#### 4.4.6 Groundwater

The stabilisation columns consist of gravel. Gravel is known to be more permeable than the host clay. Excessive rainfall might fill the columns with water. The columns are floating columns, which means they are not connected to the sandy aquifer, but what happens if there is a connection? This paragraph zooms in on these effects. The cases presented here are extreme case scenarios, the actual effect may be in between.

##### Excessive rainfall

In this case the stabilisation columns are modelled as if they are full of water and the phreatic level increases. As can be seen in Figure 4-27 excessive rainfall does not affect the FoS. The phreatic level is already high, therefore the effect of the extra amount of water is limited. The saturated weight of gravel is higher, than the unsaturated weight. These effects cancel each other out. For other configurations this can be different.

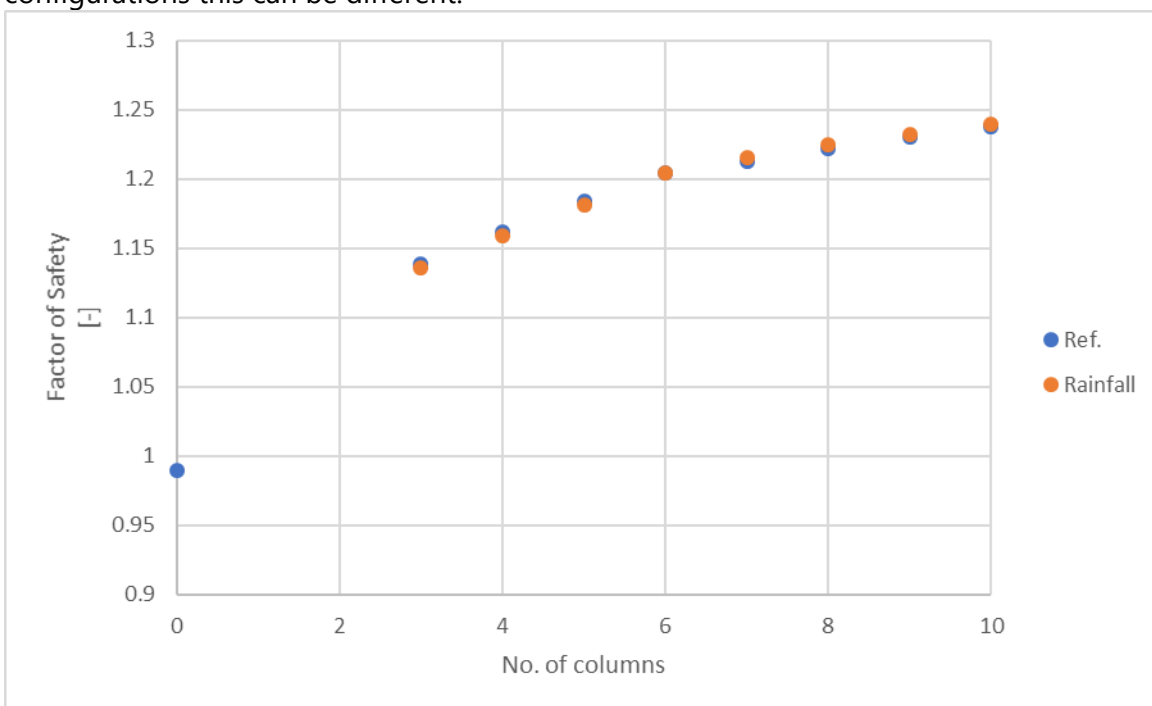


Figure 4-27: Influence of excessive rainfall on the FoS

##### Head in aquifer

The stabilisation columns are floating columns to prevent the occurrence of piping. If the stabilisation columns are in contact with the aquifer water will flow from the aquifer in the columns, for example if the host clay under the stabilisation columns bursts. The stabilisation columns will fill with water. They act as a relief well and draw the head in the aquifer down, since the head is above ground level. This will lower the lifting of the low-permeable clay (aquitard). Vertical effective stresses increase and therefore the FoS as well, which can be seen in Figure 4-28. Generally speaking this is the case or, when the head in the aquifer is lower than the phreatic level the stabilisation columns will drawdown the phreatic level, leading to an increase of the vertical effective stresses as well.

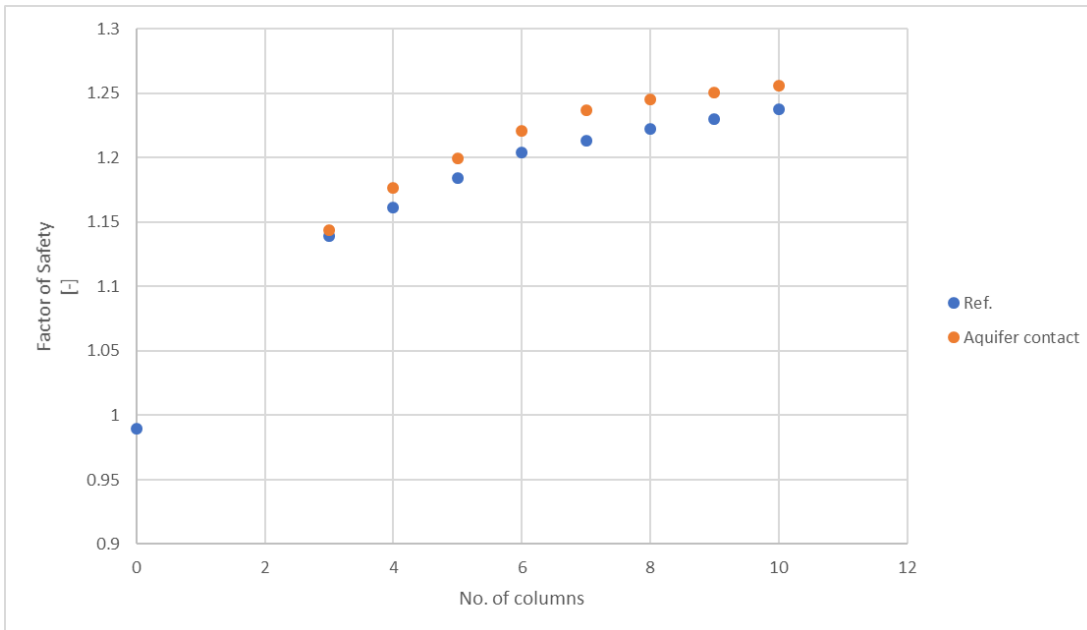


Figure 4-28: Influence of head drawdown on the FoS.

#### 4.4.7 Conclusion

Applying stabilisation columns can be an attractive alternative dike improvement method. A 20% improvement of the FoS is feasible within the current dike footprint. The present berm needs to be extended by 15 m and needs to be higher as well to improve the FoS with a classical berm solution. One interesting aspect, that is not a design choice, is the imposed volumetric strain. Plotting the coefficient of lateral earth pressure (K) versus the normalised radial distance from the stabilisation columns for various imposed volumetric strain percentages gives insight in how effective the stabilisation columns are designed with respect to the benefits arising from the lateral expansion. In the reference design an imposed volumetric strain of 100% leads to a reduction of K close to the stabilisation columns with respect to 50% imposed volumetric strain. The 100% imposed volumetric strain leads to failure of elements from which no strength can be derived anymore. As the lateral expansion is the largest contributor to the FoS, it is wise to adjust other parameters, such as spacing and diameter, in such a way that the full potential of the increase in K close to the columns can be used. Optimising the design might lead to a higher FoS or at least to a reduction of the added gravel. The effects of other aspects are limited and based on the sensitivity analysis comparable results can be achieved for other host soils.

The clay used in the reference case is relatively light weight. Application in heavier clays will decrease the positive weight effect of the gravel inclusion, this decrease is compensated by the effect of the lateral expansion. Geometric properties are logically of influence on the effectiveness of the stabilisation columns, as this influences both the weight and the lateral expansion contribution. The effect of the head drawdown is dependent on the head that is present, as it directly influences the vertical effective stresses. For the reference case this effect is limited.

---

## 5. Discussion

The main goal of this thesis is to show the technical potential of stabilisation columns to improve inner slope stability. This chapter discusses the results of this study and states for which situations the results are applicable. The first part of this study is mainly qualitatively and based on one reference case. An optimal design is case specific, the sensitivity analysis gives quantitative insight and gives directions for designing stabilisation columns.

### 5.1 Results

This study shows that for the design presented the FoS improvement is 14-24%, dependent of the number of stabilisation columns applied. The FoS is mainly improved by the effects of adding weight and a lateral expansion of the stabilisation columns.

#### Weight

The Factor of Safety (FoS) improvement is for 40-50% dependent on the added weight due to the gravel inclusion. A parallel can be seen with the classical solution to improve inner dike slope stability, namely applying a stabilisation berm, which is a well-known weight solution. This gives confidence in this part of the FoS improvement.

#### Lateral expansion

Based on the numerical analysis performed in this Thesis, the FoS improvement is for 50-60% dependent on the changes in stress field as a consequence of the lateral expansion. It is advised to check whether this new stress field represents reality in a field test. This can for example be measured by Cone Penetration Tests (CPT). As stated in chapter 2 no internationally agreed upon closed form equations are available to describe the changes in stress fields. Researchers have performed numerical analyses to better describe the effects of a lateral expansion, which corresponded well to field tests. Performing a numerical analysis in this Thesis is therefore a logical first step.

In this Thesis the effect of a lateral expansion is described in terms of changes to the coefficient of lateral earth pressure ( $K$ ) and is dependent on the radial distance from the stabilisation columns. For means of a stability analysis this is a good method as the position of the critical slip surface is stress dependent as well. The contour plot of  $K$  after column expansion matches very well to the contour plot of the calculated undrained shear strength. Which gives confidence that the changes in stress fields indeed deliver an increase in undrained shear strength. (Benmebarek et al., 2018) performed a numerical analysis where  $K$  is also dependent on the radial distance from the stabilisation columns. They found a good match between the numerical analysis and field tests, but close to the column the field measurements of  $K$  are lower than the numerical results. However, the opposite was measured in field tests by (Watts et al., 2000). (Priebe, 1995) suggests to set  $K=1$  after column installation, which simplifies modelling, but underestimates the effects of a lateral expansion.

Another parameter that is sometimes used to describe the effects of a lateral expansion is the change in soil stiffness. Stress dependent relationships have been derived to describe changes in soil stiffness. Besides that the change in soil stiffness is described indirectly by means of changes in the stress field, the match between numerical analysis and field data by (Benmebarek et al., 2018) is poor. Vice versa, a stiffer soil seems to lead to an increase of the coefficient of lateral earth pressure close to the stabilisation columns. The coefficient of lateral earth pressure is a good parameter to describe the FoS improvement, but soil stiffness can give additional insight.



The FoS improvement (14-24%) is case specific and dependent on host soil conditions. The sensitivity analysis provides some more insight in the generalisability of this solution. For heavier host clays the weight contribution of the gravel is lower. Remarkably, the net increase in FoS is almost the same, meaning the contribution of the lateral expansion is higher. Although there is only one extra case provided, this gives more confidence in the general achievable FoS improvement.

## 5.2 Design considerations

### 5.2.1 Geometry

The fictitious reference dike is simplified with respect to reality, to study the effects of stabilisation columns more precise they should be modelled in a more realistic dike. The reference dike only consists of one low permeable clay top layer, in reality this can consist of multiple soft soil layers. A Pre Overburden Pressure (POP) of 15 kPa was assigned to the entire clay layer. It's more realistic to have a higher POP value under the dike than next to the dike. The reference case is designed in such a way that the FoS is close to 1, this is useful for comparing results. A FoS of  $\pm 1$  is the lowest for which PLAXIS can perform stable calculations. This makes the reference case sensitive to changes.

The modelled ditch is very large, which can be the case, but will usually be smaller. For a smaller and/or shallower ditch relatively more of the host soil can be replaced by stabilisation columns. This will have a positive effect on the FoS.

### 5.2.2 Modelling stabilisation columns

Simplifications in material properties or column dimensions are required to translate a 3D problem into a 2D model. Generally spoken it is wise to use 2D calculations for determining the optimal design and to check this optimal design by a 3D calculation to assess whether these simplifications are justified and to exclude the possibility of soil cutting between the columns. In this Thesis a 3D calculation gave adequate results with respect to the 2D Plane Strain method with an effective width and cutting of soil between the columns did not occur, the first is in line with the results presented by (Zhang et al., 2013). The 3D calculation in this study was for a row of 6 stabilisation columns. For fewer stabilisation columns and a larger spacing the possibility of a slip surface cutting between the stabilisation columns is not investigated.

Placing stabilisation columns under and close to the ditch contributes most to the FoS. For the so called 'uplift' conditions the ditch is the weak spot, as the vertical effective stresses are low, the slip surface usually ends here. In the case presented in this study the stabilisation columns are installed under and close to the ditch, but the position of the columns is not varied to find an optimal design. Perceived slip surfaces where either 1) cutting through the stabilisation columns closest to the dike towards the ditch/ground level for 3-5 columns or 2) forced below the stabilisation columns for 6-10 columns. In the first case, the FoS can be improved by adding more stabilisation columns towards the dike, as is done in this study. In the second case the slip surface ends at the other side of the ditch seen from the dike. To further improve stability it is expected to be more beneficial to place stabilisation columns at this point than an extra column towards the dike, this is not done in this study.

In reality the stabilisation columns are installed by means of a ground displacing method, while modelling them can only be done by replacing part of the host clay by a stabilisation column. Thus, the added amount of weight is underestimated. It is a safe assumption not taking this into account, but the FoS can be higher.

The stabilisation column installation is simplified with respect to reality. Columns are installed by means of a ground displacing method. A vibrating probe is lowered to final design depth. The probe is slightly retracted and the gravel fills the cavity created. The probe then compacts the gravel and pushes it in the surrounding host soil. This is repeated stepwise up to design/ground level. The stabilisation columns are installed alternately. In the PLAXIS model the columns are installed all at once and expand all at once over full column length.

One of the assumptions is that the floating columns are not in contact with the aquifer. So, no water flows from the aquifer to the columns and piping is prevented. CPT can be used to determine the placement depth. On the other hand, the sensitivity analysis indicated that contact between the aquifer and the stabilisation columns and the accompanying flow and lowering of the head in the aquifer, can be beneficial. A flow analysis can be performed to determine the precise effect on the phreatic surface and the head in the aquifer under daily circumstances.

### 5.2.3 Modelling lateral expansion

The lateral expansion is key in the FoS improvement. The lateral expansion is based on the assumption that expanding half a column to full column width represents the changes in stress states in reality. Some researchers use other definitions of the column diameter before expansion, not deviating much. Based on the sensitivity analysis the FoS is not very sensitive to other imposed strain percentages.

The effectiveness of the lateral expansion can be determined by looking at the coefficient of lateral earth pressure ( $K$ ). (Benmebarek et al., 2018) show a clear increasing trend of  $K$  towards the stabilisation columns. In this Thesis the observed trend is similar, but the influence on  $K$  is higher. In this Thesis the depth at which  $K$  is defined is closer to ground level, in combination with the lower host clay weight the confining pressure is lower, which leads to a larger lateral expansion. Close to the stabilisation column scatter of  $K$  is perceived in contradiction to the results presented by (Benmebarek et al., 2018). If there is no scatter close to the column the effect of the lateral expansion on  $K$  is higher and therefore the FoS as well. This can be achieved by changing the stabilisation column configuration.

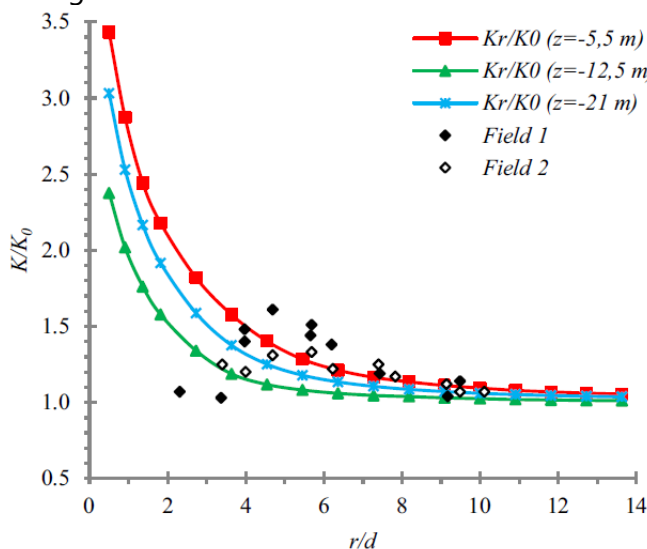


Figure 5-1: Comparison of  $K_r/K_0$  evaluated numerically with  $K/K_0$  of field measurements by (Kirsch, 2006), (Benmebarek et al., 2018).

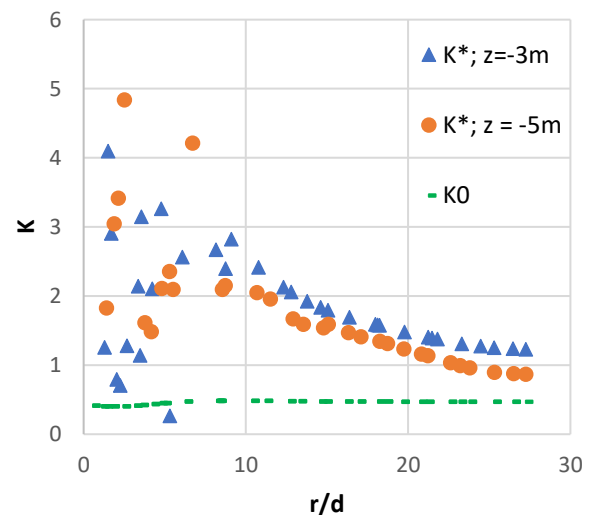


Figure 5-2:  $K^*$  at  $z=-3\text{m}$  and  $z=-5\text{m}$ , starting from the most right column to the right.  $K_0$  is the initial coefficient of lateral earth pressure,  $K^*$  is the one after column expansion.  $r$  is the distance from the column [m],  $d$  the column diameter [m].

That the influence of the lateral expansion is present at some distance from the stabilisation columns is expected. Looking at the change of the coefficient of lateral earth pressure this can still be seen at the model boundary. Although it is not likely that this boundary influences the result, since it is far away, it cannot be excluded. When the boundary is moved further away PLAXIS cannot solve the stiffness matrix. The expectation is that the low weight of the host clay plays a role in combination with the updated mesh calculations. Due to the low weight the effective stresses are low and are therefore sensitive to minor changes in the stress field. (Benmebarek et al., 2018) show a similar result, where plastic points close to ground level extent until the model boundary, as can be seen in Figure 5-3.

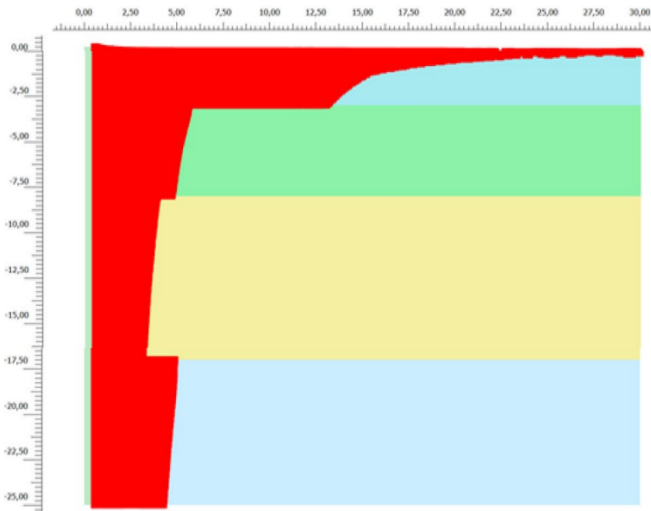


Figure 5-3: Plastic points in soft soil after column installation. (Benmebarek et al., 2018)

---

## 6. Conclusion

This chapter presents the conclusion of this study and answers the research questions. The research questions are partly answered by means of a qualitative analysis based on the theoretical background presented in chapter 2 and partly by means of a qualitative and quantitative case study in chapter 3. The main research question of this study is:

**What is the technical potential of using Stabilisation Columns for improving inner slope stability of dikes under uplift conditions in soft soils?**

In the reference case presented the FoS improvement is 14-24% for applying 3-10 stabilisation columns in a row perpendicular to the dike in a triangular grid. Achieving a comparable result in terms of FoS improvement requires the stabilisation berm to be extended by 15m and heightened by 0.5m. This classical solution for improving inner slope stability is space consuming, where the stabilisation columns can improve inner slope stability within the current footprint. From a technical potential point of view using stabilisation columns is an appealing alternative to improve inner slope stability. The sensitivity analysis in this study indicates that the FoS improvement can be achieved for different host soils as well. Optimising the stabilisation column design might even lead to a higher FoS or reducing of the fill material used.

For a large part of the dikes in Western Netherlands uplift conditions can be a problem, where a high head in the aquifer results in low effective stresses at the interface between the low permeable top layer and the permeable aquifer. By installing stabilisation columns gravel is added, which typically weighs more than the host soft soils. A higher weight leads to an increase in vertical effective stresses, in this way lifting of the low permeable top layers is prevented.

The main research question is supported by the following sub-questions:

1. *What are the effects of stabilisation columns on inner slope stability?*

Stabilisation columns are a ground improvement method. It improves the host soil, mainly clay and peat, by the inclusion of a firmer material, such as gravel. Gravel improves the host soil by 1) a higher volumetric weight and 2) a strength increase. Installing stabilisation columns by means of a vibro displacing method will also lead to 3) a lateral expansion of the stabilisation columns and, as a consequence, of the host soil as well.

In accordance with Dutch regulations the SHANSEP model is used for modelling undrained shear strength of clays below the phreatic surface. The undrained shear strength consists amongst others of a stress and a strength component. An increase in weight and strength will therefore directly lead to an increase in undrained shear strength and thereby to a higher Factor of Safety (FoS). For the increase in weight the FoS increases of 5-10% for 3-7 stabilisation columns. Applying more than 7 columns hardly contributes to the FoS.

An increase in strength, by means of an increase in friction angle ( $\varphi$ ) and undrained shear strength ratio ( $S$ ), does hardly contribute to a higher FoS. The columns are floating columns, which means that their base is not founded on a rigid sand layer, but is still in the soft top layer soil. A strength increase forces the slip surface directly below the stabilisation columns through the soft soil irrespective of the number of columns applied.

The third contribution to inner slope stability is a lateral expansion of the stabilisation columns. Due to the expansion of the columns the stress state of the host soil changes significantly. The coefficient of lateral earth pressure ( $K_r = \sigma'_r / \sigma'_z$ ) changes from its initial value  $\pm 0.5$  to 1-3, dependent on the distance from the columns. The observed trend compares well with the trend observed by (Benmebarek et al., 2018) and conducted field experiments by (Kirsch, 2006). The principal stress directions change due to the column expansion from predominantly vertical to horizontal. PLAXIS uses the principal stress direction to calculate the undrained shear strength and the FoS. Due to inclusion of gravel and the lateral expansion the FoS increases by 14-24% for 3-10 stabilisation columns. The effect of the lateral expansion on the FoS is approximately 9-14%.

## 2. *How can the effects of stabilisation columns on inner slope stability be modelled?*

In this thesis various modelling techniques are used to model the effects of stabilisation columns on inner slope stability. The methods used are the 2D Soil Homogenisation method, a 2D Plane Strain method where the width of the column is reduced (PSw), a 2D Plane Strain method where the strength is reduced (PSs) and a 3D slice model. The SH and PS methods can be used with the Uplift-Van method in D-Stability. All methods can be modelled within PLAXIS.

### **Weight and strength**

The effects of weight and strength can be modelled separately by means of the SH and PSw method. The results presented in this Thesis show good agreement between both methods for both the weight as the strength increase. The PSs method is not suited to study the effect of a weight or strength increase as this method assumes the Plane Strain column width equal to the column diameter given that all soil strength parameters are reduced.

### **Lateral expansion**

In this Thesis the lateral expansion is modelled by a 2D PSw. For one configuration the 2D model is compared to a 3D PLAXIS calculation. The outcome of these calculations matched very well, as is in line with the results presented by (Zhang et al., 2013). The effects of a lateral expansion can thus be modelled in 2D and 3D. For designing stabilisation columns the 2D method is more appropriate, as 3D calculation time is significantly longer. A final 2D design can be checked by a 3D calculation to check whether the 2D simplifications also holds for other stabilisation column configuration and to exclude the effect of soil cutting between the stabilisation columns. The latter can be done by means of an analytical check as well and did not occur in the 3D calculation in this Thesis. Other methods to model a lateral expansion are the SH method and the PSs. When field data is available the SH method can be used for back-analysis, no field data was available for this Thesis, so this method is not used. In this Thesis the PSs method did not lead to stable calculations.

The lateral expansion is applied to the stabilisation columns by applying a volumetric strain in x-direction ( $\epsilon_{xx}$ ). Based on literature expanding half a column to full column width represents the changes in the stress field well. This means an imposed volumetric strain of 100%. Imposing a lateral displacement by means of a line displacements is not possible, since the problem is not axisymmetric. When using the PSw method the lateral expansion cannot be assigned to the host clay, but only to the gravel stabilisation columns, in contradiction to the increase in weight and strength. The effects of a lateral expansion on the FoS can only be back-calculated by subtracting the effects of an increase in weight and strength.

### *Physical stability*

The ditch is the weak spot in the lateral expansion and stability calculations. It's necessary to fill the ditch with sand to prevent a local slope instability during stabilisation column installation.

### *Numerical stability*

A lateral expansion generates large strains. To perform stable calculations it's necessary to use the 'updated mesh' option in PLAXIS. This option is activated for the column expansion phase and must be switched on for all follow-up phases. The more columns are installed, the larger the displacements are. Lowering the max load fraction per step, a numerical control parameter in PLAXIS, will increase the number of steps in which the load is applied. In this way stable calculations can be performed that describe the kinetics of the deformation process well. As the number of steps increase it might be necessary to increase the maximum number of calculations steps in the expansion phase as well.

### *3. Which aspects are of influence in order to efficiently apply stabilisation columns?*

Based on the results of the reference case the improvement of the FoS is dependent on the increase in weight and the effect of the lateral expansion. Thus aspects influencing one of these effects are expected to influence in the efficiency of the stabilisation columns. The first aspect for which this holds is the column diameter. Both effects are quadratically dependent on the column diameter. The weight by means of the area and thus the total volume of added gravel and the lateral expansion by means of the effective width that is used to model stabilisation columns in 2D. Another aspect that determines the efficiency of model the column depth. The column depth needs to be picked in a way that it forces the slip surface down to the top of the aquifer. It is case specific, but 1.5m above the aquifer seems a good starting point.

One interesting aspect, that is not a design choice, is the imposed volumetric strain. Plotting the coefficient of lateral earth pressure (K) versus the normalised radial distance from the stabilisation columns for various imposed volumetric strain percentages gives insight in how effective the stabilisation columns are designed with respect to the benefits arising from the lateral expansion. In the reference design an imposed volumetric strain of 100% leads to a reduction of K close to the stabilisation columns with respect to 50% imposed volumetric strain. The 100% imposed volumetric strain leads to failure of elements from which no strength can be derived anymore. As the lateral expansion is the largest contributor to the FoS, it is wise to adjust other parameters, such as spacing and diameter, in such a way that the full potential of the increase in K close to the columns can be used. Optimising the design might lead to a higher FoS or at least to a reduction of the added gravel. The effects of other aspects are limited and based on the sensitivity analysis comparable results can be achieved for other host soils.

Modelling stabilisation columns is very much dependent on the interaction of the various aspects in relation to the effects of weight and lateral expansion. It's most efficient to start a design with a large column diameter and long columns and continue the design in such a way that the full potential of the lateral expansion can be used, preventing the host soil from failing.

## **6.1 Recommendations**

As stated earlier a field test is necessary to check the validity of the influence of the lateral expansion. This changes in the stress field can be measured by CPT. Another advantage of performing a field test is that it will give more insight in how other host soils will respond to this lateral expansion. The sensitivity analysis indicates that for a heavier host soil, the effect of the lateral expansion on the FoS

will be higher. The fictitious case presented is simplified with respect to reality. By performing a field test the initial stress field can be simulated more precise, of which the influence needs to be established.

The effect of stabilisation columns on the phreatic surface and the head in the aquifer and the possible occurrence of piping is neglected in this thesis. The sensitivity analysis in this study indicates that including the change in head might be contributory. It is worth investigating this, as it could reduce the number of stabilisation columns required.

This Thesis shows that stabilisation columns have technical potential and are a good alternative for a classical stabilisation berm. The technical potential does not include costs, it needs to be investigated whether stabilisation columns are an attractive alternative in this respect as well. Design manufacturability is not considered for cases where power lines or gas pipes are present in the stabilisation columns surrounding. Also the effect of the lateral expansion on adjacent building needs to be investigated or monitored during construction.

It is strongly advised to use remote scripting for designing dikes with stabilisation columns. Modelling a lateral expansion to multiple columns requires many actions. The sensitivity analysis provides insight in the sensitive parameters, but does not give an optimal design. It's not likely that the first design leads to an optimal design.

Large parts of western Netherlands are prone to settlements. Originally stabilisation columns are used to reduce settlements. This study shows that stabilisation columns can be used to improve inner slope stability. A follow-up study can combine both advantages, this makes applying stabilisation columns even more attractive.

## 7. Literature

- Al-Ani, W. & Wanatowski, D. (2017). *Settlement analysis of floating stone columns*. In: Proceedings of the 19th International Conference on Soil Mechanics and Geotechnical Engineering. ICSMGE 2017: 19th International Conference on Soil Mechanics and Geotechnical Engineering, 17-22
- Bakker, K. J., & Vrijling, J. K. (2013). *Levees and dikes constructed on Soft Saturated soil*. Delft: Delft University of Technology. Retrieved from <https://www.wad43.nl/publications/5a8c1394046e7363ce4861e4aa0b23cc.pdf>
- Benmebarek, S., Abdeldjalil, R., & Benmebarek, N. (2018). Numerical Modelling of Stone Column Installation Effects on Performance of Circular Footing. *International Journal of Geosynthetics and Ground Engineering*, 4. doi:10.1007/s40891-018-0140-z
- Brinkgreve, R. B. J., Zampich, L. M., & Ragi Manoj, N. (2019). PLAXIS 2D Reference Manual 2019. Delft: PLAXIS. Retrieved from [https://www.plaxis.com/?plaxis\\_download=2D-2-Reference.pdf](https://www.plaxis.com/?plaxis_download=2D-2-Reference.pdf)
- Castro, J. (2017). Modeling Stone Columns. *Materials*, 10, 782. doi:10.3390/ma10070782
- Castro, J., & Karstunen, M. (2010). Numerical simulations of stone column installation. *Canadian Geotechnical Journal*, 47, 1127-1138. doi:10.1139/T10-019
- Civieltechnisch Centrum Uitvoering Research en Regelgeving (CUR) (1996). *CUR 162: Building on soft soils*. Rotterdam: A. A. Balkema.
- Civieltechnisch Centrum Uitvoering Research en Regelgeving (CUR) (2003). *Bepaling geotechnische parameters*. Gouda: CUR.
- Egan, D., Scott, W., & McCabe, B. (2008). Observed installation effects of vibro replacement stone columns in soft clay. *Proceedings of the 2nd International Workshop on the Geotechnics of Soft Soils, Glasgow*, 23–30.
- Elshazly, H., Elkasabgy, M., & Elleboudy, A. (2007). Effect of Inter-Column Spacing on Soil Stresses due to Vibro-Installed Stone Columns: Interesting Findings. *Geotechnical and Geological Engineering*, 26(2), 225. doi:10.1007/s10706-007-9159-y
- Foray, P., Flavigny, E., Nguyen, N.T., Lambert, S., Briançon, L. (2009). *3D numerical modeling of stone columns and application*. Proceedings of the 17th International Conference on Soil Mechanics and Geotechnical Engineering. DOI: <https://doi.org/10.3233/978-1-60750-031-5-2382>, pp. 2382-2385
- Gaber, M., Kasa, A., Abdul-Rahman, N., & Alsharif, J. (2018). Simulation of Stone Column Ground Improvement (Comparison between Axisymmetric and Plane Strain). *American Journal of Engineering and Applied Sciences*, 11(1), 129-137.
- Hurley, O., Nuth, M., & Karray, M. (2015). Finite element modelling of stone column installation: review of modelling practices and case study with Plaxis 2D. *68e Conférence Canadienne de Géotechnique*.
- Iereidis, C. (2019). *Implementation of the New Dutch Guidelines on the Macrostability Assessment of Dikes using Different Constitutive Models* (Master's thesis). Retrieved from <https://repository.tudelft.nl/islandora/object/uuid%3Aa8cdf86-66a7-4251-afa4-c9a040e7ae7b>
- Jonkman, S. N., Jorissen, R. E., Schweckendiek, T., & van den Bos, J. P. (2018). *Flood defences*. (Lecture notes CIE5314). Delft: Delft University of Technology
- Keller Group. (2019). *Deep Vibro Techniques*. Retrieved from [https://www.kellerholding.com/deep-vibro-techniques.html?file=files/keller/downloads/publications/Keller\\_10-02E\\_Deep-Vibro-Techniques.pdf](https://www.kellerholding.com/deep-vibro-techniques.html?file=files/keller/downloads/publications/Keller_10-02E_Deep-Vibro-Techniques.pdf)
- Kirsch, F. (2006). Vibro Stone Column Installation and its Effect on Ground Improvement. *Numerical simulation of construction processes in geotechnical engineering for urban environment*, 115-124.
- Koopmans, R., Meindert, V., van der Krogt, M., Kanning, W., Halter, W., Steenbrink, R., ... Gerritsen, R. (2018). *POVM Grondverbeteringen*. Tiel: POVM. Retrieved from [https://www.povmacrostabiliteit.nl/wp-content/uploads/2015/03/publicatie\\_POVM-Grondverbeteringen.pdf](https://www.povmacrostabiliteit.nl/wp-content/uploads/2015/03/publicatie_POVM-Grondverbeteringen.pdf)
- Naves, T., & Lengkeek, H. J. (2017). *SHANSEP NGI-APD validatie cases*. Tiel: POVM. Retrieved from <https://www.povmacrostabiliteit.nl/wp-content/uploads/2015/03/Validatie-SHANSEP-NGI-ADP.pdf>
- Nederlands Normalisatie-instituut (NEN). (2017). *NEN-EN 1997-2*. Delft: NEN
- Ng, K. S. (2013). Cavity Expansion Approach In Modelling Stone Column Installation Effect. *International Journal of Advances in Engineering Science and Technology*, 2, 252-260. doi:10.13140/2.1.4240.8649



- Ng, K. S., & Tan, S. A. (2015). Settlement Prediction of Stone Column Group. *International Journal of Geosynthetics and Ground Engineering*, 1(4), 33. doi:10.1007/s40891-015-0034-2
- Obrzud, R. F. T., A. & Truty, A. (2018). *The Hardening Soil Model - a practical guidebook*. Prévèrènges, Switzerland: Zace Services Ltd, Software engineering.
- PLAXIS (2019). PLAXIS Materials Models Manual 2019. Delft: PLAXIS.
- Projectoverstijgende Verkenning Macrostablieiteit (POVM) (2018). *POVM Rekentechnieken - EEM toepassing binnen het ontwerp*. Tiel:POVM. Retrieved from [https://www.povmacrostablieiteit.nl/wp-content/uploads/2015/03/POVM-EEM-Versie-1\\_0-Concept.pdf](https://www.povmacrostablieiteit.nl/wp-content/uploads/2015/03/POVM-EEM-Versie-1_0-Concept.pdf)
- Priebe, H. J. (1995). *The design of vibro replacement*. Offenbach: GeTec. Retrieved from <http://citeseerx.ist.psu.edu/viewdoc/download?doi=10.1.1.476.4454&rep=rep1&type=pdf>
- Randolph, M. F., & Wroth, C. P. (1979). An analytical solution for the consolidation around a driven pile. *International Journal for Numerical and Analytical Methods in Geomechanics*, 3(3), 217-229. doi:10.1002/nag.1610030302
- Sexton, B., & McCabe, B. (2014). Modeling stone column installation in an elasto-viscoplastic soil. *International Journal of Geotechnical Engineering*, 9, 150219055907009. doi:10.1179/1939787914Y.0000000090
- Simanjuntak, Y., Goeman, D., Koning, M., & Haasnoot, J. (2018). SHANSEP Approach for Slope Stability Assessments of River Dikes in The Netherlands. *Proceedings of the 9th European Conference on NUMGE*, Porto: CRC Press, pp. 317-326.
- Sivasithamparam, N., & Castro, J. (2018). Undrained expansion of a cylindrical cavity in clays with fabric anisotropy: theoretical solution. *Acta Geotechnica*, 13(3), 729-746. doi:10.1007/s11440-017-0587-4
- 't Hart, R. (2018). *Fenomenologische beschrijving, Faalmechanismen WBI rapport 11200574-007*. Delft: Deltares. Retrieved from [https://www.helpdeskwater.nl/publish/pages/132666/11200574-007-geo-0005-r-fenomenologische\\_beschrijving\\_hgn\\_adl.pdf](https://www.helpdeskwater.nl/publish/pages/132666/11200574-007-geo-0005-r-fenomenologische_beschrijving_hgn_adl.pdf)
- Vergouwe, R. (2016). *The national flood risk analysis for the Netherlands: final report*. Rijkswaterstaat VNK Project Office. Retrieved from <https://www.helpdeskwater.nl/publish/pages/131663/vnk-rapport-eng-lr.pdf>
- Verruijt, A. (2001). Soil Mechanics. Delft: Delft University of Technology. Retrieved from <https://ocw.tudelft.nl/wp-content/uploads/SoilMechBook.pdf>
- Vrijling, J.K., Schweckendiek, T., & Kanning, W. (2011). Safety standards of flood defenses. In N. Vogt, B. Schuppener, D. Straub, & G. Brau (Eds.), *Proceedings of the 3rd International Symposium on Geotechnical Safety and Risk, ISGSR 2011* (pp. 67-84).
- Watts, K. S., Johnson, D., Wood, L. A., & Saadi, A. (2000). An instrumented trial of vibro ground treatment supporting strip foundations in a variable fill. *Géotechnique*, 50(6), 699-708. doi:10.1680/geot.2000.50.6.699
- WBI2017. (2016). *Schematiseringshandleiding macrostablieiteit*. Utrecht: Ministerie van Infrastructuur en Milieu. Retrieved from [https://www.helpdeskwater.nl/publish/pages/132667/05\\_shmacrostablieiteit\\_31jan2017.pdf](https://www.helpdeskwater.nl/publish/pages/132667/05_shmacrostablieiteit_31jan2017.pdf)
- Wikipedia. (2012). Slope stability analysis. Retrieved from [https://en.wikipedia.org/wiki/Slope\\_stability\\_analysis](https://en.wikipedia.org/wiki/Slope_stability_analysis)
- Zahmatkesh, A. (2010). Settlement Evaluation of Soft Clay Reinforced by Stone Columns, Considering the Effect of Soil Compaction. *Intl. J. of Research and Reviews in Applied Sciences*, 3(2): 159-166.
- Zhang, Z., Han, J., & Ye, G. (2013). Numerical Investigation on factors for deep-seated slope stability of stone column-supported embankments over soft clay. *Engineering Geology*, 168. doi:10.1016/j.enggeo.2013.11.004
- Zukri, A., & Nazir, R. (2018). Sustainable materials used as stone column filler: A short review. IOP Conference Series: Materials Science and Engineering, 342, 012001. doi:10.1088/1757-899x/342/1/012001
- Zwanenburg, C., van Duinen, A., & Rozing, A. (2013). *Technisch Rapport Macrostablieiteit*. Delft: Deltares. Retrieved from <http://resolver.tudelft.nl/uuid:e2653e5d-f068-46e7-b2c7-b9e14a003782>

# Appendices

# Appendix A - Stability analysis

According to (POVM, 2018) it is obligated for a so called green dike (without constructive elements) to compare calculations with a FEM (Plaxis 2D) and slip plane calculations (D-Stability). At high water conditions the position of the slip plane should match and differences in calculated stability factor should be in the range of six percent.

## A.1 Plaxis

Plaxis 2D is a Finite Element package that can be used for two-dimensional stability analysis. It consists of a number of constitutive models, the relevant ones are explained in this paragraph.

### A.1.1 Hardening Soil model

According to (Obrzud, 2018) and references therein the Hardening Soil model was designed to reproduce:

- *"densification, i.e. a decrease of voids volume in soil due to plastic deformations;*
- *stress dependent stiffness, i.e. observed phenomena of increasing stiffness moduli with increasing stress level (mean stress);*
- *soil stress history, i.e. accounting for preconsolidation effects;*
- *plastic yielding, i.e. development of irreversible strains with reaching a yield criterion;*
- *dilatation, i.e. an occurrence of negative volumetric strains during shearing."*

According to (*POVM Rekentechnieken – EEM toepassing binnen het ontwerp*, 2018) the Hardening Soil (HS) model should be applied for sand, clay and peat without time dependent effects. The HS model resembles the well-known Mohr-Coulomb (MC) model. According to (Plaxis, 2019):

*"In contrast to the MC model, the yield surface of a hardening plasticity model is not fixed in principal stress space, but it can expand due to plastic straining (...) Since the failure criteria in this model obeys Mohr-Coulomb failure criteria, the state of stress in plastic range is described by means of  $\phi$ ,  $c$  as for the MC model. However, soil stiffness is described much more accurately by defining three different stiffnesses corresponding to the loading condition as: (a) the triaxial loading stiffness ( $E_{50}^{ref}$ ), (b) the triaxial unloading stiffness ( $E_{ur}^{ref}$ ), and (c) the oedometer loading stiffness ( $E_{oed}^{ref}$ )."* Relations have been formulated to take shear hardening (deviatoric hardening) and cap hardening (volumetric/compression hardening) into account. The shear hardening is mainly dependent on the triaxial moduli  $E_{50}^{ref}$  and  $E_{ur}^{ref}$ . Whereas the cap hardening mainly depends on the pre-consolidation stress, where the  $E_{oed}^{ref}$  (c) describes the plastic strains originating from the yield cap."

The angle of the critical state line is determined by the friction angle  $\Phi_{cs}$ . The angle between the plastic strain vector and the vertical is determined by the dilatancy angle  $\psi$ .

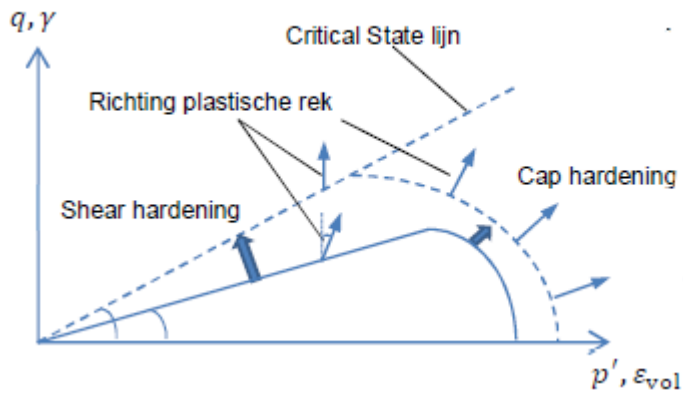


Figure A1: Hardening Soil model with shear- and cap hardening. Dutch: Richting plastische rek -> English: Towards plastic strain. Dutch: lijn -> English: Line (*POVM Rekentechnieken – EEM toepassing binnen het ontwerp*, 2018)

For the Hardening Soil model the relevant parameters are listed in Table A1.

Table A1: Hardening Soil model parameters

| Parameter                                     | Description  | [Default] value                     | Units                |
|---|--|-------------------------------------|----------------------|
| <b>Strength parameters as in Mohr-Coulomb</b> |  |                                     |                      |
| $c'$  | Effective cohesion                                 | -                                   | [kN/m <sup>2</sup> ] |
| $\phi'$                                       | Effective angle of internal friction               | -                                   | [°]                  |
| $\psi$  | Angle of dilatancy                                 | -                                   | [°]                  |
| <b>Stiffness parameters</b>                   |  |                                     |                      |
| $E_{50}^{ref}$                                | Secant stiffness in standard drained triaxial test | -                                   | [kN/m <sup>2</sup> ] |
| $E_{oed}^{ref}$                               | Tangent stiffness for primary oedometer loading    | -                                   | [kN/m <sup>2</sup> ] |
| $E_{ur}^{ref}$                                | Unloading/reloading stiffness                      | $[3 \cdot E_{50}^{ref}]^{1)}$       | [kN/m <sup>2</sup> ] |
| m   | Power for stress-level dependency of stiffness     | Sand [0.5];<br>Clay, peat [0.8-1.0] | [-]                  |
| <b>Advanced parameters</b>                    |  |                                     |                      |
| $\nu_{ur}$                                    | Poisson's ratio                                    | $[0.2]^{1)}$                        | [-]                  |
| $p^{ref}$                                     | Reference stress for stiffness                     | $[100]^{1)}$                        | [kN/m <sup>2</sup> ] |
| $K_0^{nc}$                                    | $K_0$ -value for normal consolidation              | $[1 - \sin\phi]^{1)}$               | [-]                  |
| $R_f$   | Failure ratio $q_f / q_a$                          | $[0.9]^{1)}$                        | [-]                  |
| $\sigma_{tension}$                            | Allowable tensile strength                         | $[0]^{1)}$                          | [kN/m <sup>2</sup> ] |

1) (Plaxis, 2019)

### A.1.2 Soft Soil Creep model

The Soft Soil Creep (SSC) model should be applied if time dependent processes (creep) needs to be modelled in clay and peat. The Soft Soil Creep model can simulate the behavior of normally consolidated soft soils. The SSC model resembles the HS model, but doesn't allow for shear hardening (Figure A2). Relevant parameters are listed in Table A2.

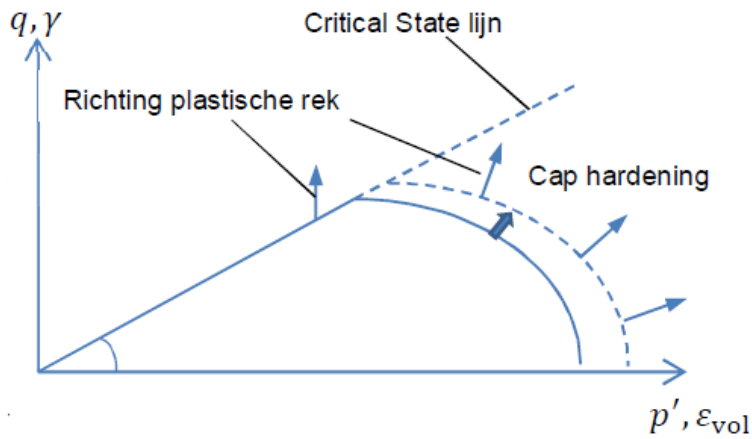


Figure A2: Soft Soil Creep model with Cap hardening. Dutch: Richting plastische rek -> English: Towards plastic strain. Dutch: lijn -> English: Line (*POVM Rekentechnieken – EEM toepassing binnen het ontwerp*, 2018)

Table A2: Soft Soil Creep [default] parameters

| Parameter                                     | Description                             | [Default] value                            | Units                |
|---|---|--|----------------------|
| <b>Strength parameters as in Mohr-Coulomb</b> |   |  |                      |
| $c'$  | Effective cohesion                      | -  | [kN/m <sup>2</sup> ] |
| $\phi'$                                       | Effective friction angle                | -  | [°]                  |
| $\psi$  | Dilatancy angle                         | -  | [°]                  |
| <b>Stiffness parameters</b>                   |   |  |                      |
| $\lambda^*$                                   | Modified compression index              | [-] $\lambda^*/\kappa^* \approx 2.5 - 7^1$ | [-]                  |
| $\kappa^*$                                    | Modified swelling index                 | [-]  | [-]                  |
| $\mu^*$                                       | Modified creep index                    | [-] $\lambda^*/\mu^* \approx 15 - 25^1$    | [-]                  |
| <b>Advanced parameters</b>                    |   |  |                      |
| $\nu_{ur}$                                    | Poisson's ratio for unloading-reloading | [0.15] <sup>1)</sup>                       | [-]                  |
| $K_0^{nc}$                                    | $K_0$ -value for normal consolidation   | [1-sin $\phi$ ] <sup>1)</sup>              | [-]                  |
| M   | $K_0^{nc}$ - related parameter          | Function of other parameters.              | [-]                  |
| $\sigma_{tension}$                            | Allowable tensile strength              | [0] <sup>1)</sup>                          | [kN/m <sup>2</sup> ] |

1) (Plaxis, 2019)

### A.13 SHANSEP NGI-ADP

The Wettelijk BeoordelingsInstrumentarium (WBI) prescribes the SHANSEP NGI-ADP model for slip plane calculations in case of highwater conditions. When switching from HS or SSC to SHANSEP Plaxis uses eq. 2.5 to calculate the undrained shear strength.

The parameters S and m are in Plaxis defined as  $\alpha$  and power respectively. The relevant parameters are given in Table A3 and a graphical representation is given in Figure A4. (Zukri & Nazir, 2018) state: "When switching from HS or SSC to SHANSEP Plaxis determines the undrained shear strength belonging to the at that moment highest principal stress." The yield stress is defined as the highest calculated principal stress during all phases.

The abbreviation ADP stands for Active/Direct-Shear/Passive. The NGI-ADP is a total stress model, so it doesn't differentiate pore pressure and effective stresses. The model is able to use different values

of the undrained shear strength in the active, neutral and passive part of the slip plane, see Figure A3. Defining the ratio between active and passive undrained shear strength can be very useful in case of uplift conditions. Via this ratio a reduced passive undrained shear strength can be modelled at the end of the slip plane.

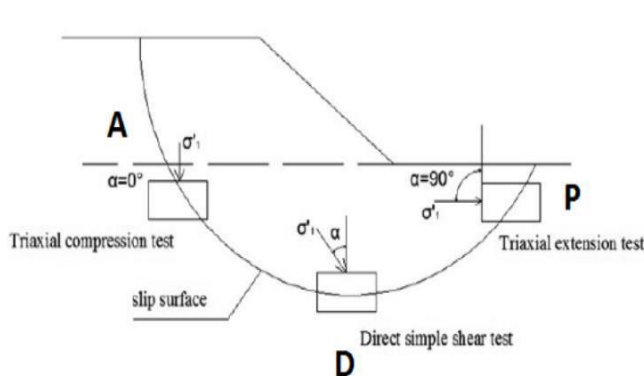


Figure A3 : A schematic overview of the ADP-model (Iereidis, 2019)

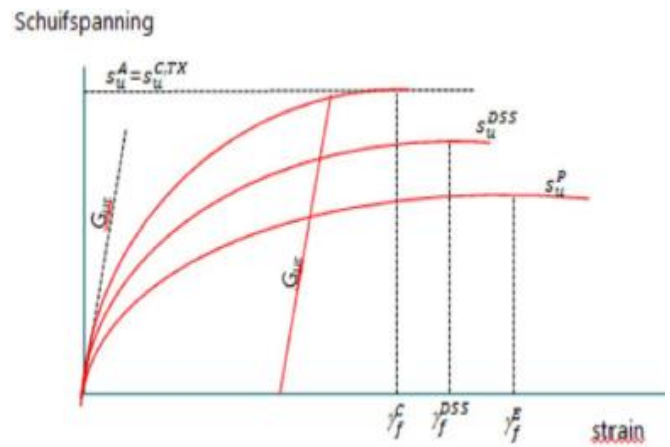


Figure A4 : Parameters of the SHANSEP NGI-ADP model, shear stress versus strain. (POVM, 2018) Dutch: Schuifspanning -> English: Shear stress

Table A3: SHANSEP NGI-ADP parameters

| Parameter           | Description   | [Default] values                                | Units                |
|---------------------|---|---|----------------------|
| $G_{ur} / s_u^A$    | Ratio unloading/reloading shear modulus over (plain strain) active shear strength                         | -   | [-]                  |
| $\gamma_f^C$        | Shear strain at failure in triaxial compression   | $[\gamma_f^C = \frac{3}{2} \cdot \epsilon_1^C]$ | [%]                  |
| $\gamma_f^E$        | Shear strain at failure in triaxial extension   | $[\gamma_f^E = \frac{3}{2} \cdot \epsilon_1^E]$ | [%]                  |
| $\gamma_f^{DSS}$    | Shear strain at failure in Direct Simple Shear  | $\gamma_f^C < \gamma_f^{DSS} < \gamma_f^E$      | [%]                  |
| $s_u^P / s_u^A$     | Ratio of (plane strain) passive shear strength over (plane strain) active shear strength.                 | [1.01] <sup>2)</sup>                            | [-]                  |
| $\tau_0 / s_u^A$    | Initial mobilization  | [0.7] <sup>1)</sup>                             | [-]                  |
| $s_u^{DSS} / s_u^A$ | Ratio of direct simple shear strength over active shear strength.   | [0.99] <sup>3)</sup>                            | [-]                  |
| $\nu'$              | Effective Poisson's ratio unloading<br>Effective Poisson's ratio past yield stress                        | [0.2] <sup>3)</sup><br>[0.33] <sup>3)</sup>     | [-]                  |
| $\nu_u$             | Poisson ratio undrained behaviour   | $\nu_u$ [0.495] <sup>3)</sup>                   | [-]                  |
| $\alpha$            | Normally consolidated undrained shear strength (Also known as S)  | Clay: 0.16 – 0.28<br>Peat: 0.28 – 0.44          | [-]                  |
| $m$                 | Power for stress-level dependency of stiffness  | $0.8 \pm 0.1$ <sup>3)</sup>                     | [-]                  |
| $s_{u,min}$         | Undrained shear strength. Default value 0 kPa, might be slightly higher in the case of uplift conditions. | [0] max. 2 kPa <sup>2)</sup>                    | [kN/m <sup>2</sup> ] |
| $OCR_{min}$         | Minimum OverConsolidation Ratio   | [1] <sup>1)</sup>                               | [-]                  |
| $POP_{min}$         | Minimum Pre Overburden Pressure   | [0] <sup>1)</sup>                               | [kPa]                |

| Parameter   | Description                                    | [Default] values | Units                  |
|---|--|------------------|------------------------|
| <b>Parameters for initial strength / activating the SHANSEP model</b> |  |                  |                        |
| $S_{u,ref}^A$   | Reference (plain strain) active shear strength | -                | [kN/m <sup>2</sup> ]   |
| $y_{ref}$   | Reference depth                                | -                | [-]                    |
| $S_{u,inc}^A$   | Increase of shear strength with depth          | -                | [kN/m <sup>2</sup> /m] |

- 1) (Plaxis, 2019)
- 2) (POVM, 2018)
- 3) (Naves & Lengkeek, 2017)

## Undrained (A)

As an alternative to the SHANSEP NGI-ADP model, the HS and SSC models can also be combined with Plaxis "Undrained (A)". For higher overconsolidation ratios this model is more conservative than the SHANSEP model. The "Undrained (A)" model enables the modelling of undrained behaviour using effective strength and stiffness parameters. The effective strength parameters are  $c'$ ,  $\varphi'$  and  $\psi$ , the effective stiffness parameters are  $E'_{50}$  and  $\nu'$ . So undrained shear strength is not an input but an output parameter.

## A.2 D-Stability (2019)

D-Stability is a two dimensional program developed by Deltares that is widely used in Dutch engineering practice for designing and checking the stability of embankments on soft soils. The most recent version (D-Stability 2019) has been optimized for undrained calculations. The stability can be calculated with built-in slip plane models.

### Slip plane models

D-Stability offers three slip plane models to calculate the slope stability: Bishop, Uplift-Van and Spencer. In the WBI the Uplift-Van model is prescribed. This is in good accordance with literature on slope stability analysis with stone columns improvement. (Zhang et al., 2013) and references therein state that Bishop's simplified method assuming a circular slip surface is probably the most commonly-used limit equilibrium method. However, it is "indicated that the critical slip surface of the deep-seated slope failure of a deep mixed column-support embankment over soft soil was not circular based on the numerical results." As a consequence "the limit equilibrium analysis using Bishop's simplified method overestimated the factor of safety of the embankment over a deep mixed column-reinforced foundation as compared with the numerical method."

*"The failure mechanism based on the Uplift-Van model is described by two circular slip circles: one on the active zone and another on the passive zone, bound by a horizontal slip line. This horizontal line, which is part of the passive zone, usually lies along the bottom of a weak soil layer (Figure A5). The safety factor for macro-stability is expressed as the ratio of the resisting moment to the driving moment. The resistance against sliding is governed by the shear strength of soils." according to (Simanjuntak et al., 2018).*

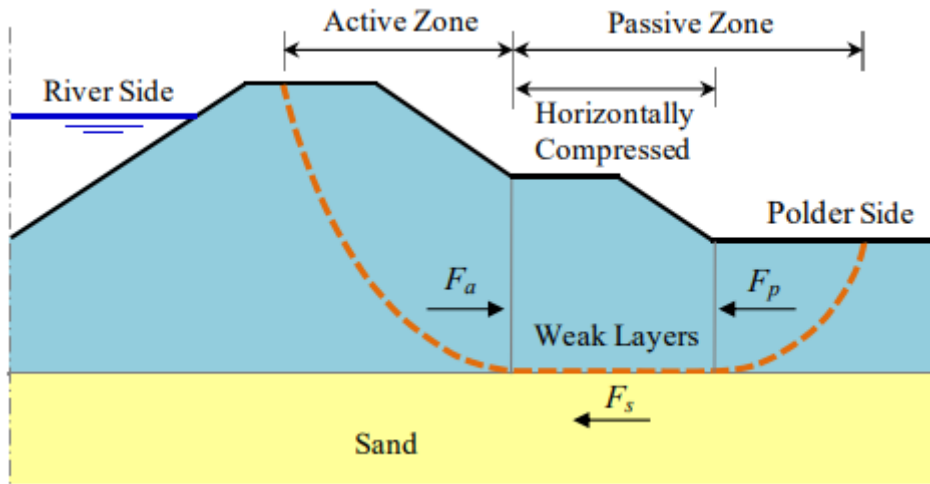


Figure A5 : The Uplift-Van Model (Simanjuntak et al., 2018)

Until 2017 the Bishop method was most used in Dutch engineering practice. It assumes loss of equilibrium of a slope by the creation of a circular slip surface. (CUR, 1996) "The circular shearing soil mass is divided into a number of vertical slices." (CUR, 1996) The resisting moment equals the summation of the shear strength of each slice along a slip surface. The driving moment is determined by summation of the multiplication of each slice weight by the horizontal force component relative to the centre of the circle (O in Figure A6). (CUR, 1996)

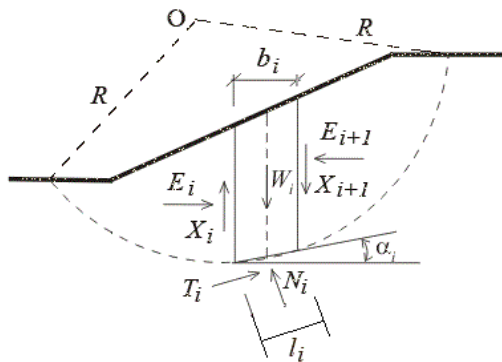


Figure A6 : Bishop method (Wikipedia, 2012)

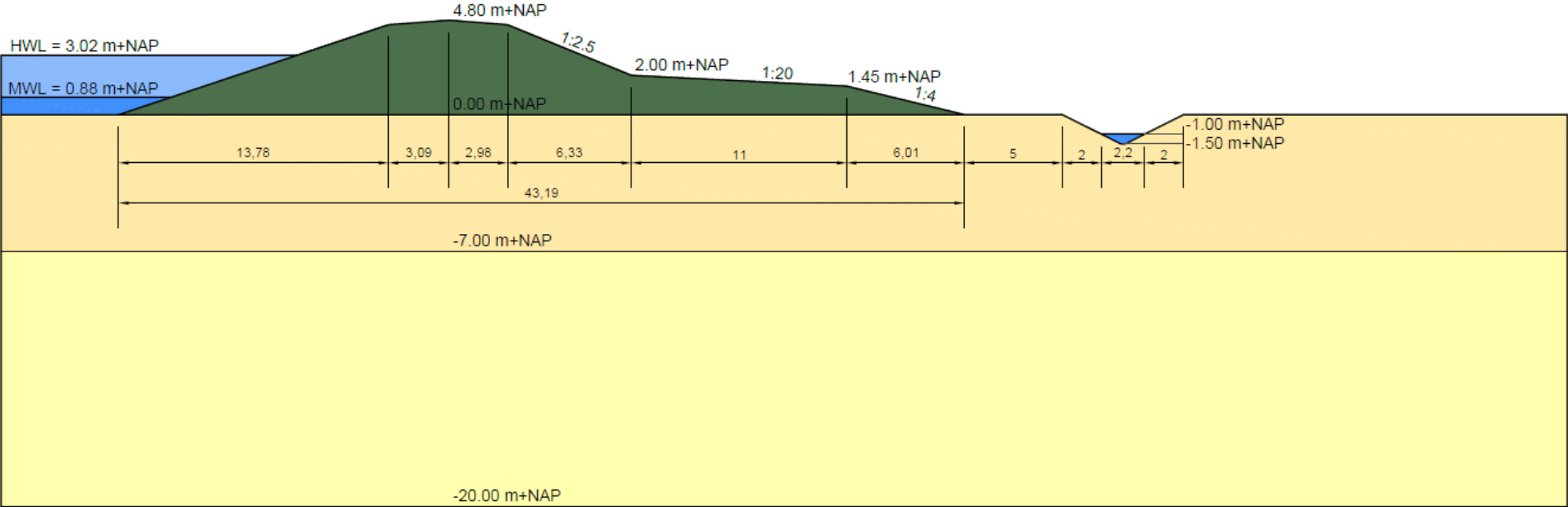
### Shear strength model

In D-Stability two shear strength model options can be selected: Drained or Undrained. If the option Drained is selected D-Stability requires the strength parameters: cohesion ( $c$ ), friction angle ( $\phi$ ) and dilatancy angle ( $\psi$ ). In case the Undrained shear strength model is chosen, D-stability requires the shear strength ratio ( $S$ ) and the strength increase component ( $m$ ).



# Appendix B – Green dike

## B.1 Green dike layout



## B.2 Soil parameters

Table 0-1: Volumetric weights

| Soil type                   | $\gamma_{\text{unsat}}$<br>[kN/m <sup>3</sup> ] | $\gamma_{\text{sat}}$<br>[kN/m <sup>3</sup> ] |
|-----------------------------|---|---|
| Clay Gorkum light (organic) | 11.86   | 11.86   |
| Dike material               | 18.45   | 18.45   |
| Sand Pleistocene            | 18.00   | 20.00   |

Table 0-2: Strength and stiffness parameters applied in the SSC-model

| Soil type                   | $\lambda^*_{\text{kar}}$ | $\kappa^*_{\text{kar}}$ | $\mu^*_{\text{kar}}$ | $c'_{\text{kar}}$<br>[kN/m <sup>2</sup> ] | $\phi'_{\text{kar}}$<br>[kN/m <sup>2</sup> ] |
|-----------------------------|--------------------------|-------------------------|----------------------|---|--|
| Clay Gorkum light (organic) | 0.1783                   | 0.0378                  | 0.0261               | 1.0                                       | 31.2   |
| Dike material               | 0.0654                   | 0.0077                  | 0.0039               | 2.0                                       | 27.2   |

Table 0-3: Strength and stiffness parameters applied in the SHANSEP-model

| Soil type                   | $\alpha$<br>[-] | $m$<br>[-] | $G/s_u^A$ | $\gamma_r^C$<br>[%] | $\gamma_r^{\text{DSS}}$<br>[%] | $\gamma_r^E$<br>[%] |
|-----------------------------|-----------------|------------|-----------|---------------------|--------------------------------|---------------------|
| Clay Gorkum light (organic) | 0.25            | 0.76       | 26        | 9.66                | 12.07                          | 14.49               |
| Dike material               | 0.25            | 0.76       | 193       | 10.08               | 12.60                          | 15.12               |

Table 0-4: Strength and stiffness parameters applied in the HS-model

| Soil type        | $E_{50}^{\text{ref}}$<br>[MN/m <sup>2</sup> ] | $E_{\text{oed}}^{\text{ref}}$<br>[MN/m <sup>2</sup> ] | $E_{\text{ur}}^{\text{ref}}$<br>[MN/m <sup>2</sup> ] | $m$<br>[%] | $c'_{\text{kar}}$<br>[kN/m <sup>2</sup> ] | $\phi'_{\text{kar}}$<br>[kN/m <sup>2</sup> ] |
|------------------|---|---|--|------------|---|--|
| Sand Pleistocene | 35  | 35  | 100  | 0.5        | 1.0                                       | 32.5   |